Highly tunable delivery of matrix-bound growth factors for therapeutic angiogenesis

Inauguraldissertation

zur

Erlangung der Würde eines Doktors der Philosophie

vorgelegt der

Philosophisch-Naturwissenschaftlichen Fakultät

der Universität Basel

von

Veronica Sacchi

von Italien

Basel, 2014

Genehmigt von der Philosophisch- Naturwissenschaftlichen Fakultät auf Antrag von

Prof Markus Affolter

Dr Andrea Banfi

Prof Michael Heberer

Prof Heinz Redl

Basel, den 18. Juni 2013

Prof Dr Jörg Schimbler
Dekan

“Dans la vie, rien n’est à craindre,
tout est a comprendre.”

Marie Curie

“Nothing in life is to be feared. It
is only to be understood.”

Marie Curie

b

1. Mechanism of physiological vessels formation

1.1 Formation of vessels in the embryo

In vertebrates, the circulatory system is the first functional organs to arise and is critical in providing both oxygen and nutrient supply to the developing tissues. The vasculature is formed through three main cellular processes: vasculogenesis, angiogenesis and arteriogenesis (1). Vasculogenesis is the first process that gives rise to blood vessels during embryonic development and the vascular plexus is established before the onset of heartbeat (2). The blood islands in the yolk sac are the earliest site of prenatal vasculogenesis. These are composed of heamangioblasts, the putative common precursors of endothelial and hematopoietic cells (3). Angioblasts, the peripheral cells of the blood islands, connect to construct a primitive network composed of capillaries, arteries and veins. Both fibroblast growth factor- 2 (FGF-2) and vascular endothelial growth factor -A (VEGF-A) have a key role in the specification of angioblasts (2). Following assembly of primitive vessels in the early embryo, remodeling transforms the plexus into a hierarchically organized network of arteries, capillaries and veins. Arterial and venous ECs possess specific molecular identities from the earliest stages of cardiovascular development. Arterial ECs in fact express the Ephrin-B2, while the venous ECs express the cognate receptor EphB4 (4). After endothelial cell specification, the vascular plexus expands by angiogenesis (reviewed in details in paragraph 1.3), that is defined as the formation of new blood vessels from pre-existing ones, i.e. capillaries and postcapillaries venule (5). After the formation of the immature plexus, vessels undergo to maturation by mural cells recruitment (reviewed in

chapter 2), a process mediated by platelet-derived growth factor-B (PDGF-B), angiopoietins, and transforming growth factor-β (TGF-β) (2).

1.2 Formation of vessels in the adult

In adults, growth and remodeling of the vascular network is essential for tissue metabolism and wound repair. Vascular growth in the postnatal life proceeds mainly through angiogenesis (reviewed in paragraph 1.3), which however is not the only mechanism of vascular growth in the adult. It has been established that vasculogenesis occurs also in postnatal life, as “postnatal vasculogenesis”, which is *de novo* vessel formation by in situ incorporation, differentiation, migration and/or proliferation of bone marrow-derived endothelial precursor cells (EPCs) that can be mobilized in response to various growth factors stimuli, as VEGF, granulocyte monocyte- colony stimulating factor (GM-CSF), FGF-2, and angiopoietins. This process it has been demonstrated in several disorders, as hypoxic conditions or tumors (6). Arteriogenesis instead define the growth of functional collateral arteries from pre-existing arteriol- arterial anastomoses after stenosis or occlusion of a major artery. This occurs in the adult to naturally bypass the vascular occlusion in response to increased blood flow or shear stress (7). It comprises the induction of vascular wall cell proliferation and migration and includes wall-remodeling processes. In consequence, the structural enlargement of collateral arterioles to arteries proceeds as an active growth rather than by a passive dilation because of the altered blood pressure (7).

1.3 Molecular mechanisms of angiogenesis

Angiogenesis is a complex multi-step process, which requires the tight coordination of several cell types and factors (8). It can take place by two different mechanisms: sprouting angiogenesis (reviewed in paragraph 1.3.2) and splitting angiogenesis (see paragraph 1.3.3). The process can be divided in two sequential phases: 1) tube formation, in which endothelial cells sense the angiogenic stimulus and start to proliferate, migrate and assemble the new vessel and 2) vascular maturation (reviewed in chapter 2), in which the new vessels are covered from mural cells (either pericytes or smooth muscle cells) and generate new extracellular matrix (9). This step is necessary to induce endothelium quiescence and promote vessel stabilization. Newly induced vessels are defined stable when they become independent from the angiogenic stimulus (10-12). In the past years have been discovered and characterized numerous angiogenic factors such as vascular VEGF, angiopoietins, TGF-β, FGF, hepatocyte growth factor (HGF) (13). Among them, VEGF is the most potent and specific growth factor. It was first identified in 1983 as a protein that promotes vascular leakage, called VPF, (14) but was not isolated and characterized. It has been isolated for the first time in 1989 from medium conditioned by bovine pituitary follicular cells as specific endothelial cell mitogen and called VEGF (15). Further cloning studies have demonstrated that VEGF and VPF are the same protein (16, 17).

1.3.1 Vascular endothelial growth factors (VEGFs) and receptors

The VEGF family of growth factors includes five members in mammals: VEGF-A, VEGF-B, VEGF-C, VEGF-D and placenta growth factor (PIGF). The VEGF homologues produced by Orf viruses are collectively termed VEGF-E, and a homologue isolated from snake venom is the VEGF-F (18). VEGFs belong to the platelet- derived growth- factor superfamily of secreted dimeric glycoprotein growth factors. The main receptors involved into the signaling cascade upon VEGFs binding are three tyrosine kinase receptors termed VEGFR-1 (Flt-1), VEGFR-2 (Flk-1), and VEGFR-3 (Flt-3). All VEGFRs have a conserved intracellular split tyrosine kinase domain and a series of immunoglobulin – like domains in the extracellular part (18). Additionally there are two co-receptors, Neuropilins 1 and 2 (Nrp-1 and Nrp-2), originally identified as semaphorin receptors that mediate repulsive signals in axon guidance (19). Binding of VEGF ligands to their respective receptors induces receptor homodimerization or heterodimerization, which activates receptor kinase activity, receptor auto-phosphorylation and downstream signaling (18)(Fig. 1). Among the mammalian VEGFs, VEGF-A is the most potent and characterized angiogenic growth factor and plays a pivotal role both in physiological and pathological conditions.

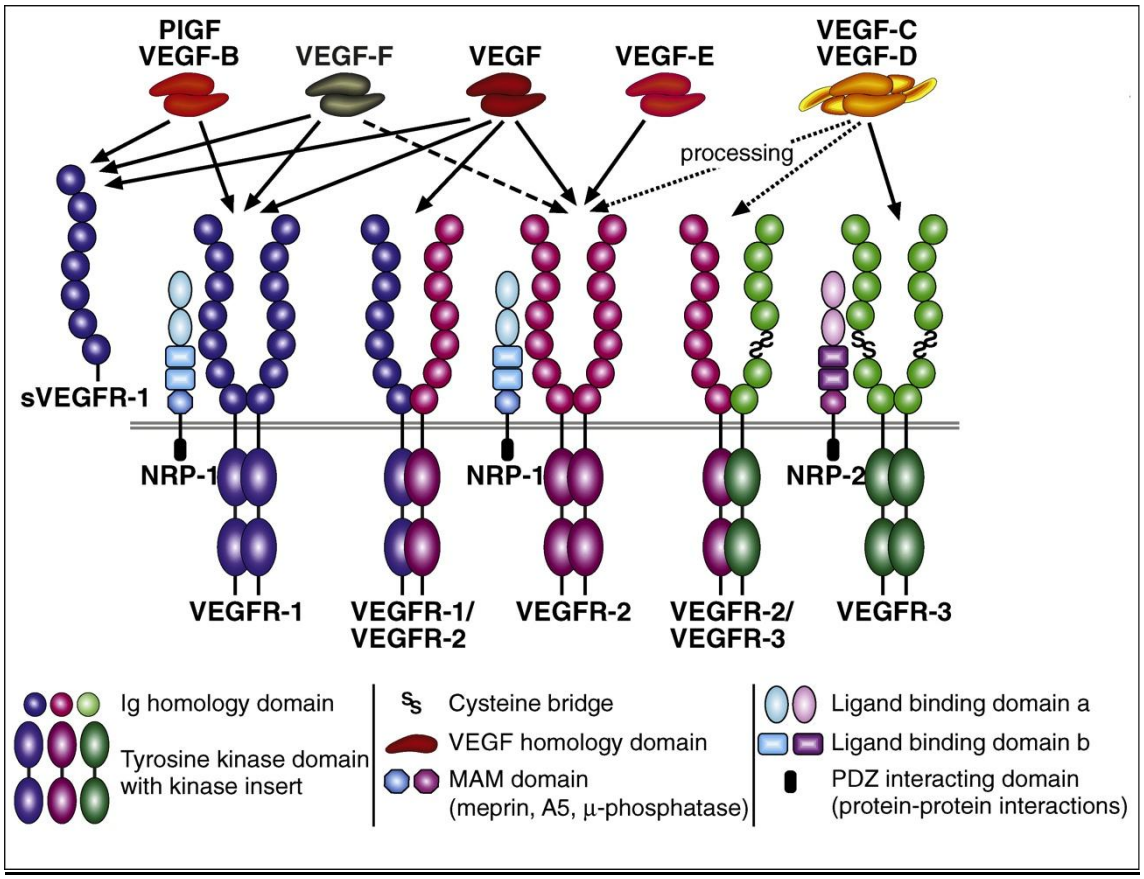

Figure 1 Structure and interactions of VEGFs, VEGFRs, and their NRP co-receptors.

The different growth factors of the VEGFs family bind to their correspondent receptors specificities (indicated by the arrows). Binding of the dimeric VEGF ligands stimulates receptor dimerization and autophosphorylation, leading to the recruitment of the downstream signaling molecules (adapted from (18)).

1.3.1.1 VEGF-A signaling and regulation

VEGF-A is essential for both vasculogenesis and angiogenesis. Heterozygous mutation of the VEGF-A gene cause embryonic lethality at day 11-12. Blood islands, ECs and major vessels fail to form in fact in the mutant embryo, and is reduced the number of red blood cells (20, 21). On the other hand, increase of a two-or three fold overexpression of VEGF-A from its endogenous locus results in severe abnormalities in hearth development and embryonic lethality (22). VEGF-A is an oxygen sensitive molecule and its transcription is under the

control of hypoxia-inducible factor (HIF)-1. HIF-1 is composed by two peptides, HIF-1α and HIF-1β. During normoxic conditions, HIF-1α is rapidly degraded, whereas in hypoxic conditions it dimerizes with HIF-1β. This complex is able to bind and activate a specific region of the VEGF-A promoter driving its transcription. Regulation of angiogenesis by hypoxia is demonstrated in many types of tumors or in wound healing processes (23). Furthermore, several growth factors, inflammatory cytokines, oncogenes and hormones have also been reported to induce VEGF-A gene expression (24). The human VEGF-A gene is composed by eight exons divided by seven introns. The VEGF-A molecule exists in several isoforms generated by alternative splicing events occurring predominantly in exons 6 and 7, encoding for two different heparin-binding domains. Among the different VEGF-A isoforms, VEGF-A_{121}, VEGF-A_{165} and VEGF-A_{189} are the forms secreted by most cell types (25). These isoforms differ from each other in the size of the heparin-binding domain. In fact, whereas VEGF-A_{121} lacks these domains completely and is thus completely soluble, VEGF-A_{165} and VEGF-A_{189} have only one or both heparin- binding regions respectively and display increasing affinity for the extracellular matrix. As a consequence, VEGF-A_{165} is partially soluble and is able to generate gradients of intermediate stepness, whereas VEGF-A_{189}, which remains tightly bound to the extracellular matrix, generates very steep gradients (26). The different biological functions of these isoforms have been extensively characterized in vivo in the mouse hindbrain and in retina using isoform-specific genetic manipulations and VEGF-A knockout mice (27). Mice VEGF-A isoforms are one aminoacid shorter compared to the human but showed the same biological properties (24). Mice having only VEGF-A_{120} died soon after birth, developed severe cardiomyopathy

(28), and showed impaired angiogenesis characterized by a reduced vascular branching and increased vascular diameter. The number of endothelia filopodia processes was reduced and their orientation compromised. On the other hand mice expressing only VEGF-A_{188} formed ectopic and abnormally thin vessel branches. Only mice expressing the intermediate-binding VEGF-A_{164} exhibited the growth of a normal vessel network. Further, double heterozygous mice, expressing both VEGF-A_{120} and VEGF-A_{188}, but not VEGF-A_{164}, induce normal vessel morphogenesis as obtained with VEGF-A_{164} alone (27). VEGF-A binds VEGFR-1 and VEGFR-2 as well as Nrp-1 (fig. 1) (29). VEGFR-1 is widely expressed even if its kinase activity is poor. It exists as a full-length form and an alternative spliced, soluble form (sFlt1) (30). Both forms of the VEGFR-1 bind VEGF-A with higher affinity than VEGFR-2, preventing the activation of this receptor. Flt1-/- died at embryonic day 9 (E9.0), whereas deletion of the tyrosine kinase domain is compatible with vascular development (31, 32). VEGFR-2 instead is the main VEGF-A receptor on endothelial cells, is essential for endothelial cell biology during development and in the adult, both in physiology and pathology. Mouse embryos lacking VEGF-R2 die at E8.5- 9.5 and lack vasculogenesis and hematopoiesis (33). Activation of VEGFR-2 from VEGF-A exerts several actions on endothelial cells, as proliferation, migration, endothelial cell survival and vascular permeability. VEGFR-2 binds VEGF-A with a 10-fold lower affinity than VEGFR-1 (29). VEGF-A_{165} additionally binds the co-receptor Nrp-1 through its heparin- binding domain (34) forming a ternary complex with VEGFR-2 (35). The formation of this complex lead to enhanced endothelial cell migration and survival (29). In particular, Nrp-1 has been shown to be essential in VEGF-A in vessel sprouting and branching (36).

1.3.1.2 Others VEGFs members signaling

VEGF-B exists in two different isoform, VEGF-B_{167} and VEGF-B_{186}, and selectively binds VEGFR-1 (fig. 1) (18). VEGF-B exerts a less pronounced role in the vascular system, is mainly involved in the maintenance of vessels in pathological conditions rather than in their formation (37). In the heart, induces revascularization and preserves cardiac function after myocardial infarction (38, 39). VEGF-C and VEGF-D are mainly involved in angiogenesis and their binding affinities for their receptor depend on proteolytic processing of their pro-peptides (fig. 1). In fact, only the mature forms bind VEGFR-2, and the affinity for VEGFR-3 increases with processing. VEGF-C/VEGF-D binding to VEGFR-3 promote lymphatic endothelial cells proliferation (29). PIGF has been discovered in the placenta but is expressed also in heat and lungs; it exists in four isoforms (PIGF1-4) in human generated by alternative splicing, of which only PIGF-2 has a homologue in mice. It signals through VEGFR-1 stimulating angiogenesis and collateral growth in ischemic limb and hearth (18).

1.3.2 Sprouting angiogenesis

Sprouting angiogenesis is the best-characterized process of vessel growth. In sprouting angiogenesis, endothelial cells (ECs) are attracted by pro-angiogenic signals, ECs loosen their cell-cell junctional contacts, start to secrete proteases to degrade the extracellular matrix (ECM) and become invasive and motile to initiate the new blood vessel sprout (8). Only some ECs are selected to initiate vessel sprouting; these leading endothelial cells, the tip cells, extend numerous

dynamic filopodia that sense and respond to attractive or repulsive guidance signals in the microenvironment (40, 41). Hence, tip cells share many morphological and functional similarities with the neuronal growth cones that guide axons (42). Endothelial stalk cells follow the tip cell, compared to the tip cells have a lumen, are less motile, produce fewer filopodia and are more proliferative. They establish the trunk of the new vessel and allow the elongation of the vessel (43); they also form junctions with neighboring and produce basement membrane components to ensure the integrity of the sprout (44). Once initiated, EC sprouting continues in a highly directional manner until tip cell connect with adjacent vessels and undergo anastomosis to form a continuous lumen, allowing blood flow (fig. 2) (8).

Several signaling pathways control EC behavior during angiogenic sprouting including Tie2 and Notch signaling. However, the vascular endothelial growth factor- A (VEGF-A) is the master regulator of new blood vessel sprouting during development, growth and disease (9). VEGF-A guides angiogenic sprouting by directing tip cell migration, polarization and directional filopodia extension depending on its local distribution and therefore on the generation of extracellular gradients (40). VEGF-A stimulation of VEGFR-2 mediate also endothelial stalk cells proliferation, but this is regulated by the concentration of the VEGF-A and not by the formation of extracellular gradient (40).

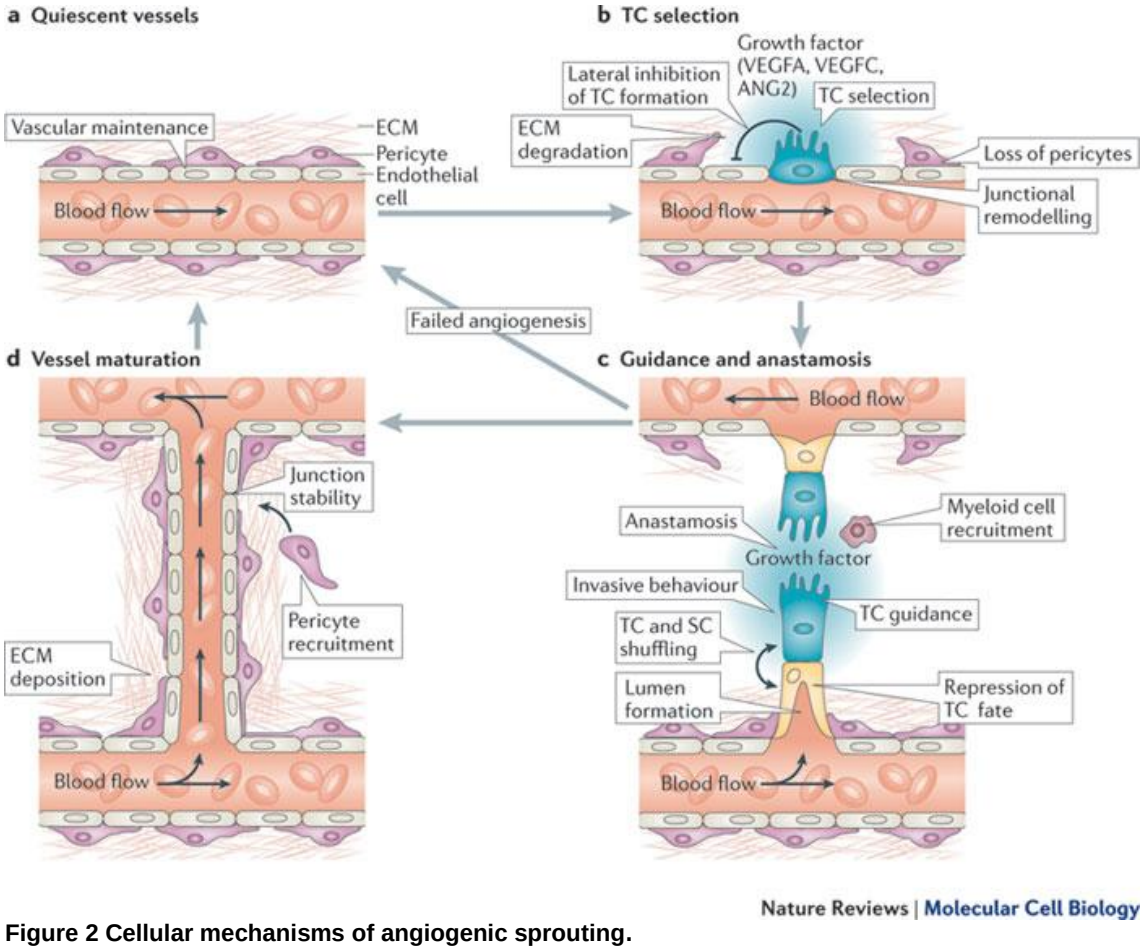

Figure 2 Cellular mechanisms of angiogenic sprouting.

During angiogenic sprouting, selected endothelial "tip cells" start to secrete proteases and migrate guided by gradients of pro-angiogenic growth factors. During sprout elongation, tip cells are followed by endothelial stalk cells, which proliferate and establish the vessel trunk. Upon contact with other vessels, tip cell behavior is repressed and vessels fused by the process of anastomosis (adapted from (8)).

A balanced correct formation of tip and stalk cells that is critical for having physiological sprouting angiogenesis. The best know regulator of endothelial tip and stalk cells specification and their ligand Dll4 and Jagged1.

1.3.2.1 Notch and VEGF-A cross-talk: regulation of tip and stalk cells formation

Notch signaling is an evolutionarily conserved pathway among vertebrate and invertebrate organisms (45). ECs express multiple Notch receptors (Notch1 and Notch4) and transmembrane Notch ligands (Delta- like 1(Dll1), Dll4, Jagged 1 and Jagged2) (8). Ligand binding induces two further proteolytic cleavages of Notch receptors. Extracellular proteases sever the Notch extracellular domain (NECD). The cleavage and subsequent conformation changes make Notch susceptible to processing by γ-secretase that releases the Notch intracellular domain (NICD). Following translocation of the NICD into the nucleus, the NICD form a complex with the transcription factor RBPj/CBF1 and Mastermind-like proteins to drive target genes-expression, as the basic helix-loop-helix (bHLH), Hairy/Enhancer of Split (Hes) and Hes-related proteins (Hey), which in turn, act as transcriptional regulators of further downstream genes (45). This complex not only activates transcription but also promotes its own turnover to prevent sustained Notch activation. Several studies have elucidated the crucial role of Notch and Dll4 in tip and stalk cell formation. Endothelial- specific inducible knock- out of Notch 1 or Dll4 heterozygous mutation cause excessive tip cell formation in mouse retinas. Further, most Notch1-deficient endothelial cells are in tip cell position (46). In addition, studies in mouse and zebrafish revealed that blocking the Notch signaling either using γ-secretase inhibitors or by disruption of Dll4 expression increase tip cell formation and sprouting, highlighting the role of Notch in suppressing the tip cell fate (47-49). VEGF interact with the Dll4/ Notch pathway in order to guarantee the balanced formation of tip and stalk cells. VEGF-A signaling through VEGFR-2 promotes tip cell induction by

upregulating the expression of the Notch ligand Dll4. Expression of Dll4 in endothelial tip cells activates Notch-1 in adjacent stalk cells to laterally inhibit tip cell fate and maintain the hierarchical organization of sprouting ECs (46). Notch-1 activation inhibits VEGFR-2 function in stalk cells, which become less responsive to VEGF-mediated tip cells inducing signals VEGFR-1 is predominantly expressed in stalk cells and involved in guidance and limiting tip cell formation(44). Interestingly, endothelial cells can rapidly exchange between the tip and stalk cell position during angiogenic sprouting in vitro and in vivo in the head of zebrafish, by regulating the expression level of VEGFR-2 and VEGFR-1 (50). The sVEGFR1 rescues vascular defects caused by VEGFR1-deficiency, defining a role of this receptor as a decoy for VEGF-A to spatially control VEGFR-2 signaling (Fig. 3) (51). Furthermore, it has been proved that activation of VEGFR-3 by VEGF-C produced by macrophages is able to reinforce Notch signaling and to promote the conversion of tip to stalk cells (52). Opposite to Dll4, stalk cells express the other Notch ligand Jagged1. Jagged1 also promotes tip cell formation and angiogenesis, even if Jagged1 poorly activates the Notch receptor. In fact, in sprouting ECs the NECD is glycosylated by the Fringe-family of glycosyltransferase.

This modification favors Notch signaling via Dll4 but represses signaling via Jagged1. Thus, stalk cells-restricted Jagged1 competes with Dll4 for binding to Notch receptors on tip cells and effectively suppress Notch signaling in tip cells. Consequently, in the retinal vessels of EC-specific Jagged1- knockout mice is impaired the formation of tip cells and vascular sprouting (53).

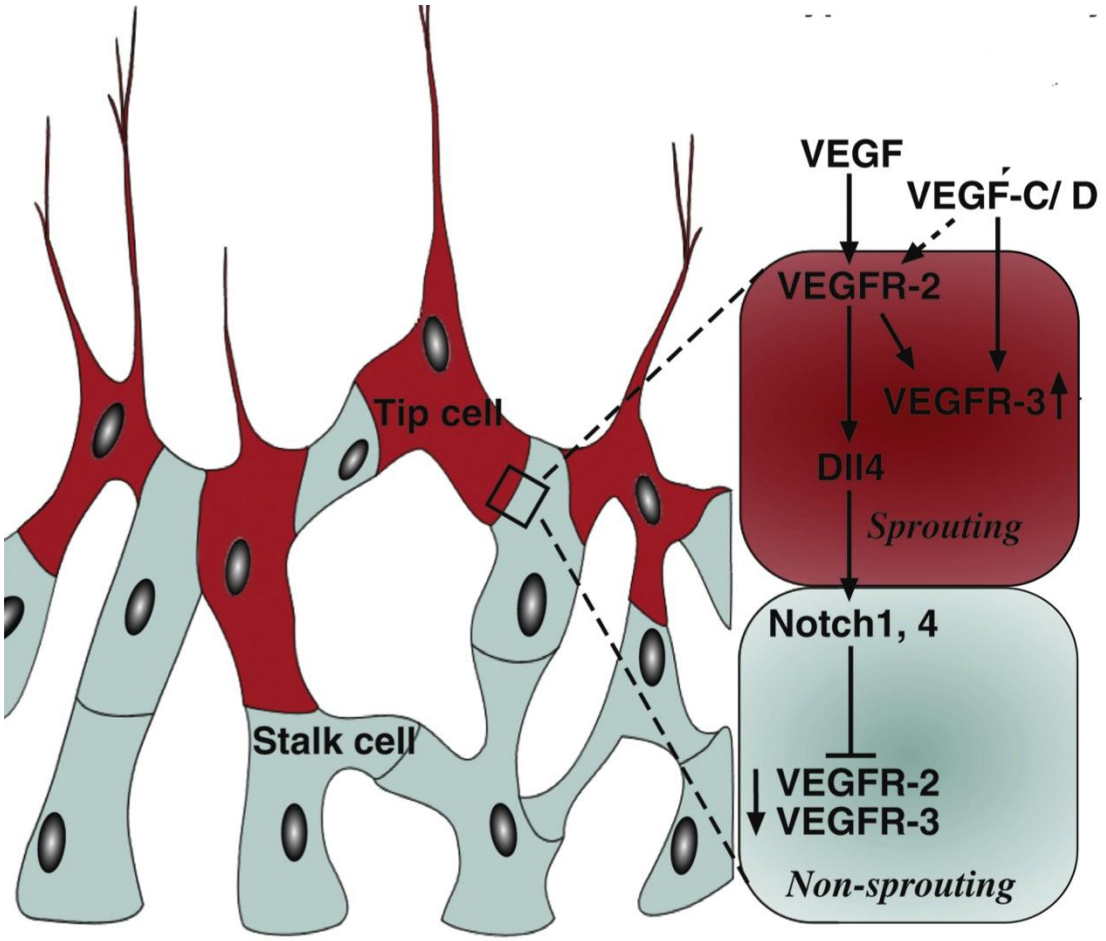

Figure 3 Molecular mechanisms of endothelial tip cell selection (Lohela M et al, Curr Opin in Biol, 2009)

Endothelial tip cells start sprouting by sending thin filopodia toward the VEGF-A gradient. Behind the tip cells, proliferating endothelial stalk cells form the lumen of the newly growing vessels. Additional factors as a VEGF-C/D may augment the angiogenic effects of VEGF-A. VEGF-A/ VEGFR-2 signaling enhances Dll4 expression in tip cells. Dll4-mediated activation of Notch1 in neighboring endothelial cells inhibits tip cells behavior in stalk cell by downregulating VEGFR-2 and VEGFR-3 while upregulating VEGFR-1. Tip and stalk cells can dynamically shuffle their position by dynamically regulating VEGFRs expression (adapted from (18))

1.3.4 Intussusceptive angiogenesis

Intussusception is defined as the formation of new blood vessels resulting from the insertion and extension of luminal tissue pillars, growing in itself (54). It was first described from Caduff et al in 1986 (55). The formation of intraluminal pillars proceeds through a multistep process (Fig. 4) (56). It starts when the

endothelial walls from opposite sides of a vessel protrude into the vascular lumen from opposite walls. Afterwards, the inter-endothelial junctions are reorganized, so that a central perforation is formed in the core of the pillar. A trans-luminal pillar is established upon contact between these processes. This is subsequently invaded by supporting cells, i.e. pericytes and fibroblast, which start to deposit ECM into the pillar. As the pillar increases in girth, it splits the vascular segment into two separated new vessels (Fig. 4). There are three forms of intussusceptive angiogenesis, based on the phenotype, the intussusceptive microvascular growth (IMG), the intussusceptive arborization (IAR), and intussusceptive branching (IBR) (56, 57). IMG is characterized by the formation of numerous pillars, which promote the expansion of the capillary plexus. In contrast, IAR contributes to the formation of a supplying vascular tree, in which major arterioles, venules and capillaries are discerned. The IBR, is important for the optimization of the branching geometry in function of the tissue demands, changing the branching pattern of blood vessels or pruning the vascular network from superfluous vessels. Blood flow has a main role in regulating intussusceptive angiogenesis. It has been described splitting angiogenesis in response to increased blood flow in the chicken chorioallantoic membrane (CAM) model (58) and in the skeletal muscle (59). Sprouting and intussusception are two complementary modes of angiogenesis, and a combination of metabolic and haemodynamic factors determine whether occurs intussusception or sprouting. In general higher levels of shear stress lead to intussusceptive angiogenesis, whereas angiogenic growth factors released from the tissue in response to hypoxia stimulate sprouting. Intussusceptive angiogenesis is a process that only occurs in a pre-existing vascular network

that was formed either through vasculogenesis or through sprouting angiogenesis (60). However, intussusception is energetically and metabolically more effective because does not require massive cell proliferation or membrane degradation (61).

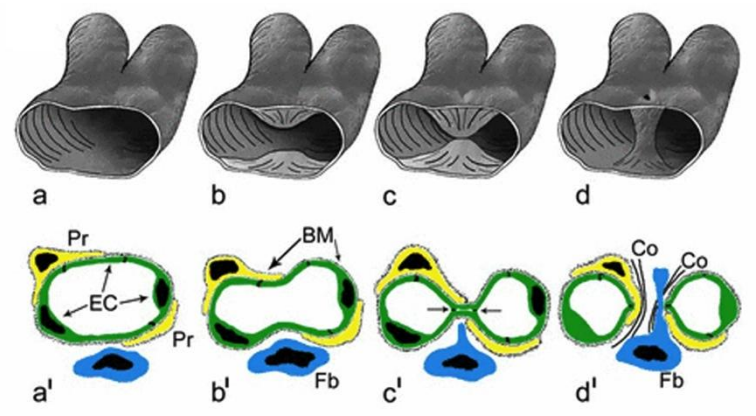

Figure 4 (a-d) Three-dimensional schema illustrating the steps in the formation of transluminal pillars during intussuscpetive angiogenesis.

The process begins with the protrusions of endothelial cells from opposite sides into the vessel lumen (a,b). After the contact has been established (c), the endothelial bilayer becomes perforated centrally and a transluminal pillar is formed (d). (a'-d') Two-dimensional representation of the phases described in (a-d). Endothelial cells from opposite sides of a capillary protrude into its lumen until they contact each other (a'-c'). After the formation of the transluminal pillar, the endothelial cells than retract, and newly formed pillars increases in girth after invasion by fibroblasts (Fb) and pericytes (Pr), which enforce collagen fibrils (Co in d') (adapted from (61)).

Intussusception has been described not only in physiological but also in pathological conditions, as for example in tumor, where after anti-angiogenic treatments or radiotherapy, tumors can rapidly recover by switching from sprouting to intussusceptive growth (62). Besides hemodynamics forces, there are also molecular mechanisms regulating intussusceptive angiogenesis. VEGF-A, the best described angiogenic growth factor, has been demonstrated necessary for shear stress dependent splitting of capillaries in skeletal muscle

and clearly induced intussusceptive angiogenesis in the CAM (63). Recent work from our group demonstrated that therapeutic overexpression of two different VEGF doses in skeletal muscle induces new vascular networks by causing initial circumferential enlargement of a pre-existing vessels and associated endothelial cell proliferation, which were accompanied with increased blood flow and shear stress in the absence of migrating endothelial tip cells. The circumferential enlargement was followed by intussusceptive remodeling (64).

A recent computational model created on the actual experimental findings defined that only a narrow range of VEGF concentrations is able to guarantee a correct balanced formation of tip and stalk cells, whereas high VEGF levels will create an oscillating-negative feedback loop, which will induce an all- stalk or an all-tip cell phenotype (65). Recent data from our group showed that the homogenous enlarged vessels induced by both two VEGF doses previously described (64) displayed synchronous Notch1 activation in long stretches of contiguous endothelial cells, which also simultaneously expressed Dll4. The activation is lost after the intussusceptive remodeling is completed. Using a computational model, it was defined that VEGF therapeutic overexpression lead to synchronous expression of Dll4 and Notch1 in contiguous endothelial cells by switching from lateral inhibition to lateral induction (66). VEGF doses and shape of its gradient thus determine whether Dll4/Notch1 axis is activated in an alternate or synchronous pattern, determining whether angiogenesis is induced by sprouting or by intussusception (66).

1.4 Vessels maturation

Once vessels are formed, vessels need to mature to return endothelium to quiescence and promote vessels stabilization. The blood flow in the new lumen remodels vessels connections and activates the shear-stress responsive transcription factor Kruppel-like factor 2. Upon perfusion, oxygen and nutrient delivery reduces VEGF-A expression and inactivates endothelial oxygen sensors, together shifting endothelial behavior toward a quiescent phenotype (43). A fundamental feature of vessel maturation is the recruitment of mural cells and deposition of ECM (67). Mural cells are commonly subdivided in vascular smooth muscle cells and pericytes, depending on their density, morphology, and specific markers expression (68). Vascular smooth muscle cells are associated with arteries and veins around which they form multiple concentric layers, and are separated from ECs by a matrix. Pericytes are associated with the microvessels, i.e. capillaries, post-capillaries venules, and terminal arterioles. These cells are either solitary associated with the endothelial tube or form a single, discontinuous layer around it. Mature pericytes are cell embedded within the vascular basement membrane (BM) (69), establishing a direct cell-to-cell contact with ECs. They probably contribute to the BM deposition, since in vitro studies demonstrated that pericytes-endothelial interaction regulates BM assembly (70). Pericytes extend primary cytoplasmic processes along the abluminal surface of the endothelial tube, which usually span several endothelial cells and occasionally bridge neighboring capillary branches. Thin secondary processes extend from the primary processes, which are normally perpendicular in their orientation relative to the primary branches,

thereby partially encircling the vessel. The contacts between endothelial cells and pericytes are usually of peg-socket type, in which pericyte cytoplasmic fingers (pegs) are inserted into endothelial invaginations (pockets)(71). Recruitment of pericytes to the growing endothelium is controlled by the platelet-derived-growth-factor-BB (PDGF-BB)/ PDGF receptor (PDGFR) β.

1.4.1 The role of PDGF/PDGFRβ in pericyte recruitment.

Human PDGF was originally identified as a disulfide-linked dimer of two different polypeptide chains, A and B. Two other polypeptide chain, PDGF-C and D have been discovered more recently (72). PDGFs act via two RTKs (PDGFR- α and PDGFR- β) with common domain structures, including five extracellular immunoglobulin (Ig) loops and a split intracellular tyrosine kinase (TK) domain. In vivo have been demonstrated interactions of the PDGF-AA and PDGF-CC via PDGFR-α, and PDGF-BB via PDGFR- β (72). The ligand receptor/pair PDGF-B/PDGFR-β has a well-characterized role in pericytes recruitment. PDGF-B is secreted has a homodimer from the endothelium of angiogenic sprouts and in the endothelium of growing arteries, at sites where pericytes are actively recruited and the vSMC population is expanding (40, 73). Perivascular mesenchimal cells representing vascular mural cells (vSMC and pericytes) progenitors express instead PDGFR-β (73). PDGF-BB promotes recruitment of pericytes to the growing vessel, the proliferation of adjacent mural cells progenitors (72). PDGFRs (α as β) dimerization allows receptor phosphorylation on tyrosine residues in the intracellular domain auto-phosphorylation activates the receptor kinases promoting then cell growth, differentiation, migration and survival. Ablation of PDGF-BB or PDGFR-β in

mice causes mural cell deficiency leading to widespread vascular leakage and perinatal lethality at E16-E19. The lack of pericytes leads to endothelial hyperplasia and an abnormally variable capillary diameter, revealing a negative control of pericytes on EC proliferation (73). Once secreted, PDGF-B is bound to heparan sulfate proteoglycans on the cell surface or in the ECM through its C-terminal retention motif. The extracellular retention of PDGF-BB is necessary to limit the range of action of PDGF-BB and ensure tight adhesion of pericytes to the vessel wall (74). Knockout of the PDGF-BB retention motif in mice results in defective investment of pericytes in the microvessels wall and delayed formation of the glomerular mesangium. Although mutants live into adulthood, they develop glomerulosclerosis, proteinuria and severe retinopathy (74). Global reduction of N-sulfated heparan sulfate proteoglycans by knockout of the N-deacetilase/ N-sulfotransferase-1 gene (ndst-1) attenuates signaling by several heparan sulfate binding growth factors, including PDGF-BB and causes pericytes detachment and delayed pericytes migration (75).

1.4.2 Endothelium-perycites cross-talk and its role in promoting vessel stabilization

Mural cell recruitment is an important step to protect new vessels against VEGF withdrawal and thus to promote stabilization. Newly induced vessels will be stable if will become VEGF-independent. Pericytes exert then their regulatory function on endothelial cells through both cell-to-cell contact and secreted signals that promote vessel stabilization. There are several molecules regulating the endothelium/pericytes cross-talk, of which two of the best characterized are angiopoietin-1 (Ang-1) and TGF-β. Ang-1 is produced by

mural cells; it activates its endothelial receptor Tie2 promoting pericytes adhesion and making vessels leakage-resistant by tightening the endothelial junctions (76). However, recent work demonstrates that Ang-1 is not essential for mural cell recruitment (77). TGF-β promotes vessels maturation by stimulating mural cell induction, differentiation, proliferation, migration and production of extracellular matrix. Loss of function of TGF-β receptor 2, endoglin, or activin receptor-like kinase 1 (Alk1) in mice causes vessel fragility in part due to impaired mural cell development (78). Thus, during these phases of vessel growth and maturation, changes in the local balance between pro- and anti-angiogenic factors, as in the blood flow may prevent vessel stabilization and lead to the elimination of the new vessels, a process known as vascular pruning.

2. Angiogenesis as a therapeutic target

Several studies highlighted the important role of VEGF-A as a major actor in embryonic and early postnatal development of the vascular system. However, angiogenesis can also take place in the adult life, as for example, during wound healing, skeletal growth, menstrual cycle and pregnancy, which all require tightly regulated VEGF upregulation (79). Disregulation of VEGF-A activity and subsequently pathological angiogenesis is a hallmark of several pathological disorders. A characteristic of pathological angiogenesis in that does not reach resolution upon the establishment of vascular perfusion. The pathological angiogenic cascade in fact is persistent and unresolved and becomes driven by the pathological condition. In several tumors as breast, kidney, brain, cervical and colon cancer, levels of VEGF- A have been correlated with poor prognosis (18). Uncontrolled neovascularization is also associated with proliferative retinopathy, and increased VEGF levels were described in the humor vitreous and aqueous of eyes of patients affected by such pathology (79). Furthermore, several studies have demonstrated that age-related macular degeneration (AMD) is caused by neovascularization and vessels leakiness (79). Since VEGF has a key role in developing pathological angiogenesis, several VEGF- blockers have been developed for clinical use in clinical cancer and eye disease (9).

On the other hand, insufficient vascular supply is also a cause of several diseases, as coronary artery disease (CAD), peripheral artery disease (PAD) and cerebrovascular disease. Atherosclerosis is the principal pathophysiological process causing ischemic disease. Treatment with anticoagulants and vasodilators can relieve symptoms in patients with intermittent ischemic symptoms but is not enough to cure such pathologies. Revascularization

procedures, as angioplasty, intravascular catheter mediated thrombolysis, or bypass surgery, are performed in patients with critical symptoms to improve blood circulation (80). However, many patients cannot be treated with conventional revascularization strategies because of a poor overall health status, and moreover a substantial portion of patients undergoing revascularization strategies does not benefit from the treatments or experience restenosis.

The lack of a functional vasculature is also one of the causes of failure of tissue engineering approaches aimed to replace complex tissues and organs with artificial ones created in vitro. In fact, unlike engineered skin, cartilage or bladder, cell viability, optimal function and/or integration of the construct used to generate tissues and organs for transplantation, cannot be sustained through diffusion alone (81). The formation and long-term survival of blood vessels within a material requires the integration of biochemical and biophysical cues (81). Also proper vascular maturation is required for the in vivo success of engineered tissue (82). In the last decades therapeutic angiogenesis has emerged as a promising alternative strategy for treating diseases suffering because of insufficient vascular supply. The aim of therapeutic angiogenesis in fact is to stimulate blood vessel growth by delivering pro-angiogenic factors, in an attempt to increase blood supply for improving ischemic tissue recovery, and promote engraftment and survival of engineered transplanted tissue.

2.1 The angiogenic therapy

Stimulation of blood vessel growth can be achieved by exogenous administration of pro-angiogenic factors. There are three main approaches that have been tested in pre-clinical settings: protein, gene and cell therapies (80). In protein therapies, recombinant proteins are used directly to induce the therapeutic effects. However, the short half-life of proteins in blood, coupled with the dose-limiting hypotension, have prevented the therapeutic efficacy of this approach into large randomized clinical trials (83). Gene therapy via non viral and viral vectors consists in carrying the gene construct encoding a therapeutic protein into the target cells (84). Initial studies were performed using plasmid vectors, which irrespective of the therapeutic gene involved, is simple and fraught of the major safety concerns. However, the efficiency of naked DNA uptake by muscle and cardiac cells is very poor and the maintenance of gene expression is short (around two weeks), thus not sufficient to exert an angiogenic stimulus able to generate a stable vasculature (85). The use of viral vectors could significantly improve the efficiency of gene delivery. Adenovirus have been so far the preferred vector, since can transduce at high efficiency both endothelial and vSMC. However, first generation adenoviral vectors are fraught with well-established, inflammatory and immunogenic potential, which raises safety concerns and limits temporal expression of the transgene (85). In contrast, a vector system that currently appears very suitable for gene therapy for cardiovascular disorders is based on AAV. These vectors presented several advantages, as the lack of relevant immunogenicity, the absence of an inflammatory response at the site of injection, the capacity to transduce cells at

high multiplicity of infection, and the tropism for postmitotic tissues (85). Cell-based therapies instead use progenitor or stem cells to promote tissue repair (86). Cells can also been engineered to express therapeutic proteins and thus induce vascular growth mainly in a paracrine manner (86). The therapeutic potential of bone-marrow derived endothelial progenitors, which still retain the ability to induce postnatal vasculogenesis (6), it has been tested in several clinical trial for PAD, showing some promising results, even if the effective cell population, isolation and processing methods must continue to be refined to gain a deeper understanding of the feature that define its potency (86).

2.2 The issues with VEGF-based therapies for therapeutic angiogenesis: total versus microenvironmental dose.

Since VEGF has a key role in inducing angiogenesis (9), it has been tested in several clinical trials, however until now with disappointing results (87). Retrospective analyses identified several issues that undetermined the efficacy of those trials, particularly the difficulty to deliver a sufficient VEGF dose into the target tissue at safe vector doses (88, 89). In fact, the delivery of recombinant VEGF-A_{165} in patients with coronary artery diseases, did not show any efficacy, despite brilliant results in the pre-clinical animal models, probably due to the short half-life of VEGF-A protein in vivo (85). Also several large randomized clinical-trial using plasmid delivery of VEGF-A for patients with peripheral and coronary artery disease did not have therapeutic efficacy. On the other hand, the growth of angioma was observed in a rat infarct model after injection of a

VEGF-encoding plasmid (90). The induction of vascular tumour (hemangiomas) because of uncontrolled VEGF delivery was also reported after delivery of retrovirally-transduced myoblast both in skeletal muscle (91) and myocardium (92). Further, injection of an adenoviral vector expressing VEGF induced a dose-dependent angiogenic response in skeletal muscle and in other tissues and caused angioma formation (93, 94). In addition, intramuscular VEGF gene transfer using recombinant Sendai virus in animals with critical limb ischemia resulted in increased leakiness of blood vessels, severe edema and accelerated limb amputation (95). Thus, VEGF has a narrow VEGF window, in which you pass from low but insufficient concentration rapidly to high but toxic concentrations. Previous work from our group has carefully investigated the dose-dependent effects of VEGF in both normal and ischemic skeletal muscle, identifying that the microenvironmental VEGF concentration, and not the total dose, determine the transition from normal to aberrant angiogenesis (11, 96), as VEGF remains tightly bound to the ECM (26). Taking advantage of an highly optimized myoblast-based gene delivery platform, which is based on selection and creation of clonal cell populations expressing each one homogenous VEGF levels, it has been identified that, as shown if figure 5, clonal cell population within the range from ≈5 ng/10^6 cells/day (low VEGF) to ≈70 ng/10^6 cells/day (VEGF threshold concentration) promoted the growth of normal capillaries, and just above the defined threshold concentration VEGF induced the growth of hemangiomas (Fig. 5). Conversely, the parental polyclonal cell population expressing heterogeneous VEGF levels led always the formation of hemangiomas, even if the total dose was almost diluted to 0 (Fig. 5).

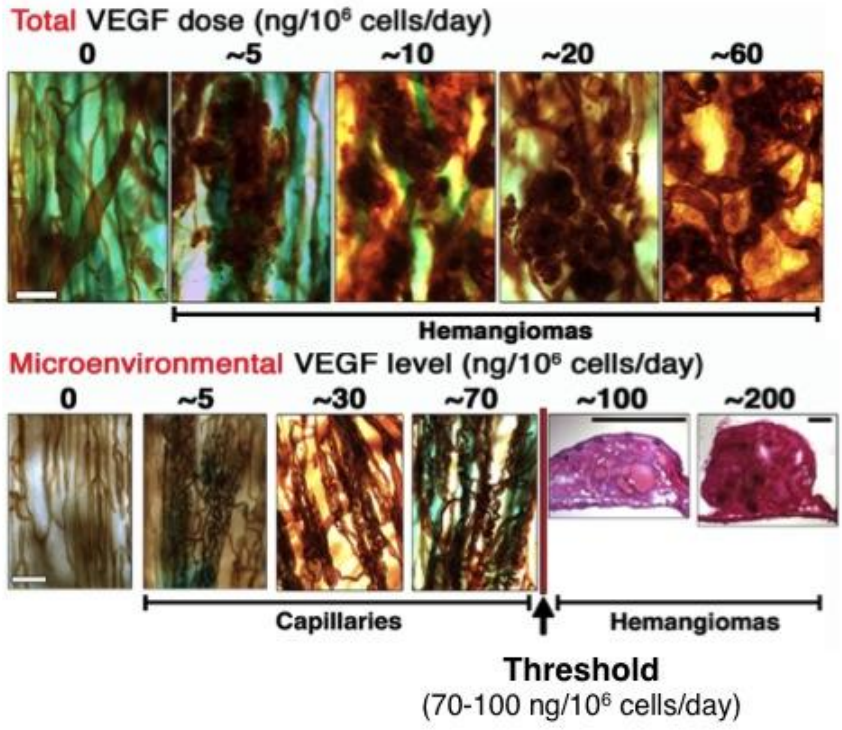

Figure 5 The microenviromental level of VEGF produced in muscle, and not the toal dose, determines a threshold between the growth of normal capillaries and hemangiomas. (adapted from (11)).

The control of the microenviromental VEGF concentration has been found crucial in determining the therapeutic efficacy of VEGF in hindlimb ischemia (96). In fact, only a clonal population expressing a defined medium VEGF concentration just below the threshold showed therapeutic efficacy, while neither the parental polyclonal population nor the clonal population expressing low VEGF levels had a therapeutic effect in hindlimb ischemia (96).

Therefore, direct *in vivo* gene therapy approaches, which generate heterogeneous expression levels around each transduced cells, lead to a waste of therapeutic window (97).

Although uncontrolled levels and long-term expression of VEGF are dangerous due to serious side effects, short-term expression is insufficient for the formation of a stable vasculature. In fact, in a transgenic mouse model the abrogation of

VEGF-expression before 4 weeks led to regression of the induced vasculature (10). VEGF-dependence of newly induced vessels has been demonstrated also by injecting inducible AAVs in skeletal muscle, confirming that sustained VEGF expression for at least 1 month is needed to induce the formation of stable vessels (12). Furthermore, VEGF withdrawal by a recombinant receptor-body (VEGF-trap) did not cause regression of new vessels only 4 weeks after implantation of myoblasts expressing VEGF (11).

2.3 Balanced coordinated co-expression of VEGF and PDGF-BB overcomes the limits of single VEGF-delivery for therapeutic angiogenesis

As discussed in the previous chapters, VEGF-A is the master regulator angiogenesis, but growth of normal and stable blood vessels requires the complex interactions of multiple cell types and growth factors that are coordinated in time and space (68). Targeting vascular maturation is an attractive strategy to overtake VEGF-A limitations that become evident in the first generation of clinical trials. The complexity and heterogeneity of factors involved in vascular maturation open different strategies to target this process. A promising candidate is represented by the PDGF-BB, that has a key role in recruiting pericytes and thus in promoting vessel normalization. This was confirmed by recent work in our group, which taking advantage of the myoblast-mediated gene delivery platform, demonstrated that myoblasts transduced with a retroviral vector carrying a bicistronic construct co-expressing VEGF-A_{164} and

PDGF-BB on a fixed ratio 1:3 promoted consistent normalization of aberrant angiogenesis induced from heterogeneous VEGF-A_{164} levels (Fig. 6) (97). Further, when tested in hindlimb ischemia, cells co-expressing VEGF-A_{164} and PDGF-BB stimulated the growth of stable collateral arteries without causing the growth of any hemangioma, whereas cells expressing only VEGF-A_{164} moderately increased blood vessel perfusion without stimulating growth of collateral arteries (97).

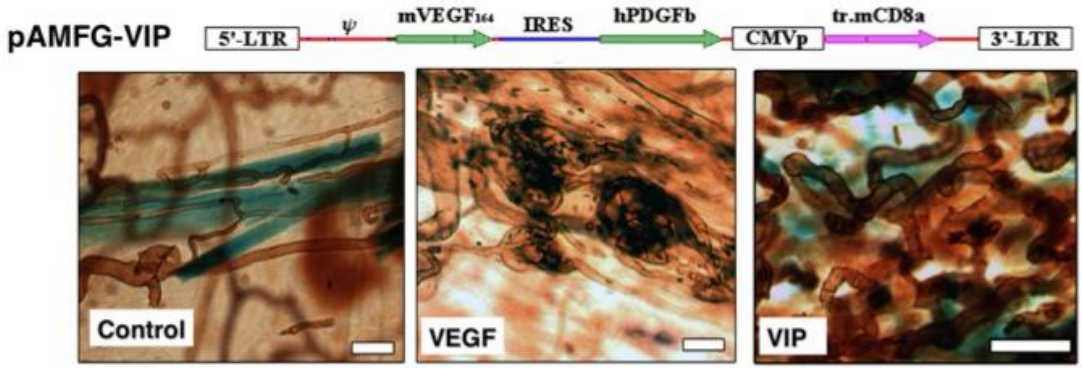

Figure 6 Coordinated co-expression of VEGF and PDGF-BB (VIP) in a fixed molar ratio 1:3 by a single bicistronic construct induced only normal and robust angiogenesis, despite of high and heterogeneous VEGF level (adapted from (97)).

Besides, unpublished data from our group indicate that PDGF-BB co-expression accelerates the stabilization of vessels induced by heterogeneous VEGF-A_{164} levels, so that 50% of new vessels were already VEGF-independent after 2 weeks, whereas none was stable when VEGF-A_{164} was expressed alone (98).

3. Recombinant growth factors delivery for therapeutic angiogenesis

Cell-based delivery of angiogenic growth factors into skeletal muscle has allowed elucidating fundamental requirements that need to be fulfilled to induce therapeutic angiogenesis. However, while very useful as a controlled model system, this approach is not suitable for a clinical application. In fact, the isolation, transduction and clonal expansion of autologous cells is too expensive and time-consuming, while the use of retroviral vectors, which integrate in the host genome and can cause malignant transformation by insertional mutagenesis, raises safety concerns (99). The use of recombinant proteins presents several desirable features for clinical translation of these biological concepts compared to gene therapy approaches, such as the lack of genetic modification, the ease of achieving a homogenous dose distribution and the limited duration of treatment. However, soluble recombinant proteins are degraded rapidly and deactivated by enzymes or other chemical and physical degrading reactions occurring at body temperature and hence have short half-life (100, 101). Growth factors are physiologically present either as matrix-bound proteins attached to the ECM or as soluble molecules secreted by cells or cleaved from the matrix by certain enzymes or proteases. In this sense, the ECM serves as a reservoir of morphogenetic signals; how this reservoir displays or releases these signals in response to cellular influences determine its role in tissues homeostasis, development, and in response to injury. Also endothelial cell function and vascular growth are critically dependent on the interactions with the surrounding ECM. The ECM controls in fact endothelial cell activities by diverse mechanisms ranging from cell anchorage, integrin-mediated activation and signaling to binding, release and activation of soluble growth factors (102). Several angiogenic growth factors as FGF, VEGF and

PDGF-BB are tightly bound to the heparin sulfate proteoglycans of the extracellular matrix. The binding of growth factors such as VEGF and PDGF-BB is crucial to establish concentration gradients and limits their action in vivo, ensuring the growth of normal blood vessels (103). Thus, polymeric materials mimicking the natural ECM are an interesting approach to deliver growth factors aiming to reproduce the physiological cell-demanded growth factor release, in order to create the necessary spatial and temporal gradients and regulate the extent and pattern of tissue formation (100). This approach would protect growth factors from rapid clearance, and allow controlled, sustained and localized delivery (100). Delivery vehicles may be fabricated from a variety of synthetic and natural polymers. While natural tissue-derived matrices have an innate capacity to interact with cells and go through cell-mediated degradation, synthetic matrices in their naive form lack cellular recognition but have well-controlled and reproducible chemical properties (104). Therefore, natural ECM-derived biomaterials have the key advantages of not requiring modifications to allow cell-adhesion and infiltration. Other key advantages are the relative easy production at low cost. Examples are collagen and fibrin that are clinically well-established and FDA-approved matrices for wound healing to treat burns and chronic wounds, and as tissue sealants, respectively (104). Fibrin matrices, as will be reviewed in detail in the next paragraph, allow to couple modified growth factors enzymatically to the fibrin monomer during their cross-linking reaction and subsequent release from cells that are locally remodeling the matrix. This property allow controlled and cell-demanded growth factor release necessary to induce therapeutic angiogenesis, providing to fibrin compared to collagen a key advantage as a reservoir for pro-angiogenic growth factors (104).

3.1 Fibrin as a growth factor delivery system

Fibrin is a biopolymer found in tissue repair but not in the otherwise healthy organism. Fibrin formation in fact occurs naturally during the blood coagulation cascade, and serves as a reservoir for proliferating cells and growth factors, degrading in synergy with tissue formation. There are three main components making a fibrin gel, fibrinogen, thrombin and factor XIII. When the components are mixed together in a calcium-enriched environment, the thrombin enzymatically cleaves fibrinogen to form fibrin and the factor XIII to factor XIIIa. Fibrin monomer then self-assembled to fibrin dimer, which are cross-linked by factor XIIIa through transglutaminase reaction to form the final fibrin gel (105).

In contrast to the more permanent ECM which are usually formed by the sequential assembly of numerous components in a spatially ordered array that is difficult or impossible to reproduce in vitro, fibrin gels formed from purified plasma proteins acquires structures and mechanical properties that are very similar to those of the blood clot (106).

There are several advantages that make fibrin a suitable material for regenerative medicine application, as the abundance of fibrinogen and its relative easy purification, the possible fine control of gelation times and mechanical properties of fibrin gels by adjusting the concentration of its components (107).

Initial attempts to use fibrin gel as a reservoir of growth factors have been done by direct loading of different proteins into the gel. However, the simple mixtures of VEGF or FGF with fibrin gels showed release kinetics indicative of an

uncontrolled burst, not useful for the purpose to use them for therapeutic angiogenesis (108). Thus, methods for incorporation of growth factors would allow taking advantage of fibrin gels as materials allowing cell-demanded and controlled growth factor release applicable in tissue regeneration and vascular growth. In this direction, Schense JC et al previously developed a mechanism by which any number of biomolecules can be grafted within a fibrin scaffold during fibrinogen cross-linking (109). Specifically, they designed a bi-domain substrate with a factor XIIIa substrate derived from α_2-plasmin inhibitor (α_2-PI_{1-8}) at the N-terminal and at the C-terminal the peptide or the growth factor of interest (Fig. 7). This domain allow covalent binding of the growth factor mediated from factor XIIIa cross-linking reaction of the fibrin monomer, and can be cleaved from cell-released proteases while they are locally remodeling the matrix (110). The first molecule modified using this approach was the heparin, which then can bind several growth factors by natural affinity. Using this approach, it has been demonstrated that controlled release of several nerve-growth promoting factors could be accomplished from the heparin-laden fibrin matrix promoting efficient neurite growth extension compared to control (111, 112).

Furthermore, several recombinant fibronectin (FN) fragments have been synthetized as bi-domain containing the α_2-PI_{1-8} substrate site at the N-terminal (113, 114). This recombinant fibronectin fragments display affinity for several integrins and growth factors as VEGF, PDGF-BB and BMP-2. The engineered FN fragment co-delivered together with VEGF and PDGF-BB *in vivo* significantly enhances wound regeneration, and further promoted bone healing in a critical size defect when co-delivered with PDGF-BB and BMP-2 (115).

In addition to heparin and FN fragments, several growth factors also can be engineered to contain the α_2-plasmin inhibitor (α_2-PI_{1-8}) at the N-terminal, for direct incorporation within the fibrin matrix, with a significant improvement of their biological activities (Fig. 7). The α_2-PI_{1-8}-VEGF-A_{121} in the CAM assay induced robust angiogenesis with a well-organized pattern of capillaries, avoiding the formation of massive edema, whereas the native form of the VEGF-A_{121} induced the growth of chaotic and abnormally enlarged vessels (116). This protein contained the α_2-PI_{1-8} transglutaminase substrate domain at the N-terminal for the covalent binding by factor XIIIa, a central plasmin substrate (pl) domain that provides a further cleavage site for local cell-mediated release, and a C-terminal human BMP-2 domain that provides the osteogenic properties (Fig. 7). The α_2-PI_{1-8} –pl-BMP-2 protein loaded in fibrin gel significantly improved bone healing compared to WT BMP-2 (117). Recently, it has been generated as a recombinant protein with at the N-terminal the α_2-PI_{1-8} peptide also the insulin growth factor- 1 (IGF-1) (118). This modified fusion protein loaded into fibrin gel applied to bladder lesions significantly enhances smooth muscle cells regenerative response compared to the wild type protein (118).

However, the brief persistence of fibrin hydrogel, with complete degradation within a week (116), has been a major obstacle to the exploitation of this system for therapeutic angiogenesis.

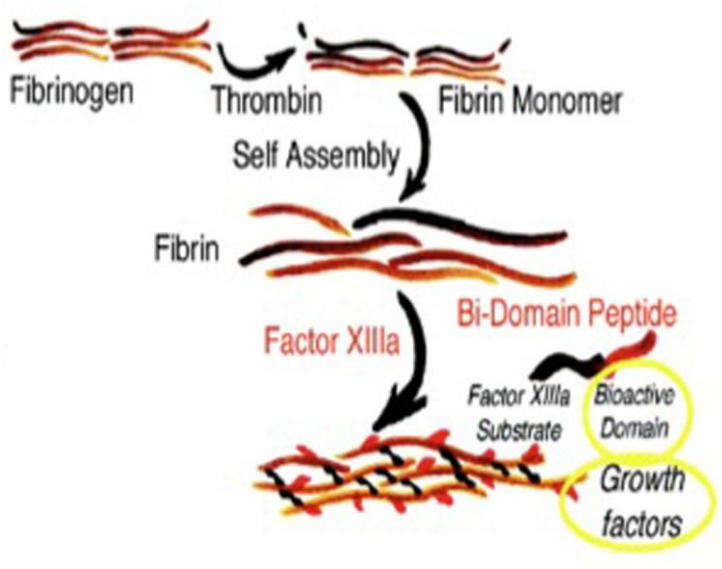

Figure 7 Incorporation of bi-domain peptide or fusion protein into fibrin gel. Heparin bi-domain peptide or engineered fusion proteins have been synthetized to contain the sequence α_2-PI_{1-8}, which is the transglutaminase substrate, at the N-terminal, to allow covalent binding and subsequent controlled release mediated from cell-associated enzymatic activities.

4. Aims of the thesis

Therapeutic angiogenesis is a promising strategy to treat pathologies characterized by insufficient blood supply to tissues, such as coronary and peripheral artery diseases, but also to promote the engraftment and survival of tissue-engineered constructs after transplantation into the host. Since the identification of the master regulator of angiogenesis, VEGF, many clinical trials have been performed but did not demonstrate clinical efficacy (87). Taking advantage of an optimized myoblast-based gene delivery system, our group previously investigated the key requirements to induce therapeutic angiogenesis either by VEGF-gene delivery alone or by balanced co-expression of VEGF and PDGF-BB from a single bicistronic construct (11, 97). However, while very useful as a controlled model system, this approach is not suitable for a clinical application. In fact, the isolation, transduction and clonal expansion of autologous cells is too expensive and time-consuming, while the use of retroviral vectors, which integrate in the host genome and can cause malignant transformation by insertional mutagenesis, raises safety concerns (99).

The delivery of recombinant growth factors presents several desirable features for clinical translation of these biological concepts compared to gene-therapy, such as a defined duration of treatment, homogenous dose distribution and the absence of genetic modifications. However, the very short half-life of recombinant growth factors after direct injection *in vivo* has limited their clinical usefulness. The controlled release of factors from biopolymers is an attractive approach to protect them from rapid clearance while ensuring homogenous and sustained release (119).

Pro-angiogenic factors such as VEGF and PDGF-BB have heparin-binding domains that localize them in the extracellular matrix after secretion and their restricted spatial organization within the microenvironment is crucial to induce physiological angiogenesis (103). Therefore, the group of J. Hubbell (EPFL, Lausanne, Switzerland) previously developed a protein engineering approach that enzymatically links recombinant growth factors to fibrin, a biopolymer physiologically degraded by cell-associated proteases (105). Engineered factors are produced as fusion proteins with the factor XIIIa substrate sequence α_2-P_{1-8} (NQEQVSPL) at the N-terminal, to allow covalent binding by factor XIIIa during the fibrin cross-linking reaction and subsequent release by enzymatic cleavage (99). However, the short persistence of fibrin hydrogels in vivo (116), which did not allow sufficiently prolonged factor release to achieve stabilization of newly induced angiogenesis, has been a major obstacle towards the application of this approach for therapeutic angiogenesis (119).

Therefore, the focus of this thesis is to determine the requirements to induce safe, stable and controlled angiogenesis by controlled delivery of recombinant angiogenic growth factors from fibrin gels. To this end, we investigated two specific aims:

1) In aim 1, we developed an optimized fibrin platform to ensure controlled and dose-dependent delivery of α_2-PI_{1-8}-$VEGF_{164}$ over at least 4 weeks, capable of inducing normal, stable and functional angiogenesis.

2) In aim 2, we tested the hypothesis that co-delivery of α_2-P_{1-8}-$VEGF_{164}$ α_2-P_{1-8}-PDGF-BB from fibrin gels could both normalize aberrant angiogenesis induced by high VEGF doses and accelerate vascular stabilization after short-term VEGF delivery.

References

1. Carmeliet, P. 2004. Manipulating angiogenesis in medicine. *J Intern Med* 255:538-561.
2. Ribatti, D., Nico, B., and Crivellato, E. 2009. Morphological and molecular aspects of physiological vascular morphogenesis. *Angiogenesis* 12:101-111.
3. Choi, K., Kennedy, M., Kazarov, A., Papadimitriou, J.C., and Keller, G. 1998. A common precursor for hematopoietic and endothelial cells. *Development* 125:725-732.
4. Swift, M.R., and Weinstein, B.M. 2009. Arterial-venous specification during development. *Circ Res* 104:576-588.
5. Risau, W. 1997. Mechanisms of angiogenesis. *Nature* 386:671-674.
6. Ribatti, D., Vacca, A., Nico, B., Roncali, L., and Dammacco, F. 2001. Postnatal vasculogenesis. *Mech Dev* 100:157-163.
7. Heil, M., Eitenmuller, I., Schmitz-Rixen, T., and Schaper, W. 2006. Arteriogenesis versus angiogenesis: similarities and differences. *J Cell Mol Med* 10:45-55.
8. Herbert, S.P., and Stainier, D.Y. 2011. Molecular control of endothelial cell behaviour during blood vessel morphogenesis. *Nat Rev Mol Cell Biol* 12:551-564.
9. Carmeliet, P., and Jain, R.K. 2011. Molecular mechanisms and clinical applications of angiogenesis. *Nature* 473:298-307.
10. Dor, Y., Djonov, V., Abramovitch, R., Itin, A., Fishman, G.I., Carmeliet, P., Goelman, G., and Keshet, E. 2002. Conditional switching of VEGF provides new insights into adult neovascularization and pro-angiogenic therapy. *EMBO J* 21:1939-1947.
11. Ozawa, C.R., Banfi, A., Glazer, N.L., Thurston, G., Springer, M.L., Kraft, P.E., McDonald, D.M., and Blau, H.M. 2004. Microenvironmental VEGF concentration, not total dose, determines a threshold between normal and aberrant angiogenesis. *J Clin Invest* 113:516-527.
12. Tafuro, S., Ayuso, E., Zacchigna, S., Zentilin, L., Moimas, S., Dore, F., and Giacca, M. 2009. Inducible adeno-associated virus vectors promote functional angiogenesis in adult organisms via regulated vascular endothelial growth factor expression. *Cardiovasc Res* 83:663-671.
13. Yancopoulos, G.D., Davis, S., Gale, N.W., Rudge, J.S., Wiegand, S.J., and Holash, J. 2000. Vascular-specific growth factors and blood vessel formation. *Nature* 407:242-248.
14. Senger, D.R., Galli, S.J., Dvorak, A.M., Perruzzi, C.A., Harvey, V.S., and Dvorak, H.F. 1983. Tumor cells secrete a vascular permeability factor that promotes accumulation of ascites fluid. *Science* 219:983-985.
15. Ferrara, N., and Henzel, W.J. 1989. Pituitary follicular cells secrete a novel heparin-binding growth factor specific for vascular endothelial cells. *Biochem Biophys Res Commun* 161:851-858.
16. Leung, D.W., Cachianes, G., Kuang, W.J., Goeddel, D.V., and Ferrara, N. 1989. Vascular endothelial growth factor is a secreted angiogenic mitogen. *Science* 246:1306-1309.

17. Keck, P.J., Hauser, S.D., Krivi, G., Sanzo, K., Warren, T., Feder, J., and Connolly, D.T. 1989. Vascular permeability factor, an endothelial cell mitogen related to PDGF. *Science* 246:1309-1312.
18. Lohela, M., Bry, M., Tammela, T., and Alitalo, K. 2009. VEGFs and receptors involved in angiogenesis versus lymphangiogenesis. *Curr Opin Cell Biol* 21:154-165.
19. Carmeliet, P. 2005. Angiogenesis in life, disease and medicine. *Nature* 438:932-936.
20. Carmeliet, P., Ferreira, V., Breier, G., Pollefeyt, S., Kieckens, L., Gertsenstein, M., Fahrig, M., Vandenhoeck, A., Harpal, K., Eberhardt, C., et al. 1996. Abnormal blood vessel development and lethality in embryos lacking a single VEGF allele. *Nature* 380:435-439.
21. Ferrara, N., Carver-Moore, K., Chen, H., Dowd, M., Lu, L., O'Shea, K.S., Powell-Braxton, L., Hillan, K.J., and Moore, M.W. 1996. Heterozygous embryonic lethality induced by targeted inactivation of the VEGF gene. *Nature* 380:439-442.
22. Miquerol, L., Langille, B.L., and Nagy, A. 2000. Embryonic development is disrupted by modest increases in vascular endothelial growth factor gene expression. *Development* 127:3941-3946.
23. Nagy, J.A., Dvorak, A.M., and Dvorak, H.F. 2007. VEGF-A and the induction of pathological angiogenesis. *Annu Rev Pathol* 2:251-275.
24. Ferrara, N. 2004. Vascular endothelial growth factor: basic science and clinical progress. *Endocr Rev* 25:581-611.
25. Robinson, C.J., and Stringer, S.E. 2001. The splice variants of vascular endothelial growth factor (VEGF) and their receptors. *J Cell Sci* 114:853-865.
26. Park, J.E., Keller, G.A., and Ferrara, N. 1993. The vascular endothelial growth factor (VEGF) isoforms: differential deposition into the subepithelial extracellular matrix and bioactivity of extracellular matrix-bound VEGF. *Mol Biol Cell* 4:1317-1326.
27. Ruhrberg, C., Gerhardt, H., Golding, M., Watson, R., Ioannidou, S., Fujisawa, H., Betsholtz, C., and Shima, D.T. 2002. Spatially restricted patterning cues provided by heparin-binding VEGF-A control blood vessel branching morphogenesis. *Genes Dev* 16:2684-2698.
28. Carmeliet, P., Ng, Y.S., Nuyens, D., Theilmeier, G., Brusselmans, K., Cornelissen, I., Ehler, E., Kakkar, V.V., Stalmans, I., Mattot, V., et al. 1999. Impaired myocardial angiogenesis and ischemic cardiomyopathy in mice lacking the vascular endothelial growth factor isoforms VEGF164 and VEGF188. *Nat Med* 5:495-502.
29. Koch, S., and Claesson-Welsh, L. 2012. Signal transduction by vascular endothelial growth factor receptors. *Cold Spring Harb Perspect Med* 2:a006502.
30. Kendall, R.L., and Thomas, K.A. 1993. Inhibition of vascular endothelial cell growth factor activity by an endogenously encoded soluble receptor. *Proc Natl Acad Sci U S A* 90:10705-10709.
31. Fong, G.H., Rossant, J., Gertsenstein, M., and Breitman, M.L. 1995. Role of the Flt-1 receptor tyrosine kinase in regulating the assembly of vascular endothelium. *Nature* 376:66-70.

32. Hiratsuka, S., Minowa, O., Kuno, J., Noda, T., and Shibuya, M. 1998. Flt-1 lacking the tyrosine kinase domain is sufficient for normal development and angiogenesis in mice. *Proc Natl Acad Sci U S A* 95:9349-9354.
33. Shalaby, F., Rossant, J., Yamaguchi, T.P., Gertsenstein, M., Wu, X.F., Breitman, M.L., and Schuh, A.C. 1995. Failure of blood-island formation and vasculogenesis in Flk-1-deficient mice. *Nature* 376:62-66.
34. Soker, S., Takashima, S., Miao, H.Q., Neufeld, G., and Klagsbrun, M. 1998. Neuropilin-1 is expressed by endothelial and tumor cells as an isoform-specific receptor for vascular endothelial growth factor. *Cell* 92:735-745.
35. Soker, S., Miao, H.Q., Nomi, M., Takashima, S., and Klagsbrun, M. 2002. VEGF165 mediates formation of complexes containing VEGFR-2 and neuropilin-1 that enhance VEGF165-receptor binding. *J Cell Biochem* 85:357-368.
36. Kawamura, H., Li, X., Goishi, K., van Meeteren, L.A., Jakobsson, L., Cebe-Suarez, S., Shimizu, A., Edholm, D., Ballmer-Hofer, K., Kjellen, L., et al. 2008. Neuropilin-1 in regulation of VEGF-induced activation of p38MAPK and endothelial cell organization. *Blood* 112:3638-3649.
37. Zhang, F., Tang, Z., Hou, X., Lennartsson, J., Li, Y., Koch, A.W., Scotney, P., Lee, C., Arjunan, P., Dong, L., et al. 2009. VEGF-B is dispensable for blood vessel growth but critical for their survival, and VEGF-B targeting inhibits pathological angiogenesis. *Proc Natl Acad Sci U S A* 106:6152-6157.
38. Li, X., Tjwa, M., Van Hove, I., Enholm, B., Neven, E., Paavonen, K., Jeltsch, M., Juan, T.D., Sievers, R.E., Chorianopoulos, E., et al. 2008. Reevaluation of the role of VEGF-B suggests a restricted role in the revascularization of the ischemic myocardium. *Arterioscler Thromb Vasc Biol* 28:1614-1620.
39. Zentilin, L., Puligadda, U., Lionetti, V., Zacchigna, S., Collesi, C., Pattarini, L., Ruozi, G., Camporesi, S., Sinagra, G., Pepe, M., et al. 2010. Cardiomyocyte VEGFR-1 activation by VEGF-B induces compensatory hypertrophy and preserves cardiac function after myocardial infarction. *FASEB J* 24:1467-1478.
40. Gerhardt, H., Golding, M., Fruttiger, M., Ruhrberg, C., Lundkvist, A., Abramsson, A., Jeltsch, M., Mitchell, C., Alitalo, K., Shima, D., et al. 2003. VEGF guides angiogenic sprouting utilizing endothelial tip cell filopodia. *J Cell Biol* 161:1163-1177.
41. De Smet, F., Segura, I., De Bock, K., Hohensinner, P.J., and Carmeliet, P. 2009. Mechanisms of vessel branching: filopodia on endothelial tip cells lead the way. *Arterioscler Thromb Vasc Biol* 29:639-649.
42. Adams, R.H., and Eichmann, A. 2010. Axon guidance molecules in vascular patterning. *Cold Spring Harb Perspect Biol* 2:a001875.
43. Potente, M., Gerhardt, H., and Carmeliet, P. 2011. Basic and therapeutic aspects of angiogenesis. *Cell* 146:873-887.
44. Phng, L.K., and Gerhardt, H. 2009. Angiogenesis: a team effort coordinated by notch. *Dev Cell* 16:196-208.
45. Roca, C., and Adams, R.H. 2007. Regulation of vascular morphogenesis by Notch signaling. *Genes Dev* 21:2511-2524.
46. Hellstrom, M., Phng, L.K., Hofmann, J.J., Wallgard, E., Coultas, L., Lindblom, P., Alva, J., Nilsson, A.K., Karlsson, L., Gaiano, N., et al. 2007. Dll4 signalling through Notch1 regulates formation of tip cells during angiogenesis. *Nature* 445:776-780.

47. Suchting, S., Freitas, C., le Noble, F., Benedito, R., Breant, C., Duarte, A., and Eichmann, A. 2007. The Notch ligand Delta-like 4 negatively regulates endothelial tip cell formation and vessel branching. *Proc Natl Acad Sci U S A* 104:3225-3230.
48. Leslie, J.D., Ariza-McNaughton, L., Bermange, A.L., McAdow, R., Johnson, S.L., and Lewis, J. 2007. Endothelial signalling by the Notch ligand Delta-like 4 restricts angiogenesis. *Development* 134:839-844.
49. Siekmann, A.F., and Lawson, N.D. 2007. Notch signalling limits angiogenic cell behaviour in developing zebrafish arteries. *Nature* 445:781-784.
50. Jakobsson, L., Franco, C.A., Bentley, K., Collins, R.T., Ponsioen, B., Aspalter, I.M., Rosewell, I., Busse, M., Thurston, G., Medvinsky, A., et al. 2010. Endothelial cells dynamically compete for the tip cell position during angiogenic sprouting. *Nat Cell Biol* 12:943-953.
51. Kappas, N.C., Zeng, G., Chappell, J.C., Kearney, J.B., Hazarika, S., Kallianos, K.G., Patterson, C., Annex, B.H., and Bautch, V.L. 2008. The VEGF receptor Flt-1 spatially modulates Flk-1 signaling and blood vessel branching. *J Cell Biol* 181:847-858.
52. Tammela, T., Zarkada, G., Nurmi, H., Jakobsson, L., Heinolainen, K., Tvorogov, D., Zheng, W., Franco, C.A., Murtomaki, A., Aranda, E., et al. 2011. VEGFR-3 controls tip to stalk conversion at vessel fusion sites by reinforcing Notch signalling. *Nat Cell Biol* 13:1202-1213.
53. Benedito, R., Roca, C., Sorensen, I., Adams, S., Gossler, A., Fruttiger, M., and Adams, R.H. 2009. The notch ligands Dll4 and Jagged1 have opposing effects on angiogenesis. *Cell* 137:1124-1135.
54. Styp-Rekowska, B., Hlushchuk, R., Pries, A.R., and Djonov, V. 2011. Intussusceptive angiogenesis: pillars against the blood flow. *Acta physiologica* 202:213-223.
55. Caduff, J.H., Fischer, L.C., and Burri, P.H. 1986. Scanning electron microscope study of the developing microvasculature in the postnatal rat lung. *The Anatomical record* 216:154-164.
56. Burri, P.H., and Djonov, V. 2002. Intussusceptive angiogenesis--the alternative to capillary sprouting. *Molecular aspects of medicine* 23:S1-27.
57. Djonov, V., Baum, O., and Burri, P.H. 2003. Vascular remodeling by intussusceptive angiogenesis. *Cell and tissue research* 314:107-117.
58. Djonov, V.G., Kurz, H., and Burri, P.H. 2002. Optimality in the developing vascular system: branching remodeling by means of intussusception as an efficient adaptation mechanism. *Developmental dynamics : an official publication of the American Association of Anatomists* 224:391-402.
59. Egginton, S., Zhou, A.L., Brown, M.D., and Hudlicka, O. 2001. Unorthodox angiogenesis in skeletal muscle. *Cardiovasc Res* 49:634-646.
60. De Spiegelaere, W., Casteleyn, C., Van den Broeck, W., Plendl, J., Bahramsoltani, M., Simoens, P., Djonov, V., and Cornillie, P. 2012. Intussusceptive angiogenesis: a biologically relevant form of angiogenesis. *Journal of vascular research* 49:390-404.
61. Makanya, A.N., Hlushchuk, R., and Djonov, V.G. 2009. Intussusceptive angiogenesis and its role in vascular morphogenesis, patterning, and remodeling. *Angiogenesis* 12:113-123.

62. Hlushchuk, R., Riesterer, O., Baum, O., Wood, J., Gruber, G., Pruschy, M., and Djonov, V. 2008. Tumor recovery by angiogenic switch from sprouting to intussusceptive angiogenesis after treatment with PTK787/ZK222584 or ionizing radiation. *Am J Pathol* 173:1173-1185.
63. Gianni-Barrera, R., Trani, M., Reginato, S., and Banfi, A. 2011. To sprout or to split? VEGF, Notch and vascular morphogenesis. *Biochemical Society transactions* 39:1644-1648.
64. Gianni-Barrera, R., Trani, M., Fontanellaz, C., Heberer, M., Djonov, V., Hlushchuk, R., and Banfi, A. 2013. VEGF over-expression in skeletal muscle induces angiogenesis by intussusception rather than sprouting. *Angiogenesis* 16:123-136.
65. Bentley, K., Gerhardt, H., and Bates, P.A. 2008. Agent-based simulation of notch-mediated tip cell selection in angiogenic sprout initialisation. *Journal of theoretical biology* 250:25-36.
66. Gianni-Barrera, R. Manuscript in preparation.
67. Jain, R.K. 2003. Molecular regulation of vessel maturation. *Nat Med* 9:685-693.
68. Gaengel, K., Genove, G., Armulik, A., and Betsholtz, C. 2009. Endothelial-mural cell signaling in vascular development and angiogenesis. *Arterioscler Thromb Vasc Biol* 29:630-638.
69. Sims, D.E. 1986. The pericyte--a review. *Tissue & cell* 18:153-174.
70. Stratman, A.N., Malotte, K.M., Mahan, R.D., Davis, M.J., and Davis, G.E. 2009. Pericyte recruitment during vasculogenic tube assembly stimulates endothelial basement membrane matrix formation. *Blood* 114:5091-5101.
71. Armulik, A., Genove, G., and Betsholtz, C. 2011. Pericytes: developmental, physiological, and pathological perspectives, problems, and promises. *Dev Cell* 21:193-215.
72. Andrae, J., Gallini, R., and Betsholtz, C. 2008. Role of platelet-derived growth factors in physiology and medicine. *Genes Dev* 22:1276-1312.
73. Hellstrom, M., Kalen, M., Lindahl, P., Abramsson, A., and Betsholtz, C. 1999. Role of PDGF-B and PDGFR-beta in recruitment of vascular smooth muscle cells and pericytes during embryonic blood vessel formation in the mouse. *Development* 126:3047-3055.
74. Betsholtz, C., Lindblom, P., Bjarnegard, M., Enge, M., Gerhardt, H., and Lindahl, P. 2004. Role of platelet-derived growth factor in mesangium development and vasculopathies: lessons from platelet-derived growth factor and platelet-derived growth factor receptor mutations in mice. *Current opinion in nephrology and hypertension* 13:45-52.
75. Abramsson, A., Kurup, S., Busse, M., Yamada, S., Lindblom, P., Schallmeiner, E., Stenzel, D., Sauvaget, D., Ledin, J., Ringvall, M., et al. 2007. Defective N-sulfation of heparan sulfate proteoglycans limits PDGF-BB binding and pericyte recruitment in vascular development. *Genes Dev* 21:316-331.
76. Augustin, H.G., Koh, G.Y., Thurston, G., and Alitalo, K. 2009. Control of vascular morphogenesis and homeostasis through the angiopoietin-Tie system. *Nat Rev Mol Cell Biol* 10:165-177.
77. Jeansson, M., Gawlik, A., Anderson, G., Li, C., Kerjaschki, D., Henkelman, M., and Quaggin, S.E. 2011. Angiopoietin-1 is essential in mouse vasculature during development and in response to injury. *J Clin Invest* 121:2278-2289.

78. Pardali, E., Goumans, M.J., and ten Dijke, P. 2010. Signaling by members of the TGF-beta family in vascular morphogenesis and disease. *Trends in cell biology* 20:556-567.
79. Chung, A.S., and Ferrara, N. 2011. Developmental and pathological angiogenesis. *Annu Rev Cell Dev Biol* 27:563-584.
80. Dragneva, G., Korpisalo, P., and Yla-Herttuala, S. 2013. Promoting blood vessel growth in ischemic diseases: challenges in translating preclinical potential into clinical success. *Dis Model Mech* 6:312-322.
81. Bae, H., Puranik, A.S., Gauvin, R., Edalat, F., Carrillo-Conde, B., Peppas, N.A., and Khademhosseini, A. 2012. Building vascular networks. *Sci Transl Med* 4:160ps123.
82. Stenman, J.M., Rajagopal, J., Carroll, T.J., Ishibashi, M., McMahon, J., and McMahon, A.P. 2008. Canonical Wnt signaling regulates organ-specific assembly and differentiation of CNS vasculature. *Science* 322:1247-1250.
83. Zachary, I., and Morgan, R.D. 2011. Therapeutic angiogenesis for cardiovascular disease: biological context, challenges, prospects. *Heart* 97:181-189.
84. Korpisalo, P., and Yla-Herttuala, S. 2010. Stimulation of functional vessel growth by gene therapy. *Integr Biol (Camb)* 2:102-112.
85. Giacca, M., and Zacchigna, S. 2012. VEGF gene therapy: therapeutic angiogenesis in the clinic and beyond. *Gene Ther* 19:622-629.
86. Raval, Z., and Losordo, D.W. 2013. Cell therapy of peripheral arterial disease: from experimental findings to clinical trials. *Circ Res* 112:1288-1302.
87. Gupta, R., Tongers, J., and Losordo, D.W. 2009. Human studies of angiogenic gene therapy. *Circ Res* 105:724-736.
88. Karvinen, H., and Yla-Herttuala, S. 2010. New aspects in vascular gene therapy. *Curr Opin Pharmacol* 10:208-211.
89. Yla-Herttuala, S., Markkanen, J.E., and Rissanen, T.T. 2004. Gene therapy for ischemic cardiovascular diseases: some lessons learned from the first clinical trials. *Trends Cardiovasc Med* 14:295-300.
90. Schwarz, E.R., Speakman, M.T., Patterson, M., Hale, S.S., Isner, J.M., Kedes, L.H., and Kloner, R.A. 2000. Evaluation of the effects of intramyocardial injection of DNA expressing vascular endothelial growth factor (VEGF) in a myocardial infarction model in the rat--angiogenesis and angioma formation. *J Am Coll Cardiol* 35:1323-1330.
91. Springer, M.L., Chen, A.S., Kraft, P.E., Bednarski, M., and Blau, H.M. 1998. VEGF gene delivery to muscle: potential role for vasculogenesis in adults. *Mol Cell* 2:549-558.
92. Lee, R.J., Springer, M.L., Blanco-Bose, W.E., Shaw, R., Ursell, P.C., and Blau, H.M. 2000. VEGF gene delivery to myocardium: deleterious effects of unregulated expression. *Circulation* 102:898-901.
93. Pettersson, A., Nagy, J.A., Brown, L.F., Sundberg, C., Morgan, E., Jungles, S., Carter, R., Krieger, J.E., Manseau, E.J., Harvey, V.S., et al. 2000. Heterogeneity of the angiogenic response induced in different normal adult tissues by vascular permeability factor/vascular endothelial growth factor. *Lab Invest* 80:99-115.
94. Sundberg, C., Nagy, J.A., Brown, L.F., Feng, D., Eckelhoefer, I.A., Manseau, E.J., Dvorak, A.M., and Dvorak, H.F. 2001. Glomeruloid microvascular proliferation

follows adenoviral vascular permeability factor/vascular endothelial growth factor-164 gene delivery. *Am J Pathol* 158:1145-1160.
95. Masaki, I., Yonemitsu, Y., Yamashita, A., Sata, S., Tanii, M., Komori, K., Nakagawa, K., Hou, X., Nagai, Y., Hasegawa, M., et al. 2002. Angiogenic gene therapy for experimental critical limb ischemia: acceleration of limb loss by overexpression of vascular endothelial growth factor 165 but not of fibroblast growth factor-2. *Circ Res* 90:966-973.
96. von Degenfeld, G., Banfi, A., Springer, M.L., Wagner, R.A., Jacobi, J., Ozawa, C.R., Merchant, M.J., Cooke, J.P., and Blau, H.M. 2006. Microenvironmental VEGF distribution is critical for stable and functional vessel growth in ischemia. *FASEB J* 20:2657-2659.
97. Banfi, A., von Degenfeld, G., Gianni-Barrera, R., Reginato, S., Merchant, M.J., McDonald, D.M., and Blau, H.M. 2012. Therapeutic angiogenesis due to balanced single-vector delivery of VEGF and PDGF-BB. *FASEB J* 26:2486-2497.
98. Groppa, E. Manuscritpt in preparation.
99. Yla-Herttuala, S., and Alitalo, K. 2003. Gene transfer as a tool to induce therapeutic vascular growth. *Nat Med* 9:694-701.
100. Tayalia, P., and Mooney, D.J. 2009. Controlled growth factor delivery for tissue engineering. *Advanced materials* 21:3269-3285.
101. Silva, A.K., Richard, C., Bessodes, M., Scherman, D., and Merten, O.W. 2009. Growth factor delivery approaches in hydrogels. *Biomacromolecules* 10:9-18.
102. Eming, S.A., and Hubbell, J.A. 2011. Extracellular matrix in angiogenesis: dynamic structures with translational potential. *Exp Dermatol* 20:605-613.
103. Banfi, A., von Degenfeld, G., and Blau, H.M. 2005. Critical role of microenvironmental factors in angiogenesis. *Current atherosclerosis reports* 7:227-234.
104. Lutolf, M.P., and Hubbell, J.A. 2005. Synthetic biomaterials as instructive extracellular microenvironments for morphogenesis in tissue engineering. *Nat Biotechnol* 23:47-55.
105. Breen, A., O'Brien, T., and Pandit, A. 2009. Fibrin as a delivery system for therapeutic drugs and biomolecules. *Tissue Eng Part B Rev* 15:201-214.
106. Janmey, P.A., Winer, J.P., and Weisel, J.W. 2009. Fibrin gels and their clinical and bioengineering applications. *J R Soc Interface* 6:1-10.
107. Spicer, P.P., and Mikos, A.G. 2010. Fibrin glue as a drug delivery system. *J Control Release* 148:49-55.
108. Zisch, A.H., Lutolf, M.P., and Hubbell, J.A. 2003. Biopolymeric delivery matrices for angiogenic growth factors. *Cardiovasc Pathol* 12:295-310.
109. Schense, J.C., and Hubbell, J.A. 1999. Cross-linking exogenous bifunctional peptides into fibrin gels with factor XIIIa. *Bioconjugate chemistry* 10:75-81.
110. Sakiyama, S.E., Schense, J.C., and Hubbell, J.A. 1999. Incorporation of heparin-binding peptides into fibrin gels enhances neurite extension: an example of designer matrices in tissue engineering. *FASEB J* 13:2214-2224.
111. Sakiyama-Elbert, S.E., and Hubbell, J.A. 2000. Controlled release of nerve growth factor from a heparin-containing fibrin-based cell ingrowth matrix. *J Control Release* 69:149-158.

112. Sakiyama-Elbert, S.E., and Hubbell, J.A. 2000. Development of fibrin derivatives for controlled release of heparin-binding growth factors. *J Control Release* 65:389-402.
113. Martino, M.M., Mochizuki, M., Rothenfluh, D.A., Rempel, S.A., Hubbell, J.A., and Barker, T.H. 2009. Controlling integrin specificity and stem cell differentiation in 2D and 3D environments through regulation of fibronectin domain stability. *Biomaterials* 30:1089-1097.
114. Martino, M.M., and Hubbell, J.A. 2010. The 12th-14th type III repeats of fibronectin function as a highly promiscuous growth factor-binding domain. *FASEB J* 24:4711-4721.
115. Martino, M.M., Tortelli, F., Mochizuki, M., Traub, S., Ben-David, D., Kuhn, G.A., Muller, R., Livne, E., Eming, S.A., and Hubbell, J.A. 2011. Engineering the growth factor microenvironment with fibronectin domains to promote wound and bone tissue healing. *Sci Transl Med* 3:100ra189.
116. Ehrbar, M., Djonov, V.G., Schnell, C., Tschanz, S.A., Martiny-Baron, G., Schenk, U., Wood, J., Burri, P.H., Hubbell, J.A., and Zisch, A.H. 2004. Cell-demanded liberation of VEGF121 from fibrin implants induces local and controlled blood vessel growth. *Circ Res* 94:1124-1132.
117. Schmoekel, H.G., Weber, F.E., Schense, J.C., Gratz, K.W., Schawalder, P., and Hubbell, J.A. 2005. Bone repair with a form of BMP-2 engineered for incorporation into fibrin cell ingrowth matrices. *Biotechnology and bioengineering* 89:253-262.
118. Lorentz, K.M., Yang, L., Frey, P., and Hubbell, J.A. 2012. Engineered insulin-like growth factor-1 for improved smooth muscle regeneration. *Biomaterials* 33:494-503.
119. Ehrbar, M., Zeisberger, S.M., Raeber, G.P., Hubbell, J.A., Schnell, C., and Zisch, A.H. 2008. The role of actively released fibrin-conjugated VEGF for VEGF receptor 2 gene activation and the enhancement of angiogenesis. *Biomaterials* 29:1720-1729.

5. Sustained and highly tunable delivery of recombinant $VEGF_{164}$ from optimized fibrin matrices ensure normal, stable and functional angiogenesis.

5.1 Introduction

Therapeutic angiogenesis is an attractive strategy for treating several ischemic conditions, such as peripheral and coronary artery diseases or chronic wounds, in which the intrinsic capacity for spontaneous vascular repair and tissue regeneration is either compromised or insufficient to restore physiological blood flow. Vascular endothelial growth factor (VEGF) is the master regulator of both physiological and pathological vascular growth (1). However, initial clinical trials of VEGF gene delivery with a variety of gene therapy vectors failed to establish clinical benefit (2). Retrospective analyses identified several issues that undermined the efficacy of those trials, particularly the difficulty to deliver a sufficient VEGF dose into the target tissue at safe vector doses (3, 4). Taking advantage of a highly controlled cell-based gene delivery platform, we previously identified a key requirement to optimize therapeutic efficacy of VEGF gene delivery. In fact, VEGF binds tightly to extracellular matrix (5) and induces normal or aberrant angiogenesis depending on its localized concentration in the microenvironment around each producing cell in vivo, rather than its total dose (6). However, it is challenging to achieve homogeneously distributed expression levels in vivo with gene therapy vectors. Further, newly induced vessels require that VEGF stimulation be sustained for at least 4 weeks in order to stabilize and persist indefinitely (6-8).

The use of recombinant VEGF presents several desirable features for clinical translation of these biological concepts compared to gene therapy approaches, such as the lack of genetic modification, the ease of achieving a homogenous dose distribution and the limited duration of treatment. A limitation towards the

clinical application of recombinant VEGF is its short half-life in vivo and the controlled release from biodegradable matrices is an attractive approach to protect VEGF from rapid clearance, while ensuring homogenous and sustained delivery (9).

Physiological angiogenesis crucially depends on a spatially restricted organization of growth factor cues through their binding to the extracellular matrix (ECM)(10). Therefore, we previously developed a protein engineering approach that links growth factors to a fibrin matrix by enzymatic reaction. In fact, fibrin is a natural product of blood coagulation, is injectable as a liquid and solidifies in situ without cytotoxicity, can be remodeled by cell-associated enzymes, and naturally serves as a cell infiltration matrix, thereby providing unique features as a platform for physiological presentation of angiogenic signals (11). Growth factors are engineered to contain the peptide sequence α_2-$P_{1\text{-}8}$ (NQEQVSPL), which is a substrate for the coagulation transglutaminase factor XIIIa, so that the recombinant factor is covalently incorporated into the fibrin matrix formed by the factor XIIIa-mediated cross-linking reaction of monomeric fibrinogen and it is subsequently released only through matrix degradation by local cell-associated proteases (12). We have previously shown that matrix-bound presentation of diverse so-engineered growth factors, such as VEGF-A_{121}, BMP-2 and IGF-1, can considerably accentuate their biological effects respect to the wild type growth factors (13-15). However, the brief persistence of fibrin hydrogels in vivo, with complete degradation within less than a week (13), is insufficient to ensure the stabilization of newly induced vessels and is a major obstacle to its exploitation for therapeutic angiogenesis (16). Therefore, here we aim to develop an optimized fibrin-based platform for

controlled and sustained delivery of α_2-P_{1-8}-VEGF-A_{164} to robustly induce normal, stable and functional angiogenesis in therapeutically relevant target tissues.

5.2 Materials and Methods

Recombinant α_2PI_{1-8}-VEGF$_{164}$ production and purification

The cDNA for mouse VEGF-A_{164} was PCR-amplified using primers designed to allow for fusion of the transglutaminase substrate sequence, NQEQVSPL (α_2-PI_{1-8}), onto the N-terminus of the amplified cDNA before insertion into the expression vector pRSET (Invitrogen Life Science, Basel, Switzerland). The fusion protein was expressed into E.coli strain BL21 (Dε3) pLys (Novagen, MerckKGaA, Darmstad, Deutschland). The recombinant α_2-PI_{1-8}-VEGF-A_{164} was isolated from inclusion bodies processed and refolded using a slightly modified version of a previously published protocol (17). Briefly, the inclusion bodies were collected from the bacterial lysate by centrifuging, washed with triton X-114 to remove membrane proteins and endotoxins, and extracted with urea buffer overnight at 4 °C under magnetic steering. Further dimerization of α_2-PI_{1-8}-VEGF-A_{164} was done with a redox system (0.5 mM oxidized glutathione, 5 mM reduced glutathione) added into the protein solution after the 2 M urea dialysis and α_2-PI1$_{-8}$-VEGF-A_{164} was dimerized under stirring for 48 h at 4°C. Then, glutathione and urea were removed by 3 sequential dialyses of 24 h against Tris buffers. Proteins were then concentrated using a 10 kD Amicon tube (Millipore, MerckKGaA, Darmstad, Deutschland) and further filtered through a 0.22 µm filter. α_2PI_{1-8}-VEGF$_{164}$ monomers and dimers were separated using size exclusion with a HiLoad 16/60 superdex 75 pg column (GE healthcare, Munich, Germany). Fractions corresponding to VEGF dimers were pulled together, concentrated with Amicon tube, and filtered through a 0.22 um

filter. VEGF dimers were verified as >99% pure by SDS-PAGE and MALDI-TOF analysis. Endotoxin level was verified as under 0.05 EU/mg of protein using LAL assay (GenScript, Aachen, Germany).

Fibrin gel preparation

Fibrin matrices were prepared by mixing human fibrinogen (plasminogen-, von Willebrand Factor-, and fibronectin-depleted; Enzymes Research Laboratories, Swansea, UK), factor XIIIa (CSL Behring, Switzerland) and thrombin (Sigma Aldrich, St Louis, Buchs, Switzerland) combined at different concentrations as described in the results section with 2.5 mM of Ca^{2+} (Sigma Aldrich, St Louis, Buchs, Switzerland) in 4-(2-hydroxyethyl)-1-piperazineethanesulfonic acid (HEPES) (Lonza, Basel, Switzerland). Matrices containing aprotinin-α_2-PI_{1-8} and α_2-PI_{1-8}-$VEGF_{164}$ were obtained by adding them to the cross-linking enzymes solution before mixing with fibrinogen. Matrices were allowed to polymerize at 37 °C for 1 hour before use or directly injected after mixing to have in situ polymerization, depending on the experimental design.

Determination of α_2-PI_{1-8}-VEGF-A_{164} release profile

Fibrin matrices of 50 µl volume were generated with 10 mg/ml fibrinogen, 2 U/ml of thrombin, 5 U/ml factor XIIIa , 5 mM calcium chloride, and 10 µg/ml of VEGF-A_{164} (R&D Systems, Abingdon, UK) or α_2-PI_{1-8}-$VEGF_{164}$, as previously described (13). Fibrin gels were polymerized at 37°C for 1 h and transferred into 24 well plate containing 500 ml of washing buffer. The 100% release control

well contained only the growth factor in buffer. Each 24 h, buffers were collected, stored at -20°C and replaced with fresh buffer. For the 100% release control well, 20ml of buffer was taken out every day and stored at -20°C. After 7 days, growth factor cumulative release was quantified using ELISA using the 100% released control as reference (DuoSet, R&D Systems, Abingdon, UK).

VEGFR-2 phosphorylation assay

HUVECs (PromoCell, Heidelberg Germany) were seeded in 96 well-plate (3000 cells/well) and starved 4 h with serum-free MCDB-131 medium (Invitrogen, Basel, Switzerland). Cells were then stimulated with 50 ng/mL of VEGF-A_{164} or α_2-PI_{1-8}-VEGF-A_{164} for 5 min. Phosphorylated VEGFR-2 was quantified using phospho-ELISA kits. Briefly, ELISA plates were coated with a capture antibody for the GF-receptors and then incubated with cell lysates. The phosphorylation state was detected with an anti-phospho-tyrosine antibody and normalized to a standard according to manufacturer instructions (phospho-VEGF R2/KDR, DuoSet IC; R&D Systems, Abingdon, UK).

In vitro gel polymerization

Fibrin matrices of 50µl volume were prepared onto a plastic mini-tray (Nunc Microwell Minitrays, Cat. No 470378, Sigma Aldrich, St Louis Buchs Switzerland), placed on ice according to the compositions described in Table 1. The fibrinogen solution was first deposited into the well with a pipette tip, avoiding the formation of bubbles, and then the cross-linking enzymes were added. Solutions were mixed three times with the pipette to guarantee

homogenous mixing. The start of polymerization was defined by the change of consistency from liquid to stiff as detected by touch with the pipette tip. For each gel composition three replicates were assessed and results (in s) are presented as mean ± SEM.

Rheology studies

Fibrin gel discs of 1 mm thickness were pre-formed into press-to-Seal silicone isolator slides (P24744 Invitrogen-Molecular Probes, Basel, Switzerland) coated with parafilm at room temperature. The gel compositions tested are described in Table 2. Gels were allowed to polymerize for 1h at 37°C, removed from the support and placed in PBS overnight at 4 °C to allow swelling. Gel stiffness was determined by performing small-strain oscillatory shear rheometry using a Bohlin CVO 120 high-resolution rheometer with plate-plate geometry at room temperature (Instrumat SA, Renens, Switzerland). Gels were sandwiched between the two plates of the rheometer with compression up to 80% of their original thickness to avoid slipping. Measurements were then conducted in a constant strain (0.05) mode as a function of frequency (from 0.1 to 10 Hz) to obtain dynamical spectra (n=3 per condition). Results (in KPa) are presented as mean ± SEM.

Intramuscular fibrin gel implantation in vivo

The protocol used for the preparation of fibrin matrices was the same described in the section fibrin gel preparation. In order to avoid an immunological response to human fibrinogen and cross-linking enzymes, 6-8

week-old immunodeficient SCID CB.17 mice (Charles River Laboratories, Sulzfeld, Germany) were used. Animals were treated in accordance with the Swiss Federal guidelines for animal welfare, after approval from the Veterinary Office of the Canton of Basel-Stadt (Basel, Switzerland). A liquid volume of 50µl was aspirated rapidly with a 0.3 ml insulin syringe with integrated 30 G needle (Micro-Fine Cat. No. 320837, Becton Dickinson, Allschwil, Switzerland) and injected into the gastrocnemius (GC) muscle of the mice previously anesthetized with 3% isofluorane. After injection, in situ polymerization was allowed for 20 seconds before slowly extracting the needle.

In vivo multispectral imaging

Fibrin gels were prepared as described in the section fibrin gel preparation, but fluorescently conjugated fibrinogen (Alexa 647, Invitrogen, Basel, Switzerland) was inserted in a concentration of 0.5 ng/ml in the gel volume to monitor the degradation of the different fibrin gel compositions *in vivo* by non-invasive multispectral imaging. The experiments were performed at the Ludwig Boltzmann Institute (Vienna, Austria) after approval by the local ethical committee. Animals were treated according to the National Institute of Health guidelines. Carprofen (2.5 mg/kg Rimadyl, Pfizer, Austria) was administered to animals preoperatively and for the following 3 days to ensure proper analgesia. A liquid volume of 50 µl was injected subcutaneously next to the spine and into GC muscles bilaterally in nude mice (n=10/ group). The fluorescence of the fibrin matrix was non-invasively followed and quantified over a period of 9 days using a multispectral imaging system (Maestro Imaging System, CRI Inc.,Brunn

am Gebirge, Austria). ROIs were defined and analyzed. The signals (counts/s) were normalized to day 1 values and expressed as their percentage. Data are represented as mean fluorescence intensity ± SEM.

Histological analyses

Mice were euthanized by vascular perfusion of 1% paraformaldehyde (Sigma Aldrich, St Louis Buchs, Switzerland) in PBS (Sigma Aldrich, St Louis Buchs, Switzerland) pH 7.4 for 3 minutes under 120 mm/Hg of pressure. Gastrocnemius muscles were harvested, post-fixed in 0.5% paraformaldehyde (PFA) in PBS pH 7.4 for 2 h at room temperature and cryoprotected by infusion in 30% sucrose (Sigma Aldrich, St Louis Buchs, Switzerland) in PBS at 4 °C overnight. Muscles were then embedded in OCT compound (CellPath, Newtown, Powys, UK), frozen in freezing isopentane and cryosectioned. Tissue sections were stained with H&E to verify the intramuscular localization of the gel. Vascular morphology was analyzed by immunofluorescence staining on 12µm-thick frozen sections cut across the longitudinal axis. The following primary antibodies and dilutions were used: rat anti-CD31 (clone MEC 13.3, BD Bioscences, Basel, Switzerland) at 1:100; mouse anti-α-SMA (clone 1A4, Sigma Aldrich, St Louis Buchs, Switzerland) at 1:400; rabbit anti-NG2 (Merck Millipore, Darmstadt, Germany) at 1:200. Fluorescently labeled secondary antibodies (Invitrogen, Basel, Switzerland) were used at 1:200. Fluorescence images were taken with a 40X objective on a Carl Zeiss LSM710 3-laser scanning confocal microscope (Carl Zeiss, Feldbach, Switzerland). In some experiments the amount of undegraded gel was assessed histologically by immunostaining with

a primary antibody that specifically recognizes fibrin, but not fibrinogen (mouse anti-human fibrin, clone E8, Beckman Coulter, CA, USA) at a dilution of 1:200. Tissue sections were obtained at 250-µm intervals, in 3 muscles/group. Images were taken in each section where gel was detectable with a 10X objective on an Olympus BX61 fluorescence microscope (Olympus, Volketswil, Switzerland) and merged using the multiple image alignment (MIA) function of the CellP imaging analysis software (Olympus, Volketswil, Switzerland) to reconstruct the total area of the tissue section in which the undegraded gel was present. The total surface area occupied by undegraded gel was quantified (in mm^2) using ImageJ software as the sum of all sections in each analyzed muscle. In some experiments, physiological perfusion of induced vessels was assessed by intravascular staining with a fluorescently labeled *Lycopersicum esculentum* (tomato) lectin (Vector Laboratories, Burlingame, CA, USA) that binds the luminal surface of blood vessels, as previously described (18). Briefly, mice were anesthetized and lectin was injected intravenously (50µl of a 2 mg/ml lectin solution per mouse) and allowed to circulate for 4 min before vascular perfusion of 1% PFA in PBS pH 7.4 for 3 minutes under 120 mm/Hg of pressure.

Vessel quantifications

Vessel diameters and vessel length density were measured in muscle frozen sections after staining for CD31, NG2 and SMA as previously described(6, 18). Briefly, vessel diameters were measured by overlaying captured microscopic images with a square grid. Squares were selected randomly and the diameter of

each vessel, if present, in the defined square was measured (in μm). Around 500 total diameter measurements were obtained from 3 independent muscles for each group (n=3). Vessel length density was measured in 5-10 fields per muscle from 3 muscles per group (n=3) by tracing the total length of vessels in each field and dividing it by the area of the field (mm of vessel length/mm^2 of surface area). All analyses were performed using the Cell P imaging software (Olympus, Volketswil, Switzerland). Results are presented as mean ± SEM.

Subcutaneous fibrin gel implantation

All animal procedures were approved by the Cantonal Veterinary Office of Canton Vaud. Female nude mice were used at about 4-5 weeks of age. Animals were anesthetized with inhalation of 2% isofluorane. Dorsal skin was disinfected with 70% ethanol. Two incisions, approximately 1.5 cm long, were made along the left and right sides of the dorsum. A 10-0 Dafilon suture (Braun, Meinsungen, Germany) was placed through each fibrin gel pellet to fasten the gel to the subcutaneous area just beneath the skin. Four gels of 20µl volume were implanted in each mouse in a random order and wounds were closed with 7-0 Prolene sutures (Ethicon, Norderstedt, Germany). Animals were euthanized 14 days later by carbon dioxide asphyxiation. Gels were excised together with the surrounding skin and samples were stored at -80°C for further analysis.

α_2-PI_{1-8}-VEGF-A_{164} protein extraction and quantification

The concentration of α_2-PI_{1-8}-$VEGF_{164}$ in the gels after in vivo implantation was measured from explanted and frozen fibrin gels. They were washed in PBS

for 8 h at 4°C, changing the PBS every hour. Afterwards, 50 mU of plasmin (Sigma Aldrich, St Louis Buchs Switzerland) in 50 µl of deionized water were added to each gel and incubated at 37 °C on a shaker at 1000 rpm. After 8h the plasmin solution was renewed and incubation at 37 °C on a shaker continued until all gels were completely dissolved (approximately 48 h). The amount of VEGF in the resulting samples was measured using an ELISA kit (R&D Systems Europe, Abingdon, UK). One hundred µl of each sample was used in triplicate, and the assay was performed according to the manufacture's instructions.

Endothelial cell proliferation assay

Human umbilical vein endothelial cells (HUVECs) were cultured in 96-well plates (5,000 cells/well) in EGM-2 fully supplemented growth medium (Lonza, Basel, Switzerland) in 5% CO_2 at 37°C. Before the proliferation assay, cells were starved for 6 hours with EMB-2 medium (Lonza, Basel, Switzerland) supplemented with 1% FCS. Stimulation was started by supplementing the EBM-2 medium with 50 ng of the protein-extract liberated from the gels for 72 h or 50 ng of recombinant VEGF protein (Peprotech, London, UK), for the reference control. Then, cell numbers were determined by adding 10μL of cell proliferation reagent (WST-1, Roche, Basel, Switzerland) to each well. After 4 hours of incubation, absorbance of the samples was measured at 650 nm using a microplate reader (HT microplate, Biotek, Bad Friedrichshall, Germany).

Fasciocutaneous flap model treatment and analysis.

The experiments were performed at the Ludwig Boltzmann Institute (Vienna, Austria), after approval by the local ethical committee. Six male Sprague Dawley rats per group, weighing 300-350 g (Harlan- Wilkemann), were used to perform the epigastric flap model as previously described (19). Briefly, the rats were anesthetized with ketamine (110 mg/kg) and xylazine (12 mg/kg). Prior to surgery a square flap of approximately 8x8 cm was delimited with a surgical marker. The flap was divided into three distinct vertical zones with equal size, the outer zone reflecting vital or ischemic areas depending which epigastric neurovascular bundle was ligated. In the outer zones a circle of 1.5 cm diameter located in the middle of the zone was additionally marked to identify the site for gel implantation. The marked square flap was elevated from cranial to caudal at the fascial plane of the abdominal muscular layer, until the entire flap was lifted and connected to the body of the animal only by the inferior epigastric neurovascular pedicles, at which time the entire flap was viable. To make half of the flap ischemic, the left or the right inferior neurovascular bundle was ligated according to a randomization protocol. The flap was then sutured back to its anatomical location. Thereafter, the circular wounds were created within the elevated flap not exceeding the fascia thus resulting in a wound complicated by ischemia in one vertical zone and an internal control wound on the opposite vertical zone. A volume of 100 µl of empty gel or of gel containing 2µg/ml of α_2-$PI_{1\text{-}8}$-$VEGF_{164}$ was applied into the sites according to a randomization protocol, allowing solidification in situ. Wounds were covered with a transparent foil dressing (Opsite, Smith and Nephew, England) and fixed with a second

dressing (Fixomull-stretch, Beiersdorf, Germany), changing them on day 1 and 3. As an analgesic treatment, rats received 1.25 mg/kg butorphanol and 0,15 mg/kg meloxicam 5mg/ml subcutaneously on the day of surgery and three days post-OP as well as 10 ml Ringer solution subcutaneously for fluid resuscitation on the day of surgery. Blood flow was measured by LDI (Moor Instruments Ltd., Devon, UK) system, preoperatively as baseline, postoperatively to assess the induction of ischemia, on day 3 and 7. Preoperative baseline values were set at 100% and subsequent scans referred to these values and expressed as percentage of baseline. The ischemic and non-ischemic vertical zones were scanned and evaluated separately. The scan modus was set at 10 ms/pixel, and a resolution of 256 x 256 pixels was chosen. Analyses were made by a software evaluation tool provided with the LDI Moor^{TM} system (Moor Instruments Ltd., Devon, UK). Perfusion values were recorded as colored pixels, giving the color-coordinated 2-D image of the flap perfusion. The wound closure was evaluated by planimetric analysis. Excision wounds were traced on a transparent acrylic sheet post surgery, at day 3 and 7. The sheets were photographed with adjacent standard ruler and analyzed by planimetric software (Lucia G1, Version 4.8, Laboratory Imaging Ltd., Czech Republic). The planimetric results were expressed as a percentage of the total postoperative wound surface area. At day 7 postoperatively the animals were euthanized by an intracardial overdose of barbiturate (Nembutal®, 150mg/kg KG), and the entire wound areas (ischemic and non-ischemic) were excised. The specimens were fixed in 4% neutral buffered formalin for 24 hours followed by dehydration in ascending concentrations of alcohol before embedding in paraffin. Sections of 4µm- thickness were cutted by using a rotatory microtome. H&E staining was

performed to analyse wound regeneration. Vascular morphology was analyzed by immunohistochemistry staining using the following primary antibodies: vWF (polyclonal rabbit anti-human, A0082, Dako, Glostrup, Denmark) at 1:100, rabbit anti-NG2 (Merck Millipore, Darmstadt, Germany) at 1:100, and SMA (monoclonal mouse anti-human, A2547, Sigma-Aldrich, St.Louis, MO) for 1h at room temperature or overnight at 4 °C. HRP- secondary antibodies anti-mouse (K4001, Dako, Glostrup, Denmark) and anti-rabbit (K4003, Dako, Glostrup, Denmark) were used for vWF and SMA, whereas biotinylated anti- rabbit (E0432, Dako, Glostrup, Denmark) was used for NG2. All the secondary antibodies were used at 1:200. Signals were developed using a peroxidase substrate kit (ImmPACT™ NovaRED™, Vector, Burlingame, CA) or an alkaline phosphatase system (VECTASTAIN ABC-AP system AK-5000, Vector Laboratories, Burlingame, CA, USA). All images were acquired with a 40X objective using an Olympus BX61 microscope or an Olympus BXP80 microscope (Olympus, Volketswil, Switzerland). Vessel diameters and vessel length density were quantified on samples stained for vWF using the method described in 5.2.10.

Statistics

Data are presented as mean ± SEM. The significance of differences was evaluated using analysis of variance (ANOVA) followed by the Bonferroni test (for multiple comparisons) or using a Mann-Whitney test (for single comparisons). $P < 0.05$ were considered statistically significant.

5.3 Results

Generation of a recombinant murine $VEGF_{164}$ variant, α_2PI_{1-8} - $VEGF_{164}$.

The recombinant murine $VEGF_{164}$ protein fused to the α_2-PI_{1-8} peptide at the N-terminal was produced by a method of protein engineering developed by one of us (J.H.) (20). The coupling efficiency of the α_2-PI_{1-8}-$VEGF_{164}$ in fibrin gels of previously described standard composition (13) was assessed determining the growth factor released into buffer every 24 hours over a period of 7 days. About 5.1±1.2% of the initially incorporated amount of α_2-PI_{1-8}-$VEGF_{164}$ was released during the first day and this amount did not significantly increase after 7 days (6.9±1.2%) (Fig.1a). In contrast, the native $VEGF_{164}$ was almost completely released already after 1 day (88.2±2.4%) (Fig.1a). The bioactivity of α_2-PI_{1-8}-$VEGF_{164}$ was determined by its ability to phosphorylate VEGFR-2 on HUVEC cells. As shown in Fig. 1b, the variant α_2-PI_{1-8}-$VEGF_{164}$ was as effective as WT $VEGF_{164}$ in inducing VEGFR-2 phosphorylation (Fig.1b).

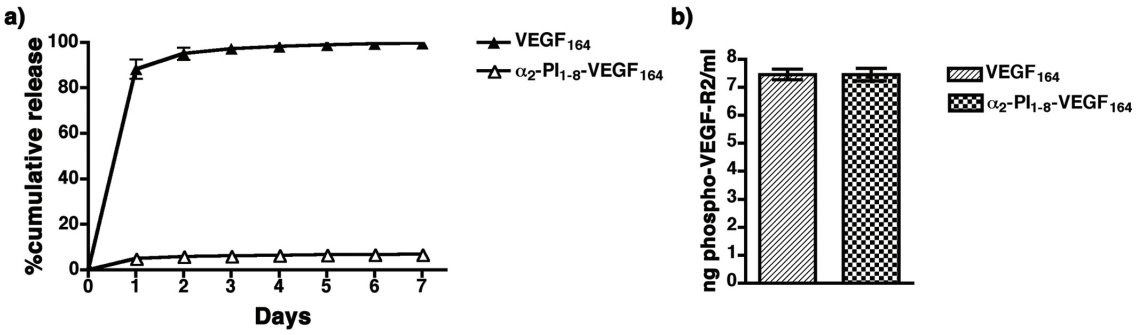

Figure 1 Characterization of the murine fusion protein α_2-PI_{1-8}-$VEGF_{164}$.

(a) Percent cumulative release of α_2-PI_{1-8}-$VEGF_{164}$ and WT $VEGF_{164}$ from fibrin gel. Quantity of WT and variant $VEGF_{164}$ was measured on buffer collected and replaced daily for 7 days using an ELISA kit. Values are reported as mean ± SEM; N=3.

(b) Phosphorylation assay. Serum starved HUVEC cells were incubated with 50 ng/ml of $VEGF_{164}$ or α_2-PI_{1-8}-$VEGF_{164}$ and the phosphorylated VEGF-R2 was quantified by ELISA. Values are reported as mean ± SEM; N=3.

In vivo fibrin gel persistence as a function of composition.

The polymerization time of different gel compositions was assessed in vitro to define gel compositions that would remain liquid longer than 10 seconds, which is the minimum time needed to allow in vivo injection in the gastrocnemius muscle of mice. Gels of 50µl volume were pre-formed on a plastic mini tray (Nunc, Microwell Minitrays) placed on ice to slow down gel polymerization as much as possible. Based on the results in Table 1, compositions based on a fibrinogen concentration of 50 mg/ml were excluded because of excessively fast polymerization.

	Gel composition			
	Fibrinogen (mg/ml)	Factor XIII (U/ml)	Thrombin (U/ml)	Polimerization time (s)
1	5	1	4	37± 2.2
2	5	5	4	12.3± 0.5
3	5	10	4	6.3± 0.5
4	25	1	2	22.5± 0.4
5	25	1	4	19.4± 0.3
6	25	2	2	20.5± 0.4
7	25	2	4	16.5± 0.4
8	25	5	2	14.5± 0.4
9	25	5	4	11.9± 0.1
10	50	1	2	9.6± 0.6
11	50	1	4	8.1± 1
12	50	2	2	5.8± 0.3
13	50	2	4	5.8± 1.1

Table1. In vitro polymerization times of fibrin gels as a function of the concentrations of Fibrinogen, Factor XIII and Thrombin. Results (in seconds) are shown as mean±SEM; n=3.

Since fibrinogen concentration determines the maximum amount of α_2-$PI_{1\text{-}8}$-growth factor that can be loaded into the gel, the compositions with the highest fibrinogen concentration compatible with in vivo injection, i.e. 25 mg/ml, were selected for subsequent in vivo experiments. The stiffnesses of these gel

compositions were determined on swollen gels by performing small-strain oscillatory shear rheometry (Table 2).

Cross-linking enzyme concentration (Fixed fibrinogen concentration = 25 mg/ml)		
FXIIIa (U/ml)	Thrombin (U/ml)	Gel stiffness (KPa)
1	2	4.8±0.62
1	4	5.4±1.15
2	2	3.2±0.37
2	4	3.7±0.17
5	2	6.9±1.17
5	4	6.2±1.68

Table2. Determination of Fibrin gel stiffness as a function of cross-linking enzyme concentration. Results (in KPa) are shown as mean±SEM; n=3.

In order to determine the gel composition that ensured the longest in vivo duration 50µl of each were injected into the GC muscle of SCID mice, and the amount of undegraded gel was assessed by histological analysis 4 days later. Gel compositions spanning the range of stiffnesses were also labeled with fluorescent fibrinogen and injected under the skin of the dorsum and into GC muscles in nude mice to monitor the *in vivo* daily degradation rate by non-invasive multispectral imaging. The different gel compositions did not show appreciable differences either in gel persistence (Fig.2a) or degradation rate (Fig. 2b). Further, the amount of remaining gel did not correlate with each composition's stiffness.

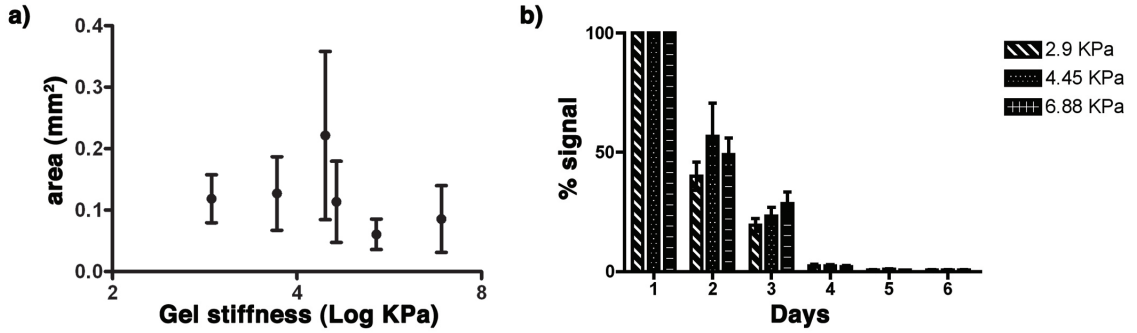

Figure 2 Determination of in vivo gel degradation.

(a) The different gel compositions were injected into the GC muscle of SCID mice and after 4 days the amount of remaining gel was quantified by immunofluorescence analysis of serial tissue sections, using an antibody that specifically recognizes fibrin, but not fibrinogen. Values are reported as mean area (mm^2) ± SEM; N=3.

(b) The different gel compositions made with fluorescently-labeled fibrinogen were injected subcutaneously next to the spine and intramuscularly into the GC muscle and the degradation was monitored in vivo daily for a period of 9 days by non-invasive imaging of fibrin fluorescence. Values are reported as mean ± SEM; N=9.

Therefore, the composition with the lowest stiffness (3.2 KPa: Fibrinogen 25 mg/ml, Factor XIII 2 U/ml, Thrombin 2 U/ml) was selected as the platform to investigate growth factor delivery in vivo, in order to maximize compliance and minimize invasiveness for host tissues.

Aprotinin-α_2-PI_{1-8} concentration determines both rate and duration of VEGF release.

In order to prolong in vivo persistence of fibrin hydrogels and the duration of VEGF release, required for vascular stabilization, the gel composition was supplemented with aprotinin, which inhibits gel degradation by plasmin. An engineered aprotinin-α_2-PI_{1-8} previously developed from one of us (J.H.) (21)

was used to allow covalent cross-linking into the hydrogels. Both the rate and duration of VEGF release from fibrin hydrogels are a function of the gel degradation rate, according to these relationships:

Dose = α_2-P_{1-8}-$VEGF_{164}$ concentration x gel degradation rate

Duration = volume/gel degradation rate

Therefore, since a reduction in degradation rate is expected to increase the duration of VEGF release, but to reduce its rate of release (i.e. the effective delivered dose), we first sought to determine the optimal aprotinin concentration that would ensure both sufficient in vivo persistence and an adequate VEGF release rate. Fibrin gels were prepared with 2 different concentrations of α_2-PI_{1-8}-$VEGF_{164}$, 100 µg/ml (the highest that could be incorporated without compromising their mechanical stability) and 25 µg/ml, in combination with 3 different concentrations of aprotinin-α_2-PI_{1-8}, 17, 56 and 85 µg/ml, and the quality of induced angiogenesis, if any, was evaluated 9 days after intramuscular injection. As shown in Fig. 3, the negative control gels, which contained only aprotinin-α_2-PI_{1-8} at the 3 different concentrations, did not induce any angiogenesis, whereas 100 µg/ml of α_2-PI_{1-8}-$VEGF_{164}$ always induced the growth of aberrant vessels, with irregular morphology, enlarged diameters and multiple lumens, devoid of pericytes and covered with a thick layer of smooth muscle cells, similar to previously described angioma-like structures (6). However, the effects of the 4-fold lower α_2-PI_{1-8}-$VEGF_{164}$ concentration of 25 µg/ml were clearly dependent on aprotinin concentration: in fact, no angiogenesis was detectable with the 85 µg/ml of aprotinin-α_2-PI_{1-8}, aberrant angioma-like structures were induced with 17 µg/ml of aprotinin-α_2-PI_{1-8}, and an abundant network of morphologically normal capillaries, associated with typical

pericytes, was generated with 56 µg/ml of aprotinin-α_2-PI_{1-8}, even if rare enlarged vessels were still detectable (white asterisk in Fig. 3e).

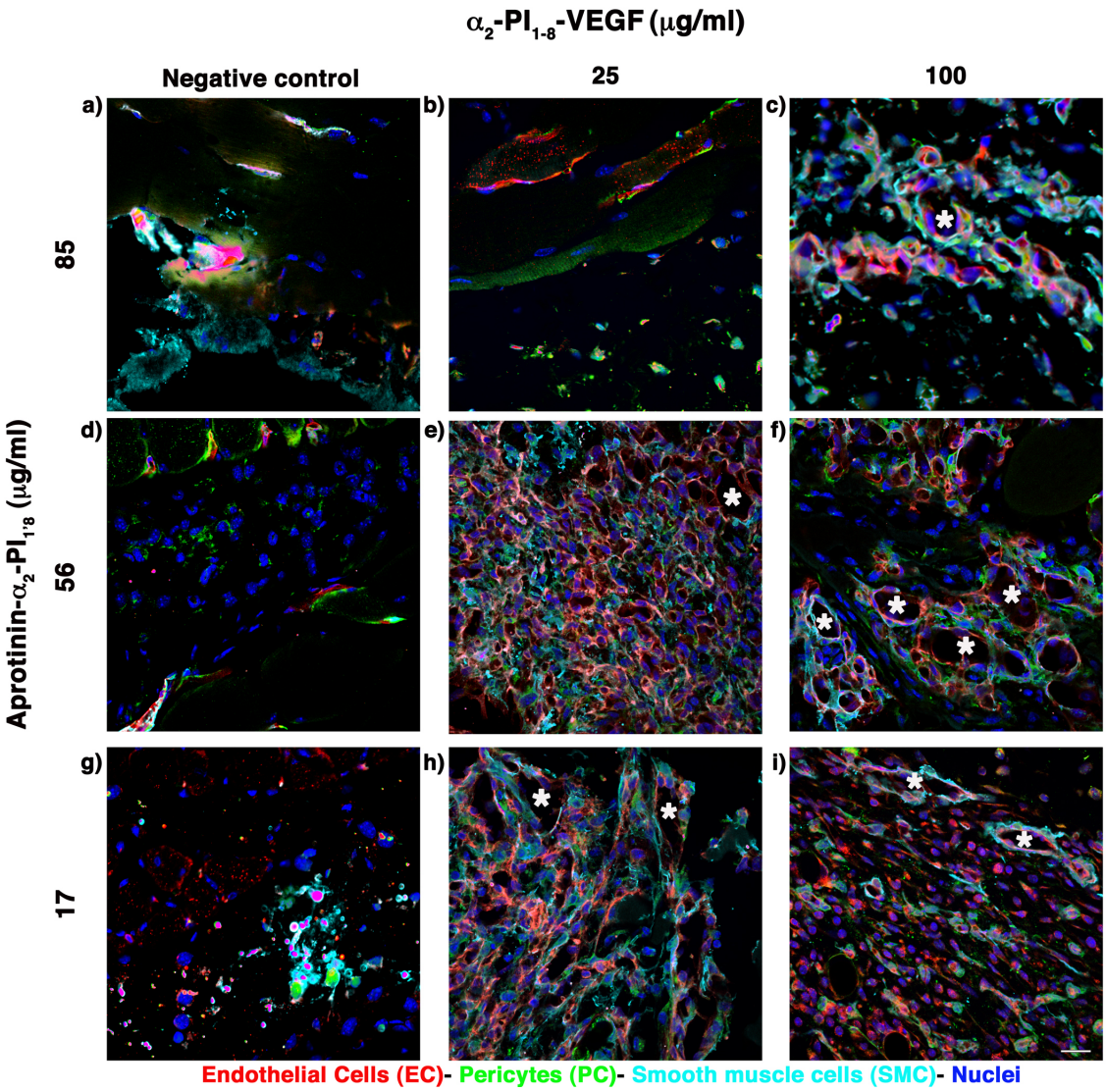

Figure 3 Aprotinin-α_2-PI_{1-8} concentration determines the effective released dose of α_2-PI_{1-8}-$VEGF_{164}$ and the consequent angiogenic phenotype.

Fibrin gels of 50µl volume were injected into the gastrocnemius muscle of SCID mice, with two different concentrations of α_2-PI_{1-8}-$VEGF_{164}$, 100µg/ml and 25µg/ml tested in combination with three concentrations of aprotinin-α_2-PI_{1-8} (17-56-85 µg/ml). Muscles were harvested 9 days later after perfusion-fixation with PFA 1%. Endothelial cells (CD31, in red), pericytes (NG2, in green), smooth muscle cells (α-SMA, in cyan) and nuclei (DAPI, in blue) were immunostained on frozen sections. Scale bar= 20µm; n=3 samples per group.

In all cases abundant residual gel was detectable in implanted muscles 9 days after injection (data not shown). Thus, an aprotinin-α_2-PI_{1-8} concentration of 56µg/ml was used in subsequent experiments to investigate the dose-dependent effects of α_2-PI_{1-8}-$VEGF_{164}$.

α_2-PI_{1-8}-$VEGF_{164}$ bioactivity after gel incorporation and in vivo implantation.

We next determined whether the α_2-PI_{1-8}-$VEGF_{164}$ could retain its bioactivity while incorporated into the fibrin gel and implanted *in vivo*, before being released. Gels were prepared with the highest feasible concentration of α_2-PI_{1-8}-$VEGF_{164}$ (100 µg/ml) and 56 µg/ml of aprotinin-α_2-PI_{1-8}. Gels of 20 µl volume were pre-formed at 37°C and implanted subcutaneously on the dorsum of nude mice (n=4 per group). After 2 weeks gels were explanted and frozen at –80°C, while gels that were frozen directly after preparation, without in vivo implantation, were used as controls (day 0). After two sequential digestions with plasmin for a total of approximately 56 h, the amount of extracted α_2-PI_{1-8}-$VEGF_{164}$ was measured by ELISA. After 2 weeks gels still contained a significant proportion of the amount of α_2-PI_{1-8}-$VEGF_{164}$ incorporated at day 0 (Fig. 4a). Furthermore, after 2 weeks of in vivo incubation gel-extracted α_2-PI_{1-8}-$VEGF_{164}$ was capable of inducing HUVEC proliferation as efficiently as without in vivo implantation (Day 0; Fig. 4b), indicating that gel incorporation effectively protects VEGF bioactivity despite prolonged permanence under in vivo conditions. The extracted factor showed a slightly reduced activity compared to

fresh recombinant VEGF (about 80% relative efficacy), likely as a consequence of the prolonged manipulations necessary for the gel extraction procedure.

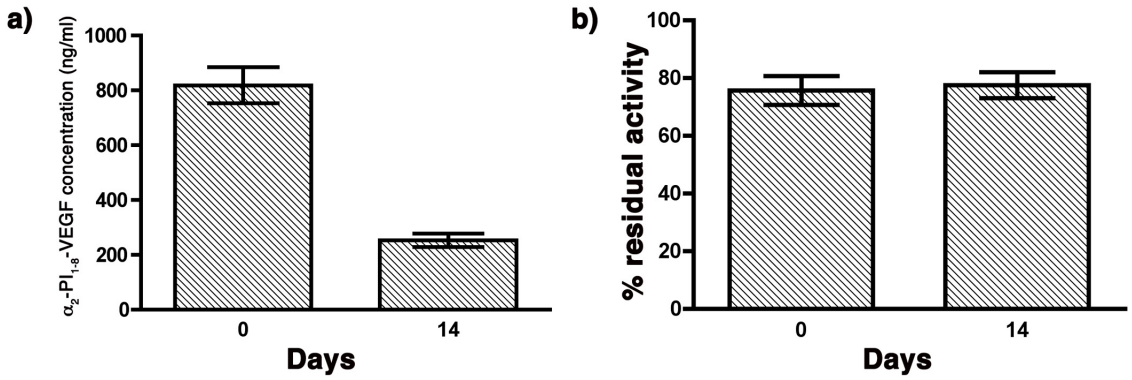

Figure 4 In vivo biological activity of α_2-PI_{1-8}-$VEGF_{164}$ is preserved after 2 weeks of in vivo implantation.

Fibrin gels of 20µl volume with 100µg/ml of α_2-PI_{1-8}-$VEGF_{164}$ and 56µg/ml of aprotinin-α_2-PI_{1-8} were pre-formed in vitro and either immediately frozen at -80 °C (day 0) or implanted subcutaneously into nude mice (n=4 per group), explanted 2 weeks later and frozen at -80 °C (day 14). (a) Measure of the extracted α_2-PI_{1-8}-$VEGF_{164}$ by ELISA. Results are reported as mean concentration (ng/ml)±SEM; n=4. (b) The biological activity of the extracted α_2-PI_{1-8}-$VEGF_{164}$ was determined by a HUVEC proliferation assay. Recombinant fresh $VEGF_{164}$ was used as positive control. Results are shown as the percentage residual activity compared to fresh recombinant VEGF (mean± SEM); n=4.

Dose-dependent angiogenesis by fibrin-bound α_2-PI_{1-8}-$VEGF_{164}$.

Since decreasing α_2-PI_{1-8}-$VEGF_{164}$ concentration from 100 to 25 µg/ml caused a shift from completely aberrant to mostly normal angiogenesis (Fig. 3), we investigated whether lower α_2-PI_{1-8}-$VEGF_{164}$ concentrations could reliably avoid aberrant vascular structures. GC muscles were injected with gels based on the optimized composition described above, with 56µg/ml of aprotinin-α_2-PI_{1-8}, and loaded with a 50-fold range of α_2-PI_{1-8}-$VEGF_{164}$ concentrations (5, 1 or 0.1 µg/ml). After 9 days, all three α_2-PI_{1-8}-$VEGF_{164}$ doses induced exclusively networks of morphologically normal and mature capillaries, associated with

NG2-positive and α-SMA-negative pericytes, with a clearly increased vascular density compared to controls (Fig.5).

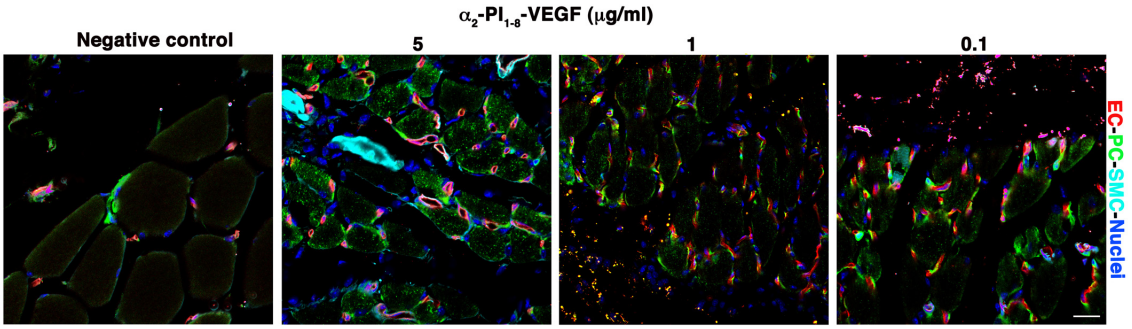

Figure 5 A wide range of α_2-PI_{1-8}-$VEGF_{164}$ doses induces robust and normal angiogenesis.

Fibrin gels loaded with 56 μg/ml of aprotinin-α_2-PI_{1-8} and 5, 1 or 0.1 μg/ml of α_2-PI_{1-8}-$VEGF_{164}$ were injected into the GC muscle of SCID mice. Muscles were harvested after perfusion-fixation with PFA 1% 9 days later. Frozen sections were immunostained to detect endothelial cells (CD31, in red), pericytes (NG2, in green), smooth muscle cells (α-SMA, in cyan) and nuclei (DAPI, in blue). All α_2-PI_{1-8}-$VEGF_{164}$ concentrations induced the formation of a normal network of capillaries uniformly covered with pericytes and lacking smooth muscle cells. Scale bar= 20 μm; n=3 per group.

Long-term stability of angiogenesis induced by optimized α_2-PI_{1-8}-$VEGF_{164}$ delivery.

It has been previously shown that VEGF gene delivery needs to be sustained for at least 4 weeks to allow newly induced vessels to stabilize and become independent of further VEGF signaling (6-8). Therefore, we investigated whether delivery of fibrin-bound α_2-PI_{1-8}-$VEGF_{164}$ by the optimized platform described above could be sustained long enough to allow vascular stabilization. Gels carrying four different concentrations of α_2-PI_{1-8}-$VEGF_{164}$ (0.01, 0.1, 5 and 100 μg/ml) were injected in GC muscles of SCID mice. In all conditions small amounts of undegraded gel were still detectable in implanted tissues (data not shown) and robust angiogenesis was present 4 weeks after implantation.

Similarly to the 9 days-results shown above, 100 µg/ml of α_2-$PI_{1\text{-}8}$-$VEGF_{164}$ generated large aberrant angioma-like structures mixed with more regular capillaries, which were however completely devoid of mural cell coverage, and both 0.1 and 5 µg/ml concentrations induced exclusively normal networks of pericyte-covered mature capillaries (Fig. 6a). Interestingly, the further 10-fold lower VEGF concentration of 0.01 µg/ml also induced efficient capillary growth, suggesting that normal angiogenesis can be effectively induced by a very wide range (at least 500-fold) of α_2-$PI_{1\text{-}8}$-$VEGF_{164}$ concentrations from 5 µg/ml to 10 ng/ml.

Quantification of vessel diameters showed that all normal vessels induced by α_2-$PI_{1\text{-}8}$-$VEGF_{164}$ concentrations up to 5 µg/ml had homogeneous diameter distributions in a narrow range, similar to normal capillaries in control tissues, whereas aberrant structures induced by 100 µg/ml displayed very heterogeneous and enlarged sizes (Fig. 6b). Interestingly, very low concentrations of α_2-$PI_{1\text{-}8}$-$VEGF_{164}$ (10 and 100 ng/ml) induced vessels with the same average diameter as control tissue, whereas the capillaries induced by 5 µg/ml were significantly larger (Fig. 6c, $P< 0.001$), although homogeneous in size and normal in morphology. In contrast to vessel diameters, the amount of angiogenesis (quantified as vessel length density) did not depend on the dose of α_2-$PI_{1\text{-}8}$-$VEGF_{164}$. In fact, all α_2-$PI_{1\text{-}8}$-$VEGF_{164}$ concentrations between 0.01 and 5 *µ*g/ml caused a similar 50-60% increase in vessel length density compared to controls (Fig. 6d, $P< 0.001$ or $P< 0.001$).

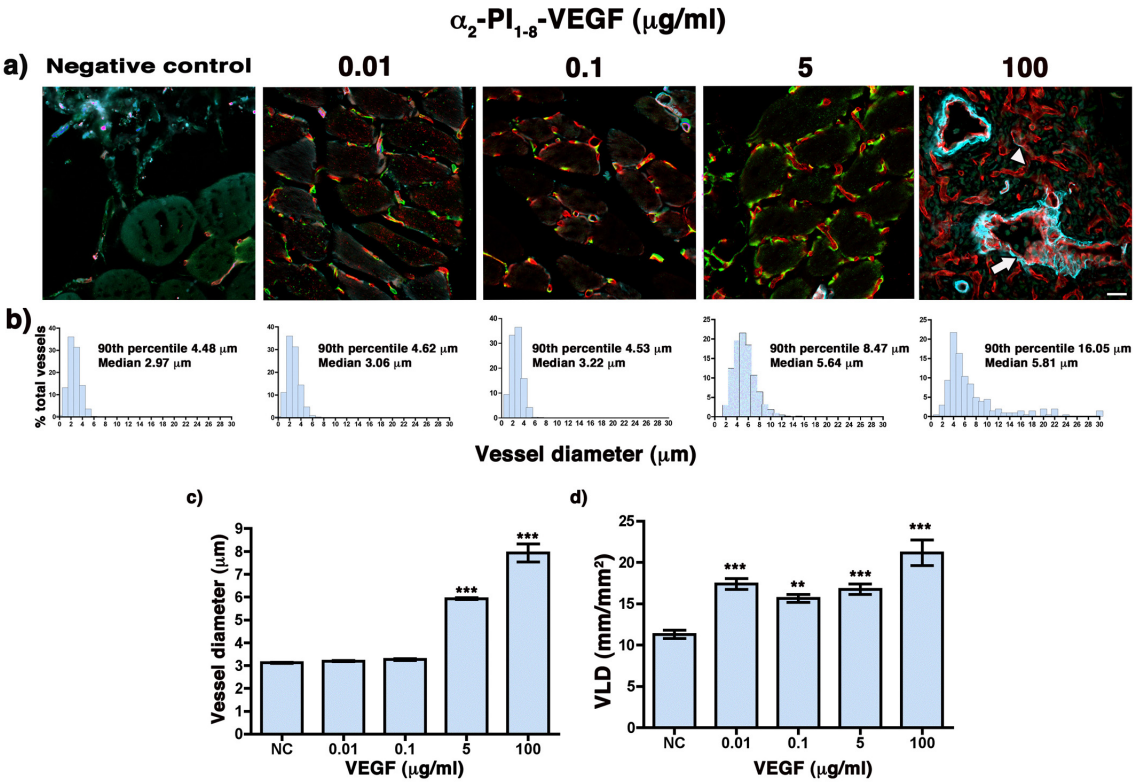

Figure 6 Sustained angiogenesis 4 weeks after optimized delivery of fibrin-bound α_2-PI_{1-8}-$VEGF_{164}$.

Fibrin gels loaded with 56 µg/ml of aprotinin-α_2-PI_{1-8} and 0 (negative control), 0.01, 0.1, 5 and 100 µg/ml of α_2-PI_{1-8}-$VEGF_{164}$ were injected into GC muscles of SCID mice. After 4 weeks muscles were harvested after perfusion-fixation with PFA 1%. (a) Frozen sections were immunostained to detect endothelial cells (CD31, in red), pericytes (NG2, in green) and smooth muscle cells (α-SMA, in cyan) were immunostained on frozen section. Scale bar = 20µm. (b-c) Vessel diameters were quantified in each group and their distribution (b) and average values (µm) (c) were calculated. (d) The amount of angiogenesis was quantified as vessel length density (VLD), calculated as the ratio between the total vessel length and the area of each measured field (mm/mm^2). Results in (c) and (d) are shown as mean ± SEM; n = 3 muscles/group; ***, P< 0.001, ** P<0.01 vs negative control.

In order to assess whether α_2-PI_{1-8}-$VEGF_{164}$-induced vessels had stabilized and achieved complete independence from exogenous VEGF, we investigated their persistence 3 months after gel injection. Angiogenesis was still present in all conditions, displaying the same morphologies as after 4 weeks (Fig. 7a), although no trace of the injected gels could be found anymore. The quantification of vessel length density confirmed that all α_2-PI_{1-8}-$VEGF_{164}$ concentrations causing normal angiogenesis (0.01 to 5 µg/ml) induced a similar

amount of new vessels, leading to about a 2-fold increase in vascular density (Fig. 7b). However, contrary to the results at 4 weeks, the amount of vessels still present 3 months after delivery of 100 µg/ml of α_2-PI_{1-8}-$VEGF_{164}$, which induced aberrant angiogenesis, was significantly less than for the other 3 lower concentrations, which induced normal angiogenesis (Fig. 7b). A quantitative comparison between vessel length densities induced by the different conditions at 4 weeks and 3 months revealed that the normal vessels generated by all α_2-PI_{1-8}-$VEGF_{164}$ concentrations between 0.01 and 5 µg/ml were completely stable and even further increased, while greater than 60% of the aberrant vasculature induced by 100 µg/ml regressed by 3 months (Fig. 7c).

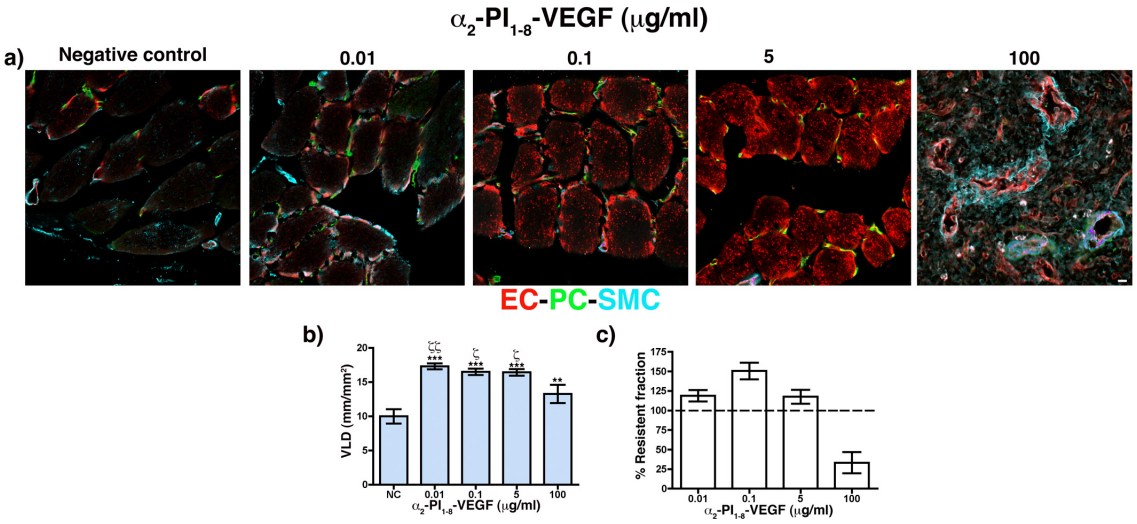

Figure 7 Long-term stability of normal, but not aberrant, angiogenesis induced by optimized delivery of fibrin-bound α_2-PI_{1-8}-$VEGF_{164}$.

Fibrin gels loaded with 56µg/ml of aprotinin-α_2-PI_{1-8} and 0 (negative control), 0.01, 0.1, 5 and 100 µg/ml of α_2-PI_{1-8}-$VEGF_{164}$ were injected into GC muscles of SCID mice. After 3 months muscles were harvested after perfusion-fixation with PFA 1%. (a) Frozen sections were immunostained to detect endothelial cells (CD31, in red), pericytes (NG2, in green) and smooth muscle cells (α-SMA, in cyan). Scale bar= 20 µm. (b) The amount of angiogenesis was quantified as vessel length density (VLD), calculated as the ratio between the total vessel length and the area of each measured field (mm/mm^2). Results are shown as mean±SEM; n = 3 muscles/group; *** P< 0.001 or ** P< 0.01 vs negative control, δδ P < 0.01, δ P < 0.05 vs the 100 µg/ml condition. (c) The stabilization rate of vessels induced in each condition was calculated as the ratio between vessel densities 3 months and 4 weeks after gel injection (% Resistant Fraction), with a

value of 100% or higher indicating complete stabilization and a value lower than 100% indicating the amount of vascular regression between the two time-points.

Newly-induced vessels by α_2-PI_{1-8}-$VEGF_{164}$ are functionally perfused.

In order to determine whether newly induced vessels by α_2-PI_{1-8}-$VEGF_{164}$ were functionally connected to the circulation, their perfusion was assessed by injecting mice 4 minutes before sacrifice with a fluorescein-labeled tomato lectin (FITC-lectin), which binds to the lumen of all vessels connected to the general circulation. Perfused endothelial structures were identified by immunostaining on frozen sections as double-positive for CD31 and FITC-lectin. As shown in Figures 8 and 9, essentially all vessels induced by the different α_2-PI_{1-8}-$VEGF_{164}$ concentrations were functionally perfused both after 4 weeks (Fig. 8) and 3 months (Fig. 9). Therefore, optimized delivery of fibrin-bound α_2-PI_{1-8}-$VEGF_{164}$ induced the growth of morphologically normal and mature vessels that are both stable and functionally perfused.

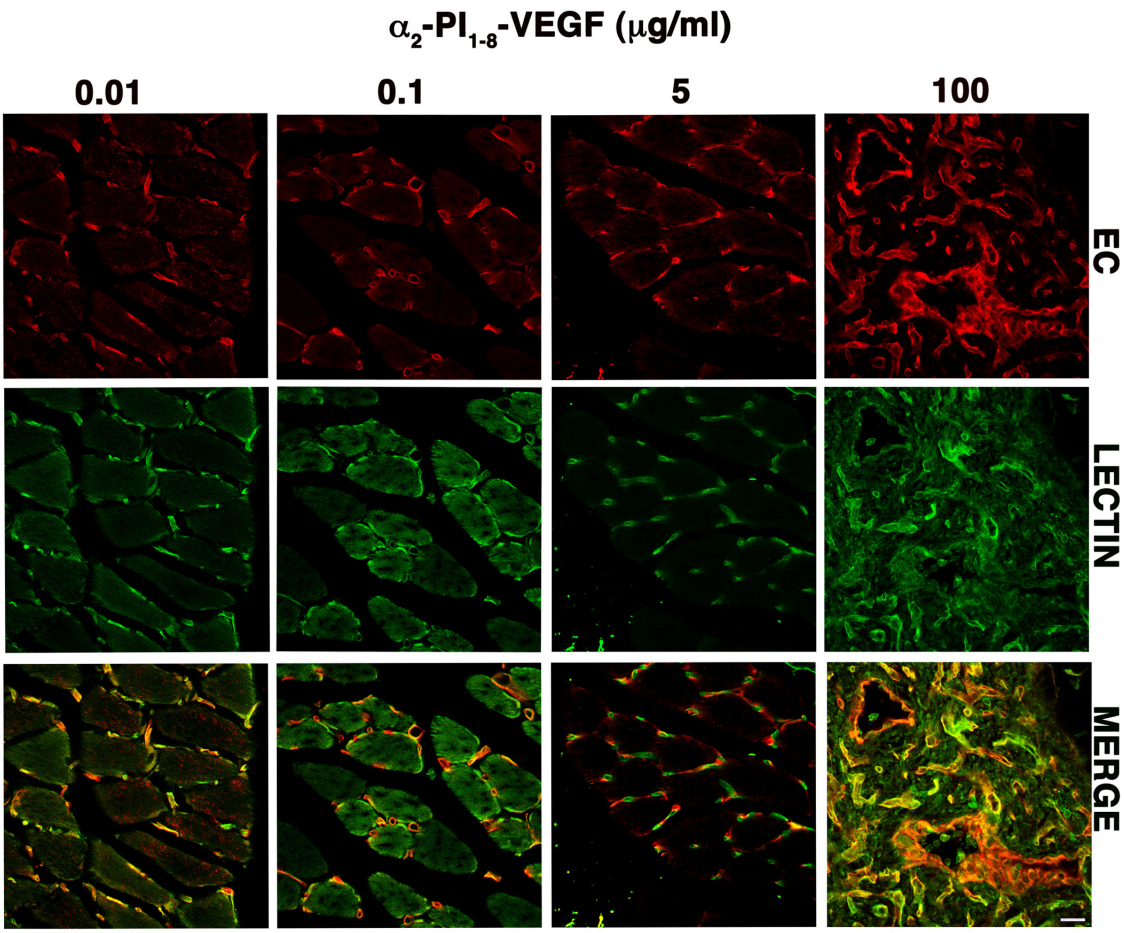

Figure 8 α_2-PI_{1-8}-$VEGF_{164}$ induced vessels are functionally perfused after 4 weeks.

FITC-lectin was injected intravenously into mice 4 weeks after gel injection, just before perfusion with PFA 1% and sacrifice. Muscles cryosections were immuno-stained to detect endothelial cells (CD31, in red), while lectin shows in green. Perfused vessels were identified as double-positive for CD31 and FITC-lectin, appearing yellow in the merged image. Scale bar = 20 μm.

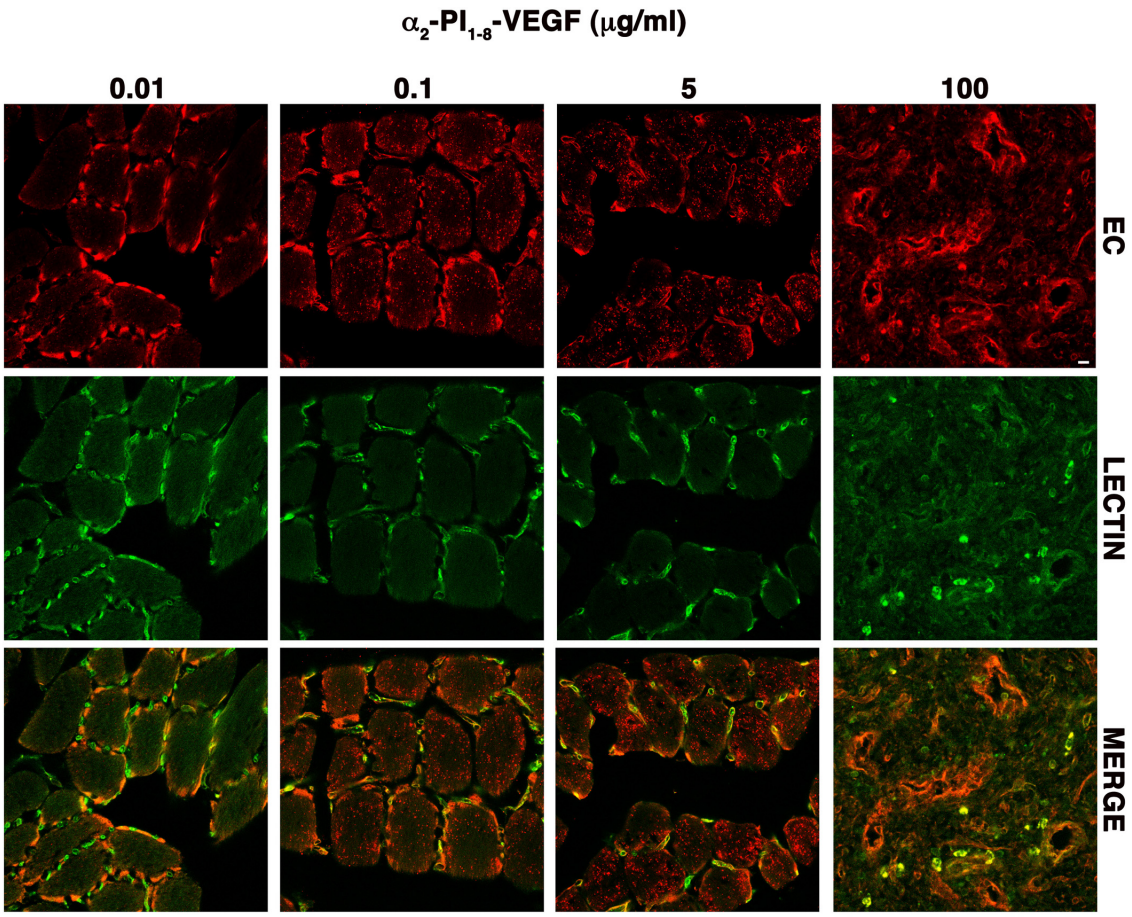

Figure 9 α_2-PI_{1-8}-$VEGF_{164}$ induced vessels are functionally perfused after 3 months.

FITC-lectin was injected intravenously into mice 3 months after gel injection, just before perfusion with PFA 1% and sacrifice. Muscles cryosections were immuno-stained to detect endothelial cells (CD31, in red), while lectin shows in green. Perfused vessels were identified as double-positive for CD31 and FITC-lectin, appearing yellow in the merged image. Scale bar = 20 μm.

Ischemic wound healing model.

Next we tested the efficacy of optimized delivery of fibrin-bound α_2-PI_{1-8}-$VEGF_{164}$ to cause functional improvement in a rat model of ischemic wound healing. A full-thickness skin flap was elevated in the epigastric region, which was supplied by two vascular bundles, one on each side. One of the two vascular pedicles was ligated to create ischemic necrosis on that side, while the other side remained physiologically perfused and was used as normal control.

This model induces an area of full-thickness necrosis spanning approximately the distal 25% of the flap, if left untreated. A circular wound of 1.5 cm diameter was induced on each side in the center of the flap and following a randomization protocol a gel disc was applied onto each wound. Based on the results described in Figures 6 and 7, a α_2-PI_{1-8}-$VEGF_{164}$ concentration of 2 µg/ml in the optimized fibrin matrix composition was used as the therapeutic condition, whereas an empty gel of the same composition was the negative control. Immunostaining for the endothelial marker von Willebrand Factor (vWF) showed that α_2-PI_{1-8}-$VEGF_{164}$ increased the vascularization of the dermis after 7 days, both in non-ischemic and ischemic tissue (Fig. 10a, d, g and j). A quantitative analysis confirmed that treatment with α_2-PI_{1-8}-$VEGF_{164}$ caused a significant increase in vessel length density in both non-ischemic and ischemic conditions (Fig. 10m-n, P=0.0002). Micro-vessels were associated with NG2-positive pericytes in all the groups (Fig. 10b, e, h and k), although the intensity of the staining was weaker for technical reasons. Furthermore, α-SMA-positive mural cells were found associated with both micro-vessels and small-caliber arterioles and venules (Fig. 10c, f, i and l, arrowheads), since, contrary to muscle tissue, in the skin a proportion of capillary pericytes also expresses α-SMA (22). The α_2-PI_{1-8}- $VEGF_{164}$-treated tissues displayed a greater density of regularly shaped larger vessels (>15 µm) with the features of arterioles, i.e. covered by a regular smooth muscle layer and homogeneous in size, consistently with the previously described effect of VEGF to cause arteriolization of pre-existing vessels (23). Tissue perfusion was measured by Doppler imaging immediately after surgery, as well as at 3 and 7 days after gel implantation. The results showed that the increased vessel density in the α_2-PI_{1-8}-$VEGF_{164}$-treated

tissues correlated with a significantly improved perfusion both in the non-ischemic and ischemic sites by 7 days (Fig. 10o-p, P<0.05).

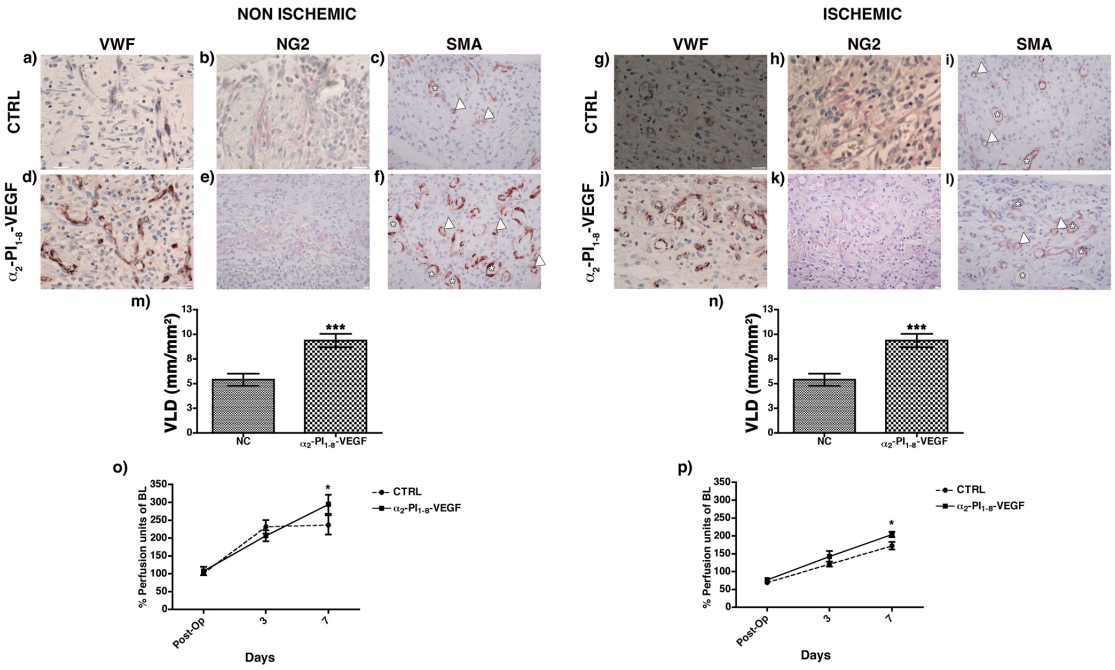

Figure 10 α_2-PI_{1-8}-$VEGF_{164}$ significantly improved wound regeneration in an ischemic wound-healing model after 7 days of gel implantation.

(a-i) Tissues were harvested 7 days after gel implantation, subsequently fixed in formalin before embedding in paraffin. Immunoistochemistry was performed on paraffin sections for endothelial cells (vWF), pericytes (NG2) and smooth muscle cells (α-SMA). Size bar= 20 μm. (m-n) The amount of angiogenesis was quantified as vessel length density (VLD), calculated as the ratio between the total vessel length and the area of each measured field. Results are shown as mean±SEM; n = 3 samples /group; P= 0.0002. (o-p) Measure of blood flow by Doppler imaging after arterial ligation, and at 3 and 7 days gel post implantation. Results are shown as mean±SEM; n = 3 samples /group; * P< 0.05.

In order to evaluate the functional effects of increased angiogenesis and perfusion in the treated tissues, healing of the wounds produced in the flaps was analyzed. In the non-ischemic condition, the control-treated tissue showed sign of very mild inflammation, with hyper/parakeratosis (Fig. 11a, arrowheads). There was not a clearly identifiable dermis beneath the epidermis, whereas bleeding areas could be detected (Fig. 11a, arrow). The underlying muscle layer

(Fig. 11b) was fully infiltrated by inflammatory cells and several muscle fibers displayed signs of partial necrosis, evidenced by infiltration of mononuclear inflammatory cells inside the myofiber (Fig. 11b, asterisks). α_2-PI_{1-8}-$VEGF_{164}$ treatment slightly reduced epidermal hyperplasia (Fig. 11c, arrowheads). Above the epidermis a layer of keratinized tissue with several apoptotic bodies was visible (Fig. 11c, white arrows) and the stratus corneus was partially present, indicating that the α_2-PI_{1-8}-$VEGF_{164}$-treated tissue had reached a more advanced stage of regeneration of the skin physiological structure. Further, α_2-PI_{1-8}-$VEGF_{164}$ treatment reduced the inflammatory infiltrate in the underlying muscle layer and completely prevented myofiber damage (Fig. 11d). The control ischemic tissues displayed moderate hyperplasia of the epidermis (Fig. 11e, arrowheads), which was covered with a thick keratinized tissue full of apoptotic bodies (Fig. 11e, white arrows). Both the dermis and the underlying muscle layer were prominently infiltrated with inflammatory cells, the muscle fibers were completely disorganized, many were invaded by monocytes and several degenerative vacuoles were visible within the muscle layer (Fig. 11f, asterisks). In the α_2-PI_{1-8}-$VEGF_{164}$-treated tissues, both epidermal hyperplasia and the thickness of the keratinized tissue with apoptotic bodies were reduced compared to controls (Fig. 11e and g). Further, α_2-PI_{1-8}-$VEGF_{164}$ treatment reduced the inflammatory infiltrate in the muscle layer and prevented myofiber damage, avoiding tissue necrosis (Fig. 11f and h). Therefore, histological analysis showed that the treatment with α_2-PI_{1-8}-$VEGF_{164}$ significantly improved the tissue regeneration process towards the physiological structure. Consistently with the histological results, the quantification of the wound healing rate showed that α_2-PI_{1-8}-$VEGF_{164}$ promoted a significant acceleration of the

ischemic wound closure 7 days after gel implantation (Fig.11j, P< 0.05). Non-ischemic wounds were also smaller both 3 and 7 days after α_2-PI$_{1-8}$-VEGF$_{164}$ treatment, although the differences were not statistically significant (Fig. 11i).

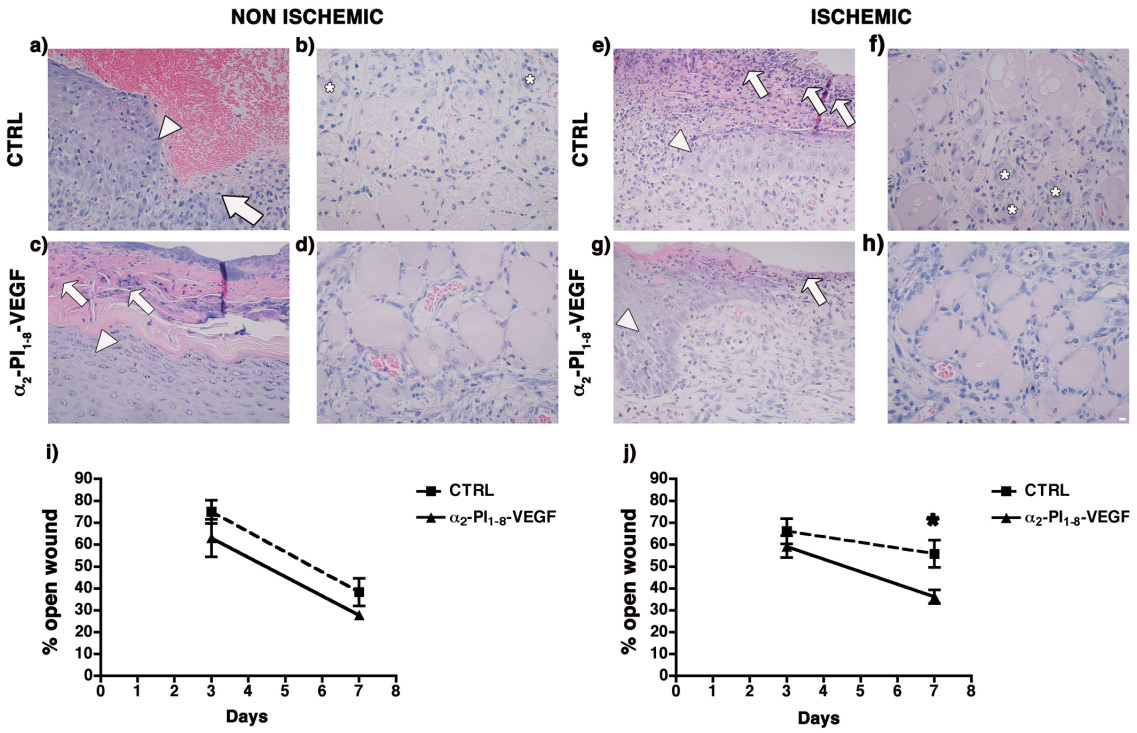

Figure 11 α_2-PI$_{1-8}$-VEGF$_{164}$ significantly improved wound regeneration in an ischemic wound-healing model after 7 days of gel implantation.

(a-h) Tissues were harvested after 7 days, subsequently fixed in formalin and embedded in paraffin. Paraffin sections were stained with Hematoxylin and Eosin, and representative images were taken to show the status of the epidermis (a, c, e, g) and beneath muscle layer (b, d, f, h). Size bar= 20 µm.

(i-j) The wound healing rate was measured by planimetric analysis after 3 and 7 days, and represented as % of open wound. Results are showed as mean ± SEM; n= 6 samples/ group * P< 0.05.

5.4 Discussion

Here we showed that fibrin-bound α_2-PI_{1-8}-$VEGF_{164}$ provides a highly tunable platform to precisely control the VEGF dose that is delivered to tissues and to efficiently induce stable and functional angiogenesis. Our data indicated that incorporation of aprotinin-α_2-P_{I1-8} at an optimal concentration is a key requirement to efficiently induce normal angiogenesis *in vivo*, since the same α_2-PI_{1-8}-$VEGF_{164}$ concentration can cause disparate effects, from none to aberrant angiogenesis, depending on its rate of release, which is controlled by the aprotinin-α_2-PI_{1-8} concentration. Under optimized conditions, which ensure a neither too fast nor too slow gel degradation rate, fibrin-bound α_2-PI_{1-8}-$VEGF_{164}$ could reliably induce exclusively normal and mature micro-vascular networks, which were stable and functionally perfused, over a very wide range (at least 500-fold) of α_2-PI_{1-8}-VEGF-A_{164} concentrations. Remarkably, newly induced vessels did not regress for at least 3 months, whereas the implanted gels were almost completely consumed by 4 weeks, demonstrating that they achieved independence from exogenous VEGF signaling for their survival and suggesting that they could likely persist indefinitely. This is particularly relevant for the therapeutic potential of this approach, since until now one of the main limits of recombinant protein delivery for therapeutic angiogenesis has been the insufficient duration of GF release to achieve stable and persistent effects (16).

On the other hand, aberrant angiogenesis induced by a α_2-PI_{1-8}-$VEGF_{164}$ concentration of 100 μg/ml failed to recruit physiological pericyte coverage by 4 weeks, when gel-bound factor was still present, consistently with the described function of VEGF as a negative regulator of pericyte function through formation

of non-functional VEGFR-2/PDGFR-β complexes and consequent inhibition of PDGFR-β phosphorylation (24). When exogenous α_2-PI_{1-8}-VEGF-A_{164} became exhausted, more than 60% of the vascular structures induced by this excessively high dose disappeared, indicating that they could not stabilize despite sustained VEGF release for at least 4 weeks.

The high tunability of the fibrin-bound delivery platform allowed us to span an extremely wide range of VEGF doses, including those determining the transition between normal and aberrant angiogenesis, which is a key feature for the design of preclinical dose-escalation studies. It should be noted that we chose to deliver the syngenic mouse recombinant factor $mVEGF_{164}$ instead of the clinically used human homolog $hVEGF_{165}$ because the experiments were performed in a mouse model and we recently found that the dose-dependent effects of VEGF are species-specific (25). In fact, even though hVEGF is similarly efficient to mVEGF in inducing angiogenesis in mouse muscle at lower doses, species-dependent differences in the relative activation of the respective receptors specifically mask the toxic effects of high doses of the human factor in mouse tissue.

The concentration of α_2-PI_{1-8}-$VEGF_{164}$ had not effect on the amount of induced vasculature, since already the lowest dose caused the maximum increase in vessel length density, which was maintained over a 500-fold range. However, the dose of α_2-PI_{1-8}-$VEGF_{164}$ influenced the size of induced vessels, which remained unaffected by doses up to 0.1 µg/ml, but was significantly increased by 5 µg/ml. These results are relevant for the therapeutic potential of α_2-PI_{1-8}-$VEGF_{164}$ delivery, as others and we have previously found that the size of newly induced vessels is key to determine the efficacy of therapeutic

angiogenesis approaches (18, 26). In fact, using a highly controlled cell-based VEGF gene delivery approach in a hindlimb ischemia model, we found that blood flow could be restored only if vessels were increased both in number and size, while a similar increase in number without change in size provided no therapeutic benefit (18).

Based on these considerations we chose a concentration of 2 μg/ml to test the ability of fibrin-bound α_2-PI_{1-8}-$VEGF_{164}$ delivery to induce functional improvement in an ischemic wound healing model. The treatment with α_2-PI_{1-8}-$VEGF_{164}$ stimulated a significant increase in normal angiogenesis, which significantly improved tissue perfusion both in non-ischemic and ischemic tissues. The angiogenic stimulus induced a significant improvement of the wound closure in ischemic conditions and a positive trend towards improvement in non-ischemic tissues. Interestingly, in control (untreated) conditions ischemia significantly slowed wound healing compared to normal tissue (55% vs 38% still open wound size by 7 days) and α_2-PI_{1-8}-$VEGF_{164}$ treatment restored healing in ischemia to the non-ischemic level (36% still open wound size by 7 days). In non-ischemic tissue α_2-PI_{1-8}-$VEGF_{164}$ treatment provided a further benefit (28% still open wound size by 7 days), but the magnitude of the difference was insufficient to reach statistical significance. These data suggest that, in the absence of ischemia, tissue repair proceeds already at physiological speed and increased blood flow could improve it only marginally, whereas in ischemic conditions impaired perfusion is the critical factor limiting wound healing and α_2-PI_{1-8}-$VEGF_{164}$ treatment may unfold its therapeutic effect.

5.5 Conclusions

In conclusion, here we developed an optimized and highly tunable platform for controlled in vivo delivery of fibrin-bound α_2-PI_{1-8}-$VEGF_{164}$, capable of reliably inducing normal, stable and functional angiogenesis in skeletal muscle, as well as improved perfusion and accelerated healing in ischemic wounds. Further studies should take advantage of the exquisite dose control afforded by this system to identify the therapeutic window of fibrin-bound α_2-PI_{1-8}-$VEGF_{164}$ for the treatment of limb and cardiac ischemia. In fact, while we found a wide range of VEGF concentrations that induce normal angiogenesis with equal efficiency, differences in the size of induced micro-vessels may produce significant disparities in therapeutic efficacy, which should be carefully determined in view of a clinical application.

References

1. Carmeliet, P., and Jain, R.K. 2011. Molecular mechanisms and clinical applications of angiogenesis. *Nature* 473:298-307.
2. Gupta, R., Tongers, J., and Losordo, D.W. 2009. Human studies of angiogenic gene therapy. *Circ Res* 105:724-736.
3. Yla-Herttuala, S., Markkanen, J.E., and Rissanen, T.T. 2004. Gene therapy for ischemic cardiovascular diseases: some lessons learned from the first clinical trials. *Trends Cardiovasc Med* 14:295-300.
4. Karvinen, H., and Yla-Herttuala, S. 2010. New aspects in vascular gene therapy. *Curr Opin Pharmacol* 10:208-211.
5. Park, J.E., Keller, G.A., and Ferrara, N. 1993. The vascular endothelial growth factor (VEGF) isoforms: differential deposition into the subepithelial extracellular matrix and bioactivity of extracellular matrix-bound VEGF. *Mol Biol Cell* 4:1317-1326.
6. Ozawa, C.R., Banfi, A., Glazer, N.L., Thurston, G., Springer, M.L., Kraft, P.E., McDonald, D.M., and Blau, H.M. 2004. Microenvironmental VEGF concentration, not total dose, determines a threshold between normal and aberrant angiogenesis. *J Clin Invest* 113:516-527.
7. Dor, Y., Djonov, V., Abramovitch, R., Itin, A., Fishman, G.I., Carmeliet, P., Goelman, G., and Keshet, E. 2002. Conditional switching of VEGF provides new insights into adult neovascularization and pro-angiogenic therapy. *EMBO J* 21:1939-1947.
8. Tafuro, S., Ayuso, E., Zacchigna, S., Zentilin, L., Moimas, S., Dore, F., and Giacca, M. 2009. Inducible adeno-associated virus vectors promote functional angiogenesis in adult organisms via regulated vascular endothelial growth factor expression. *Cardiovasc Res* 83:663-671.
9. Tayalia, P., and Mooney, D.J. 2009. Controlled growth factor delivery for tissue engineering. *Advanced materials* 21:3269-3285.
10. Banfi, A., von Degenfeld, G., and Blau, H.M. 2005. Critical role of microenvironmental factors in angiogenesis. *Current atherosclerosis reports* 7:227-234.
11. Breen, A., O'Brien, T., and Pandit, A. 2009. Fibrin as a delivery system for therapeutic drugs and biomolecules. *Tissue Eng Part B Rev* 15:201-214.
12. Schense, J.C., Bloch, J., Aebischer, P., and Hubbell, J.A. 2000. Enzymatic incorporation of bioactive peptides into fibrin matrices enhances neurite extension. *Nat Biotechnol* 18:415-419.
13. Ehrbar, M., Djonov, V.G., Schnell, C., Tschanz, S.A., Martiny-Baron, G., Schenk, U., Wood, J., Burri, P.H., Hubbell, J.A., and Zisch, A.H. 2004. Cell-demanded liberation of VEGF121 from fibrin implants induces local and controlled blood vessel growth. *Circ Res* 94:1124-1132.
14. Schmoekel, H.G., Weber, F.E., Schense, J.C., Gratz, K.W., Schawalder, P., and Hubbell, J.A. 2005. Bone repair with a form of BMP-2 engineered for incorporation into fibrin cell ingrowth matrices. *Biotechnology and bioengineering* 89:253-262.

15. Lorentz, K.M., Yang, L., Frey, P., and Hubbell, J.A. 2012. Engineered insulin-like growth factor-1 for improved smooth muscle regeneration. *Biomaterials* 33:494-503.
16. Ehrbar, M., Zeisberger, S.M., Raeber, G.P., Hubbell, J.A., Schnell, C., and Zisch, A.H. 2008. The role of actively released fibrin-conjugated VEGF for VEGF receptor 2 gene activation and the enhancement of angiogenesis. *Biomaterials* 29:1720-1729.
17. Zisch, A.H., Schenk, U., Schense, J.C., Sakiyama-Elbert, S.E., and Hubbell, J.A. 2001. Covalently conjugated VEGF--fibrin matrices for endothelialization. *J Control Release* 72:101-113.
18. von Degenfeld, G., Banfi, A., Springer, M.L., Wagner, R.A., Jacobi, J., Ozawa, C.R., Merchant, M.J., Cooke, J.P., and Blau, H.M. 2006. Microenvironmental VEGF distribution is critical for stable and functional vessel growth in ischemia. *FASEB J* 20:2657-2659.
19. Michlits, W., Mittermayr, R., Schafer, R., Redl, H., and Aharinejad, S. 2007. Fibrin-embedded administration of VEGF plasmid enhances skin flap survival. *Wound repair and regeneration : official publication of the Wound Healing Society [and] the European Tissue Repair Society* 15:360-367.
20. Schense, J.C., and Hubbell, J.A. 1999. Cross-linking exogenous bifunctional peptides into fibrin gels with factor XIIIa. *Bioconjugate chemistry* 10:75-81.
21. Lorentz, K.M., Kontos, S., Frey, P., and Hubbell, J.A. 2011. Engineered aprotinin for improved stability of fibrin biomaterials. *Biomaterials* 32:430-438.
22. Armulik, A., Genove, G., and Betsholtz, C. 2011. Pericytes: developmental, physiological, and pathological perspectives, problems, and promises. *Dev Cell* 21:193-215.
23. Springer, M.L., Ozawa, C.R., Banfi, A., Kraft, P.E., Ip, T.K., Brazelton, T.R., and Blau, H.M. 2003. Localized arteriole formation directly adjacent to the site of VEGF-induced angiogenesis in muscle. *Mol Ther* 7:441-449.
24. Greenberg, J.I., Shields, D.J., Barillas, S.G., Acevedo, L.M., Murphy, E., Huang, J., Scheppke, L., Stockmann, C., Johnson, R.S., Angle, N., et al. 2008. A role for VEGF as a negative regulator of pericyte function and vessel maturation. *Nature* 456:809-813.
25. Mujagic, E., Gianni-Barrera, R., Trani, M., Patel, A., Gurke, L., Heberer, M., Wolff, T., and Banfi, A. 2013. Induction of aberrant vascular growth, but not of normal angiogenesis, by cell-based expression of different doses of human and mouse VEGF is species-dependent. *Human gene therapy methods* 24:28-37.
26. Korpisalo, P., Hytonen, J.P., Laitinen, J.T., Laidinen, S., Parviainen, H., Karvinen, H., Siponen, J., Marjomaki, V., Vajanto, I., Rissanen, T.T., et al. 2011. Capillary enlargement, not sprouting angiogenesis, determines beneficial therapeutic effects and side effects of angiogenic gene therapy. *European heart journal* 32:1664-1672.

6. Recombinant PDGF-BB and $VEGF_{164}$ balanced co-delivery from fibrin gel normalizes aberrant angiogenesis induced from high $VEGF_{164}$ concentrations.

6.1 Introduction

Therapeutic angiogenesis, i.e. the growth of new blood vessels promoted by delivery of vascular growth factors, is an attractive strategy for treating debilitating occlusive vascular diseases, but also to promote engraftment and survival of engineered transplanted tissue. Vascular endothelial growth factor (VEGF) is the master regulator of both physiological and pathological vascular growth (1). Despite the VEGF potency, results of placebo-controlled clinical trials of VEGF gene therapy for both peripherical and coronary artery disease have been unsuccessful until now (2). Retrospective analyses determined several issues that have not been adequately considered in the first generation of clinical trials and that could benefit for the therapeutic results (3, 4). Among these, two limitations of VEGF-based gene therapy arise from biological properties of the VEGF, specifically the need to control the microenviromental VEGF distribution *in vivo* to induce safe and therapeutic angiogenesis, and the requirement of prolonged expression for 4 weeks to avoid regression (5-7).

VEGF is absolutely required to induce new blood vessel growth; nevertheless physiological growth of blood vessels is a complex multi-step process that requires the temporal and spatial co-ordination of different cell populations and cell types (1). In fact blood vessel maturation and subsequent stabilization depends on the coordinated cross-talk of multiple signaling pathways between the endothelium and pericytes (8). VEGF indeed initiate endothelial cells proliferation and migration to form the new tubular structures, whereas platelet-derived growth factor –BB (PDGF–BB) expressed by the migrating tip cells

promotes vessels stabilization by recruiting pericytes (8). Therefore, combinatorial therapy based on growth factors promoting both endothelial cell proliferation and pericyte recruitment is an attractive strategy to overcome VEGF limitations that became evident in the first generation of clinical trials (9). Taking advantage on an highly controlled cell-based gene delivery platform, we recently found that the balanced co-expression of PDGF-BB with $VEGF_{164}$ from a single retroviral bicistronic construct prevented aberrant vascular growth by uncontrolled VEGF levels, inducing only mature and stable capillary networks. Further, the balanced co-expression of PDGF-BB and VEGF significantly improved blood flow and collateral arteries growth in hindlimb ischemia, whereas cells expressing VEGF alone just modestly improved blood flow (10). Besides, recent data from our group indicate that PDGF-BB co-expression accelerates the stabilization of vessels induced by heterogeneous VEGF levels, so that 50% of new vessels were already VEGF-independent after 2 weeks, whereas none was stable when VEGF was expressed alone (11).

The use of recombinant growth factor (GFs) for clinical application of these biological concepts would present several desirable aspects compared to gene therapy approaches, such as the lack of genetic modifications, the homogenous dose-distribution and the limited duration of the treatment. However, clinical application of GFs delivery for therapeutic angiogenesis *in vivo* it has been limited until now because of their rapid degradation. Controlled-release of recombinant protein through biodegradable matrices is an attractive approach to protect the growth factor from rapid clearance, while guarantying homogenous and sustained delivery (12). Pro-angiogenic factors such as VEGF

and PDGF-BB have heparin-binding domains that localize them in the extracellular matrix after secretion and their restricted spatial organization within the microenvironment is crucial to induce physiological angiogenesis.

(13). Thus, we previously developed a protein engineering approach that enzymatically links recombinant growth factors (GFs) to fibrin (14), which is a convenient reservoir for growth factors, since is physiologically present during blood coagulation cascade, can be injected as liquid and allow solidification in situ without cytotoxicity, and can be degraded by cell-associated proteases that are naturally remodeling the matrix (15). Engineered proteins are fused with the factor XIIIa substrate sequence α_2-P_{1-8} (NQEQVSPL), to allow covalent binding by factor XIIIa during cross-linking reaction, and subsequent release by cell-associated proteases that are locally remodeling the matrix (16). In chapter 5, we demonstrated that the controlled release of α_2-PI_{1-8}-$VEGF_{164}$ from an optimized fibrin matrix is a suitable system to induce normal, stable and functional angiogenesis. However, the co-delivery of α_2-PI_{1-8}-PDGF-BB with α_2-PI_{1-8}-$VEGF_{164}$ is a strategy to potentially expand the range of α_2-PI_{1-8}-$VEGF_{164}$ concentrations within which normal angiogenesis can be reliably induced and enhance vessels stabilization. Therefore, here we aim to determine if α_2-PI_{1-8}-PDGF-BB co-delivery with α_2-PI_{1-8}-$VEGF_{164}$ from fibrin gel can prevent aberrant angiogenesis induced from high α_2-PI_{1-8}-$VEGF_{164}$ levels alone and promote the growth of mature and stable vessels.

6.2 Material and Methods

α_2PI_{1-8}-proteins production and purification

Recombinant α_2-PI_{1-8}-$VEGF_{164}$ and aprotinin- α2-PI1-8 were produced as previously described (Sacchi et al, Chapter 1;(17)). PDGF-BB was designed to contain the factor XIIIa sensitive sequence derived from α_2-plasmin inhibitor (α_2-$PI_{1-8,}$ NQEQVSPL) at the N-terminus. Sequence encoding for α_2-PI_{1-8}-PDGF-BB was synthetized by Genscript and subcloned into the mammalian expression vector pXLG (Protein Expression Core Facility, Ecole Polytechique Fédérale de Lausanne, Switzerland). In addition, a 6 x His tag was added at the C-terminus for further purification. Suspension-adapted HEK-293E cells were routinely maintained in serum-free ExCell 293 medium (SAFC Biosciences, Lenexa, KS, USA) with 4 mM glutamine as described (18). The day of transfection cells were resuspended at a density of 100 x 10^6 cells in 5 mL of RPMI 1640 medium with 0.1% pluronic F68 (SAFC Biosciences, Lenexa, KS, USA) in a TubeSpin bioreactor 50 tubes (TPP, Trasadingen, Switzerland). Plasmid DNA of α_2-PI_{1-8}-PDGF-BB (125 µg) and polyethylenimine (250 *µ*g; 1 mg/mL in H_2O; Polysciences, Eppelheim, Germany) were sequentially added and mixed. Seven days post-transfection, the cell culture medium containing α_2-PI_{1-8}-PDGF-BB was recovered by centrifugation at 1'500 rpm for 10 min and filtered through a 0.22 µm filtre. Medium containing α_2-PI_{1-8}-PDGF-BB was loaded into a HisTrap HP 5 mL column (GE Healthcare, Munich, Germany), using a ÄKTA Explorer (GE Healthcare, Munich, Germany). After extensive washing of the column with

binding buffer, α_2-PI_{1-8}-PDGF-BB was eluted with a gradient of 1 M imidazole for 15 column volums. Fractions of proteins were analyzed by SDS-PAGE and those containing $\alpha 2PI_{1-8}$-PDGF-BB were pulled together and further dialyzed against PBS overnight at 4 °C. The solution was then sterile-filtered through a 0.22 µm filter and concentrated with Amicon tube (10 kDA cutoff, Millipore, MerckKGaA, Darmstadt, Germany), before storage at –80°C. The concentration of $\alpha 2PI_{1-8}$-PDGF-BB was determined using ELISA (Human PDGF-BB DuoSet, R&D systems, Abingdon, UK) and the protein was verified as >99% pure by SDS-PAGE and MALDI-TOF.

Fibrin gels preparation

Fibrin matrices were prepared by mixing human fibrinogen at 25 mg/ml (plasminogen-, von Willebrand Factor-, and fibronectin-depleted; Enzymes Research Laboratories, Swansea, UK), factor XIIIa at 2 U/ml (CSL Behring, Switzerland) and thrombin at 2 U/ml (Sigma Aldrich, St Louis, Buchs, Switzerland) with 2.5 mM of Ca^{2+}(Sigma Aldrich, St Louis, Buchs, Switzerland) in 4-(2-hydroxyethyl)-1-piperazineethanesulfonic acid (HEPES) (Lonza, Basel, Switzerland). Matrices containing aprotinin-α_2-PI_{1-8}, α_2-PI_{1-8}-$VEGF_{164}$ and α_2-PI_{1-8}-PDGF-BB were obtained by adding the specific concentrations of them to the cross-linking enzymes solution. Matrices were directly injected after mixing to have in situ polymerization.

Intramuscular fibrin gel implantation in vivo

Matrices were prepared as described in in the previous paragraph. In order to avoid an immunological response to human fibrinogen and cross-linking enzymes, we used 6-8 week-old immunodeficient SCID CB.17 mice (Charles River Laboratories, Sulzfeld, Germany). Animals were treated in accordance with the Swiss Federal guidelines for animal welfare, after approval from the Veterinary Office of the Canton of Basel-Stadt (Basel, Switzerland). A liquid volume of 50µl was aspirated rapidly with a 0.3 ml insulin syringe with integrated 30 G needle (Micro-Fine Cat. No. 320837, Becton Dickinson, Allschwil, Switzerland) and injected into the gastrocnemius (GC) muscle of the mice previously anesthetized with 3% isofluorane. After injection, in situ polymerization was allowed for 20 seconds before slowly extracting the needle.

Histological analyses

Mice were anesthetized and the tissues were fixed by vascular perfusion of 1% paraformaldehyde (Sigma Aldrich, St Louis Buchs, Switzerland) in PBS (Sigma Aldrich, St Louis Buchs, Switzerland) pH 7.4 for 3 minutes under 120 mm/Hg of pressure. GC muscles were harvested, post-fixed in 0.5 % paraformaldehyde (PFA) in PBS pH 7.4 for 2 h at room temperature and cryoprotected by infusion in 30% sucrose (Sigma Aldrich, St Louis Buchs, Switzerland) in PBS at 4 °C overnight. After, muscles were embedded in OCT compound (CellPath, Newtown, Powys, UK), frozen in freezing isopentane and cryosectioned. Tissue sections were stained with H&E to verify the intramuscular localization of the gel. Vascular morphology was analyzed by immunofluorescence staining on 12µm-thick frozen sections of muscle tissue cut across the longitudinal axis.

The following primary antibodies and dilutions were used: rat anti-CD31 (clone MEC 13.3, BD Bioscences, Basel, Switzerland), at 1:100; mouse anti-α-SMA (clone 1A4, Sigma Aldrich, St Louis Buchs, Switzerland), at 1:400; rabbit anti-NG2 (Millipore, MerckKGaA, Darmstadt, Germany), at 1:200. Fluorescently labeled secondary antibodies (Invitrogen, Basel, Switzerland) were used at 1:200. Fluorescent image were taken with 40X objectives on a Carl Zeiss LSM710 3-laser scanning confocal microscope (Carl Zeiss, Feldbach, Switzerland). In some experiments, physiological perfusion of induced vessels was assessed by intravascular staining with a fluorescently labeled *Lycopersicum esculentum* (tomato) lectin (Vector Laboratories, Burlingame, CA,USA), that binds all the luminal surface of blood vessels, as previously described (19). Briefly, mice were anesthetized and lectin was injected intravenously (50µl of a 2 mg/ml lectin solution per mouse) and allowed to circulate for 4 min before vascular perfusion of 1% PFA in PBS pH 7.4 for 3 minutes under 120 mm/Hg of pressure.

Vessel quantifications

Vessels diameters and length density were measured in muscle tissue cryosection after staining for CD31, NG2 and SMA as previously described (6, 19). Briefly, vessel diameters were measured by overlaying captured microscopic images with a square grid. Squares were selected at random, and the diameter of each vessel (if any) in the defined square was measured (in µm). Around 500 total vessels diameter measurements were obtained from 3 independent muscles per each group (n=3). Vessel length density was

measured from 5 to 10 fields per muscle and 3 muscles per each group (n=3) by tracing the total length of vessels in each field and dividing it by the area of the field (mm of vessel length/mm^2 of surface area). All analyses were performed using the Cell P imaging software (Olympus, Volketswil, Switzerland). Results are presented as mean ± SEM. All the analyses were performed using the Cell P imaging software (Olympus, Volketswil, Switzerland).

Statistics

Data are presented as means ± SEMs. The significance of differences was evaluated using analysis of variance (ANOVA) followed by the Bonferroni test (for multiple comparisons). $P < 0.05$ were considered statistically significant.

6.3 Results

α_2-PI_{1-8}-PDGF-BB normalizes aberrant angiogenesis induced from high α_2-PI_{1-8}-$VEGF_{164}$ levels

The potential of α_2-PI_{1-8}-PDGF-BB to promote consistent normalization of aberrant angiogenesis was assessed in a previously defined gel composition (fibrinogen 25 mg/ml, factor XIII 2 U/ml, thrombin 2 U/ml) with 25 µg/ml of α_2-PI_{1-8}-$VEGF_{164}$ and 17 µg/ml of aprotinin- α_2-PI_{1-8}, which clearly induced the growth of aberrant vascular structures 9 days after *in vivo* injection (Chapter 5). The α_2-PI_{1-8}-PDGF-BB was inserted in a concentration ratio with α_2-PI_{1-8}-$VEGF_{164}$ 1:3 for proof of the concept, since it has been previously demonstrated that balanced co-delivery from a single bicistronic construct in molar ratio 1:3 was sufficient to normalize aberrant angiogenesis (10), and the quality of induced angiogenesis was assessed after 2 weeks.

As shown in Fig. 1, the negative control group, which contained only aprotinin-α2-PI_{1-8}, did not induce any angiogenesis. α_2-PI_{1-8}-$VEGF_{164}$ per se induced the growth of aberrant vessels, with irregular shape and enlarged diameter, devoid of pericytes and covered with a thick layer of smooth muscle cells (Fig. 1b, asterisks), similar to previously described angioma-like structures (6). The co-delivery of α_2-PI_{1-8}-PDGF-BB with α_2-PI_{1-8}-$VEGF_{164}$ instead completely prevented the growth of aberrant structures and induced an abundant network of only normal and mature capillaries covered by NG2-positive and α-SMA-negative pericytes (Fig. 1c).

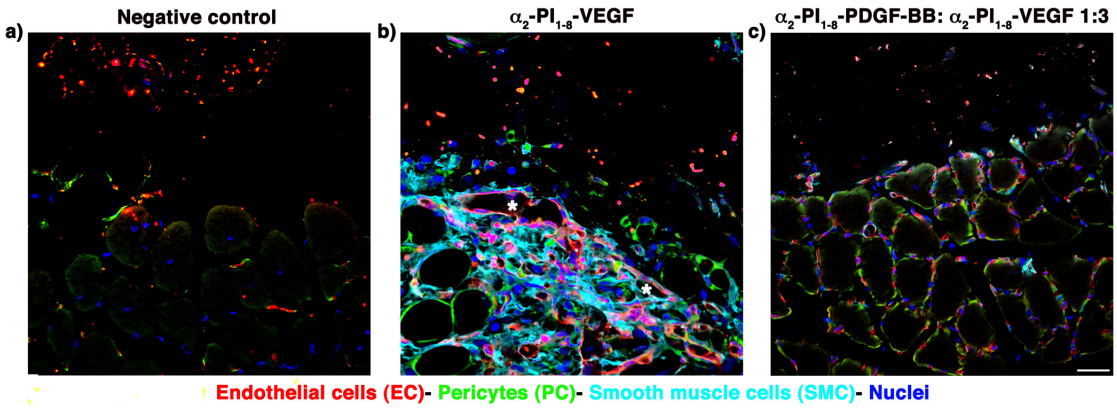

Figure 1 Balanced co-delivery of α_2–$PI_{1\text{-}8}$-PDGF-BB and α_2–$PI_{1\text{-}8}$–$VEGF_{164}$ from fibrin gels in a ratio w/w 1:3 promotes consistent normalization of aberrant angiogenesis.

Fibrin gels of 50 µl containing 17µg/ml of aprotinin-α_2-$PI_{1\text{-}8}$, 25 µg/ml of α_2-$PI_{1\text{-}8}$-$VEGF_{164}$ alone or combined with 8.3 µg/ml of α_2-$PI_{1\text{-}8}$-PDGF-BB (α_2-$PI_{1\text{-}8}$-PDGF-BB:α_2-$PI_{1\text{-}8}$-$VEGF_{164}$ ratio=1:3) were injected into GC muscles and harvested after perfusion-fixation with PFA 1% 2 weeks later. Histological sections were stained for endothelial cells (CD31, in red), pericytes (NG2, in green), and smooth muscle cells (α-SMA, in cyan) and nuclei (DAPI, in blue). Muscles were analyzed for N=3 per group. Scale bar= 20 µm.

A concentration ratio α_2-$PI_{1\text{-}8}$-PDGF-BB: α_2-$PI_{1\text{-}8}$-$VEGF_{164}$ 1:20 is sufficient to normalize aberrant angiogenesis induced from high α_2-$PI_{1\text{-}8}$-$VEGF_{164}$ levels

Since α_2-PI1$_{\text{-}8}$-PDGF-BB and α_2-$PI_{1\text{-}8}$-$VEGF_{164}$ in concentration ratio 1:3 induced the growth of normal and stable capillaries, we sought to determine the minimum concentration of α_2-PI1$_{\text{-}8}$-PDGF-BB necessary to consistently normalize aberrant angiogenesis. Gastrocnemius muscles were injected with gels based on the selected composition described above, with 17µg/ml of aprotinin-α_2-$PI_{1\text{-}8}$ and 25µg/ml, and a 20- fold range of α_2-PI1$_{\text{-}8}$-PDGF-BB concentrations (5µg/ml (1:5), 2.5µg/ml (1:10), 1.25µg/ml (1:20) and 0.25 µg/ml (1:100)). After 2 weeks, α_2-$PI_{1\text{-}8}$-PDGF-BB amounts as low as 1/20th of the α_2-$PI_{1\text{-}8}$-$VEGF_{164}$ concentration consistently normalized aberrant angiogenesis,

promoting the growth of normal capillaries wrapped by pericytes having the characteristically branches processes, with a clearly increased vascular density compared to control (Fig. 2, arrowheads). Conversely, reducing α_2-PI_{1-8}-PDGF-BB down to 1/100th of the α_2-PI_{1-8}-$VEGF_{164}$ concentration abolished this effect and caused the growth of aberrant enlarged vessels, covered by an external coat of smooth muscle cells, as with α_2-PI_{1-8}-$VEGF_{164}$ alone (Fig. 2, asterisks) and pericyte naked-capillaries (Fig.2, arrows).

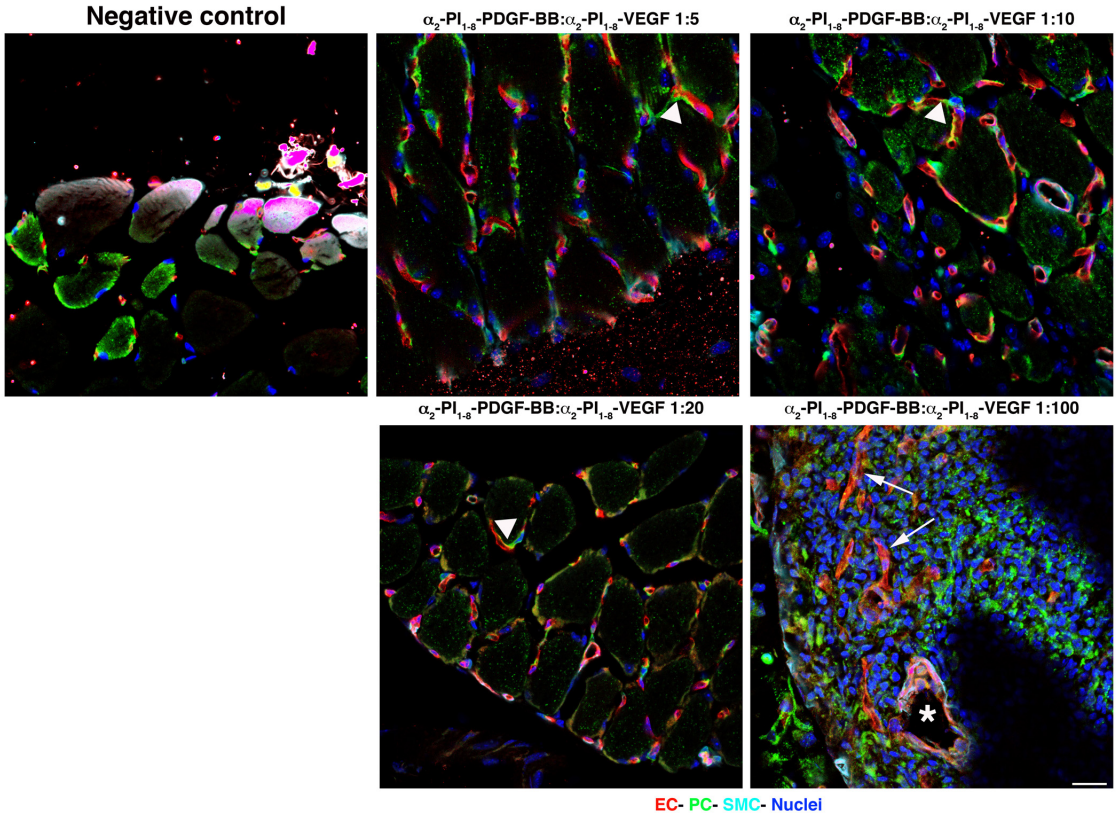

Figure 2 The ratio α_2-PI_{1-8}-PDGF-BB: α2-PI1-8-$VEGF_{164}$ 1:20 is the minimum necessary to induce angiogenesis normalization.

Fibrin gels of 50 µl containing 17µg/ml of aprotinin-α_2-PI_{1-8}, 25 µg/ml of α_2-PI_{1-8}-$VEGF_{164}$ and α_2-PI_{1-8}-PDGF-BB at a concentration of 1/5th, 1/10th, 1/20th and 1/100th of the α_2-PI_{1-8}-$VEGF_{164}$ concentration were injected into GC muscles and harvested after perfusion-fixation with PFA 1% 2 weeks later. Frozen sections were immuno-stained for endothelial cells (CD31, in red), pericytes (NG2, in green), smooth muscle cells (α-SMA, in cyan) and nuclei (DAPI, in blue). Muscles were analyzed for N=3 per group. Scale bar= 20 µm

Co-delivery of α_2-PI_{1-8}-PDGF-BB with a two-fold higher concentration of α_2-PI_{1-8}-$VEGF_{164}$ (50µg/ml) in ratio 1:20 also completely abolished the growth of the angioma-like vessels induced by α_2-PI_{1-8}-$VEGF_{164}$ alone (Fig. 3, asterisks) and promoted the growth of only normal and mature capillaries covered by pericytes (Fig. 3, arrowheads). This confirmed that α_2-PI_{1-8}-PDGF-BB co-delivered in ratio 1:20 with α_2-PI_{1-8}-$VEGF_{164}$ is sufficient to promote consistent aberrant angiogenesis normalization. α_2-PI_{1-8}-PDGF-BB injected alone did not perturb pre-existing angiogenesis into the skeletal muscle (Fig. 3).

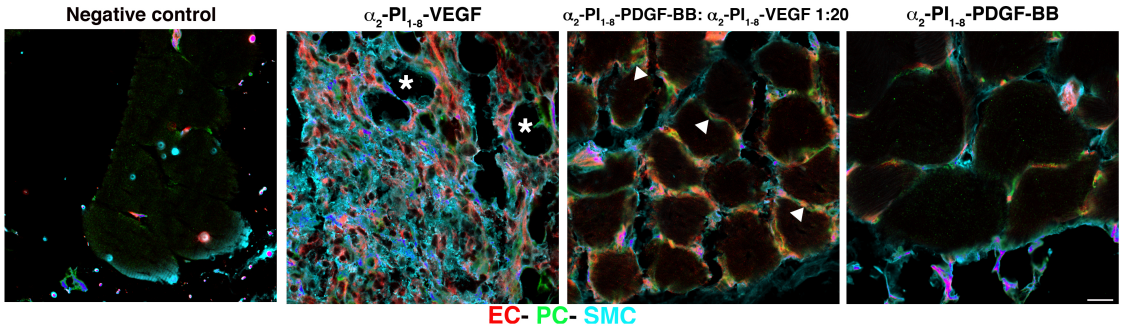

Figure 3 The ratio α_2-PI_{1-8}-PDGF-BB: α_2-PI_{1-8}-$VEGF_{164}$ and not the absolute concentration of the two growth factors is determinant to induce normal angiogenesis.

Fibrin gels of 50 µl containing 17µg/ml of aprotinin-α_2-PI_{1-8}, 50 µg/ml of α_2-PI_{1-8}-$VEGF_{164}$ alone or co-delivered with α_2-PI_{1-8}-PDGF-BB at 1/20th of the α_2-PI_{1-8}-$VEGF_{164}$ concentration were injected into GC muscles and harvested after perfusion-fixation with PFA 1% 2 weeks later. Frozen sections were immuno-stained for endothelial cells (CD31, in red), pericytes (NG2, in green), and smooth muscle cells (α-SMA, in cyan). Scale bar= 20 µm.

Long-term stability of vessels induced by α_2-PI_{1-8}-PDGF-BB and α_2-PI_{1-8}-$VEGF_{164}$ co-delivery

In order to assess whether vessels induced by balanced co-delivery of α_2-PI_{1-8}-PDGF-BB and α_2-PI_{1-8}-$VEGF_{164}$ had stabilized and achieved complete independence from exogenous pro- angiogenic stimulus, we investigated their persistence 2 months after gel injection. Gels loaded with 50 µg/ml of α_2-PI_{1-8}-$VEGF_{164}$ alone or co-delivered with α_2-PI_{1-8}-PDGF-BB at $1/20^{th}$ of the concentration, as well as 50 µg/ml of α_2-PI_{1-8}-PDGF-BB alone, were injected into the GC muscles of SCID mice. In all conditions no trace of the injected gels could be found anymore. Similarly to the 2 weeks-results shown above, α_2-PI_{1-8}-PDGF-BB: α_2-PI_{1-8}-$VEGF_{164}$ balanced co -delivery after 2 months induced normal capillaries wrapped by pericytes (Fig. 4a). On the other hand, α_2-PI_{1-8}-$VEGF_{164}$ alone at this time promoted the growth of only normal and mature capillaries, covered by pericytes, without growth of aberrant vascular structures (Fig. 4a). Quantification of vessels diameter showed that all the three groups, α_2-PI_{1-8}-$VEGF_{164}$ or α_2-PI_{1-8}-PDGF-BB each one alone, or combined together, had homogenous diameter distributions in a narrow range, similar to normal capillaries in control tissues (Fig. 4b). α_2-PI_{1-8}-PDGF-BB induced vessels with the same average diameter as control tissue, whereas the capillaries induced by α_2-PI_{1-8}-$VEGF_{164}$ alone or combined with α_2-PI_{1-8}-PDGF-BB where significantly larger, although homogeneous in size and normal in morphology. Interestingly, co-delivery of α_2-PI_{1-8}-PDGF-BB and α_2-PI_{1-8}-$VEGF_{164}$ induced vessels significantly larger than those induced by α_2-PI_{1-8}-$VEGF_{164}$ alone (fig. 4c, εε $P< 0.01$). In contrast to vessel diameter, the amount of induced vasculature (quantified as vessel length density) was not increased by $_2$-PI_{1-8}-PDGF-BB co-delivery with α_2-PI_{1-8}-$VEGF_{164}$ compared to α_2-PI_{1-8}-$VEGF_{164}$

alone, since both induced about a 2-fold increase in vascular density compared to the negative control (Fig. 4d, ** P< 0.01, *** P< 0.001). Furthermore, α_2-PI_{1-8}-PDGF-BB and α_2-PI_{1-8}-$VEGF_{164}$ co-delivery induced a significant higher amount of vasculature compared to the α_2-PI_{1-8}-PDGF-BB injected alone (Fig. 4d, δ P< 0.05).

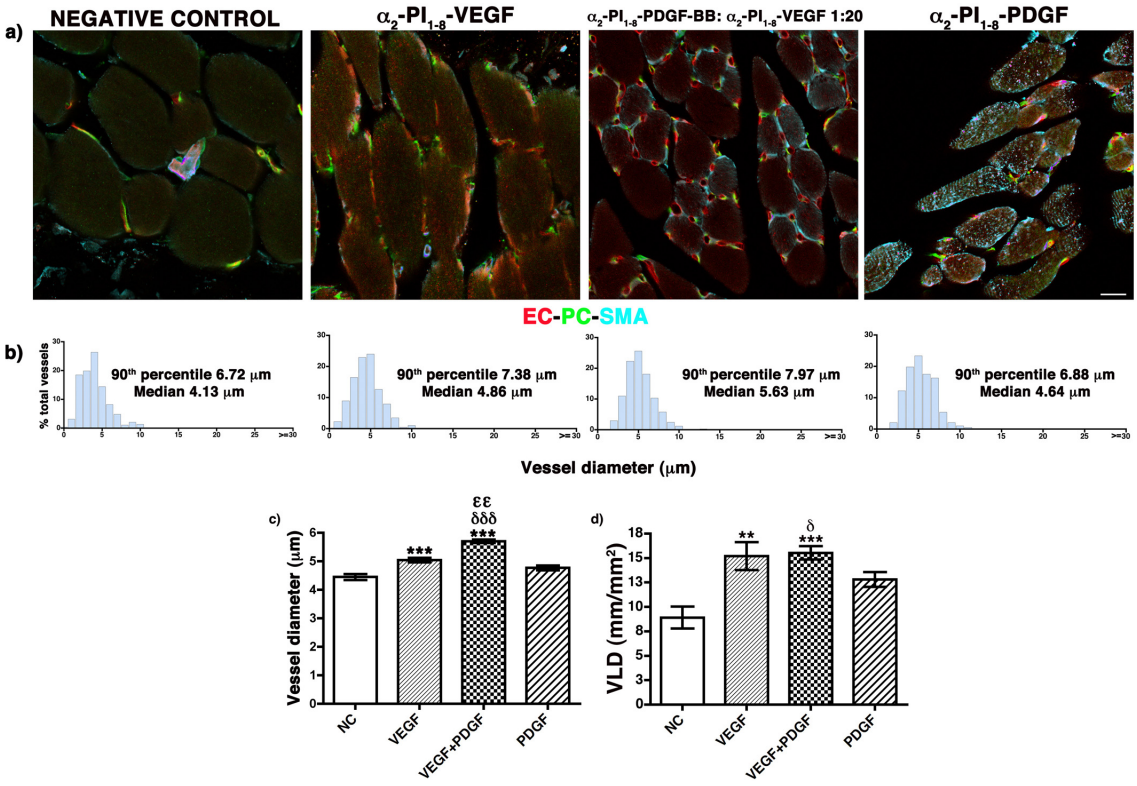

Figure 4 Long-term stability of angiogenesis induced by balanced co-delivery of α_2-PI_{1-8}-PDGF-BB and α_2-PI_{1-8}-$VEGF_{164}$

(a) Fibrin gels of 50µl volume with inserted an aprotinin-α_2-PI_{1-8} concentration of 17µg/ml, 50 µg/ml of α_2-PI_{1-8}-$VEGF_{164}$ alone or in combination with α_2-PI_{1-8}-PDGF-BB at $1/20^{th}$ of the α_2-PI_{1-8}-$VEGF_{164}$ concentration were injected into the GC of SCID mice. α_2-PI_{1-8}-PDGF-BB was tested alone in a concentration of 50 µg/ml to verify its angiogenic potential after 2 months. Endothelial cells (CD31, in red), pericytes (NG2, in green), smooth muscle cells (α-SMA, in cyan) were immuno-stained on frozen section. Scale bar= 20 µm

(b-c) Vessel diameters were quantified in each group and their distribution (b) and average values (µm) (c) were calculated. (d) The amount of angiogenesis was quantified as vessel length density (VLD), calculated as the ratio between the total vessel length and the area of each measured field (mm/mm^2). Results in (c)

and (d) are shown as mean ± SEM; n = 3 muscles/group; ***, P< 0.001, ** P<0.01 vs negative control, δδδ P< 0.001, δ P< 0.05 vs α_2-PI_{1-8}-PDGF-BB group, εε P< 0.001 vs α_2-PI_{1-8}-$VEGF_{164}$ group.

Newly induced vessels by balanced co-delivery of and α_2-PI_{1-8}-PDGF-BB and α_2-PI_{1-8}-$VEGF_{164}$ are functionally perfused

In order to determine whether newly induced vessels were functionally connected to the circulation, their perfusion was assessed by injecting mice 4 minutes before sacrifice with a fluorescein-labeled tomato lectin (FITC-lectin), which binds to the lumen of all vessels connected to the general circulation. Perfused endothelial structures were identified by immuno-staining as double-positive for CD31 and FITC-lectin on frozen sections. As shown in Figures 5 and 6, essentially all vessels induced both by α_2-PI_{1-8}-$VEGF_{164}$ alone and by co-delivery of α_2-PI_{1-8}-PDGF-BB and α_2-PI_{1-8}-$VEGF_{164}$ were functionally perfused after 2 weeks (Fig. 5) and 2 months (Fig. 6). Therefore, balanced co-delivery of α_2-PI_{1-8}-PDGF-BB and α_2-PI_{1-8}-$VEGF_{164}$ induced the growth of morphologically normal and mature vessels that are both stable and functionally perfused.

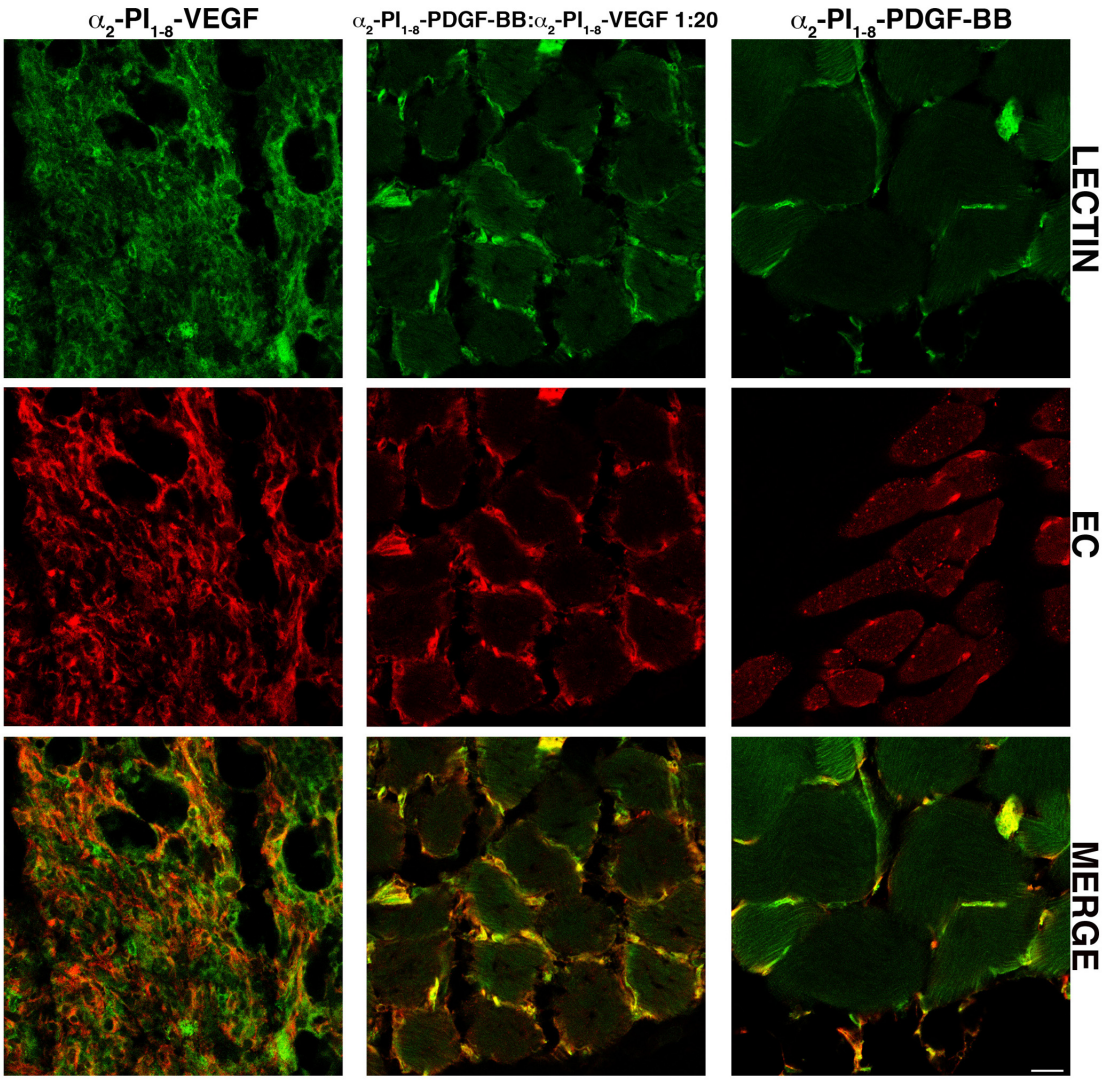

Figure 5 Newly Induced vessels by balanced co-delivery of α_2-PI$_{1-8}$-PDGF-BB and α_2-PI$_{1-8}$-VEGF$_{164}$ are functionally perfused after 2 weeks.

FITC-lectin was injected intravenously into mice 4 weeks after gel injection, just before perfusion with PFA 1% and sacrifice. Muscles cryosections were immuno-stained to detect endothelial cells (CD31, in red), while lectin shows in green. Perfused vessels were identified as double-positive for CD31 and FITC-lectin, appearing yellow in the merged image. Scale bar = 20 µm

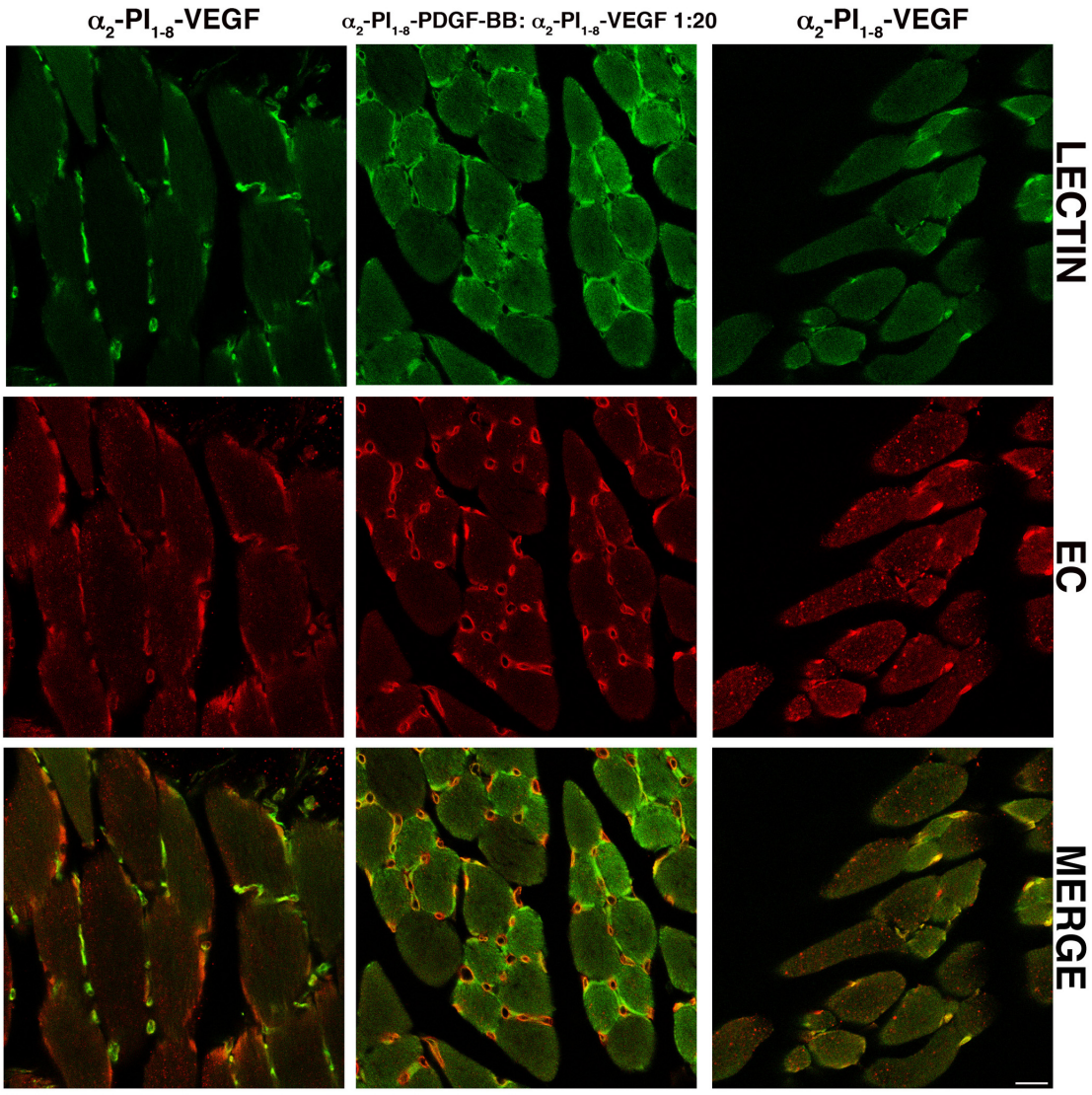

Figure 6 Newly Induced vessels by balanced co-delivery of α_2-PI$_{1-8}$-PDGF-BB and α_2-PI$_{1-8}$-VEGF$_{164}$ are functionally perfused after 2 months.

FITC-lectin was injected intravenously into mice 4 weeks after gel injection, just before perfusion with PFA 1% and sacrifice. Muscles cryosections were immuno-stained to detect endothelial cells (CD31, in red), while lectin shows in green. Perfused vessels were identified as double-positive for CD31 and FITC-lectin, appearing yellow in the merged image. Scale bar = 20 µm.

Short-term co-delivery of α_2-PI$_{1-8}$-PDGF-BB and α_2-PI$_{1-8}$-VEGF$_{164}$ not only normalizes aberrant angiogenesis induced by high α_2-PI$_{1-8}$-VEGF$_{164}$ levels, but also increases diameters of morphologically normal vessels induced by α_2-PI$_{1-8}$-VEGF$_{164}$ at a safe concentration

In order to determine whether the balanced co-delivery of α_2-PI$_{1-8}$-PDGF-BB: α_2-PI$_{1-8}$-VEGF$_{164}$ not only promoted normalization of aberrant angiogenesis induced from high α_2-PI$_{1-8}$-VEGF$_{164}$ levels but also accelerates vascular stabilization, we used the same gel composition as previous experiment but without aprotinin-α_2-PI$_{1-8}$, thus lasting *in vivo* around 9 days (Chapter 5). Fibrin gels were prepared with two different α_2-PI$_{1-8}$-VEGF$_{164}$ concentrations, 5µg/ml and 50µg/ml, individually or combined with α_2-PI$_{1-8}$-PDGF-BB at 1/20th of the α_2-PI$_{1-8}$-VEGF$_{164}$ concentration. After 2 weeks in all conditions the gel was completely exhausted. α_2-PI$_{1-8}$-VEGF$_{164}$ was delivered alone at a concentration of 5 µg/ml induced the growth of normal capillaries covered by pericytes (fig. 7b). Interestingly, quantification of vessel diameters showed that 5µg/ml of α_2-PI$_{1-8}$-VEGF$_{164}$ induced vessels significantly larger than negative control (Fig. 7k, *** $P< 0.001$), but co-delivery of α_2-PI$_{1-8}$-PDGF-BB and α_2-PI$_{1-8}$-VEGF$_{164}$ further increased the induced vessels size compared to α_2-PI$_{1-8}$-VEGF$_{164}$ alone (Fig. 7k, δδδ $P< 0.001$), while both having homogenous diameter distribution on the range of normal capillaries (Fig. 7 g-i). α_2-PI$_{1-8}$-VEGF$_{164}$ injected alone at a concentration of 50 µg/ml caused the growth of enlarged angioma-like structures coated by a thick layer of smooth muscle cells (fig. 7c, asterisks) and capillaries devoid of pericytes (fig. 7c, arrows). The balanced co-delivery

prevented the growth of aberrant vessels induced from the highest α_2-PI_{1-8}-$VEGF_{164}$ concentration *per se* at the highest concentration and promoted the maturation of capillaries, which are in this group tightly covered by pericytes (fig. 7e).

Quantification of vessels diameters showed that interestingly, the highest α_2-PI_{1-8}-$VEGF_{164}$ concentration had homogenous vessels distribution in the range of normal capillaries, as when co-delivered with α_2-PI_{1-8}-PDGF-BB, and rare enlarged aberrant vessels (Fig. 7 h-j). This small group of aberrant did not increase the 90th percentile towards value characteristic of aberrant angiogenesis, indicating the most of the vessels are in the range size of normal capillaries (Fig. 7h). Both α_2-PI_{1-8}-$VEGF_{164}$ injected alone or combined with α_2-PI_{1-8}-PDGF-BB induced similar average vessels size, both statistically significantly higher than control (Fig. 7, *** $P< 0.001$). Quantification of the amount of induced angiogenesis as vessel length density (VLD), showed that the co-delivery of α_2-PI_{1-8}-PDGF-BB and α_2-PI_{1-8}-$VEGF_{164}$, when α_2-PI_{1-8}-$VEGF_{164}$ at a concentration of 5µg/ml, did not significantly increase the amount of vasculature induced compared to α_2-PI_{1-8}-$VEGF_{164}$, since both lead about a 2-fold increase compared to negative control (Fig. 7l *** $P< 0.001$ vs negative control). Both co-delivery of α_2-PI_{1-8}-PDGF-BB and α_2-PI_{1-8}-$VEGF_{164}$ when α_2-PI_{1-8}-$VEGF_{164}$ was at a concentration of 50 µg/ml induced a similar increase of vessel length density compared to control without statistical significant differences between the two groups (** $P< 0.01$, * $P< 0.05$ vs negative control). Further investigations are necessary to define if such a short-term co-delivery is sufficient to achieve vessels stabilization.

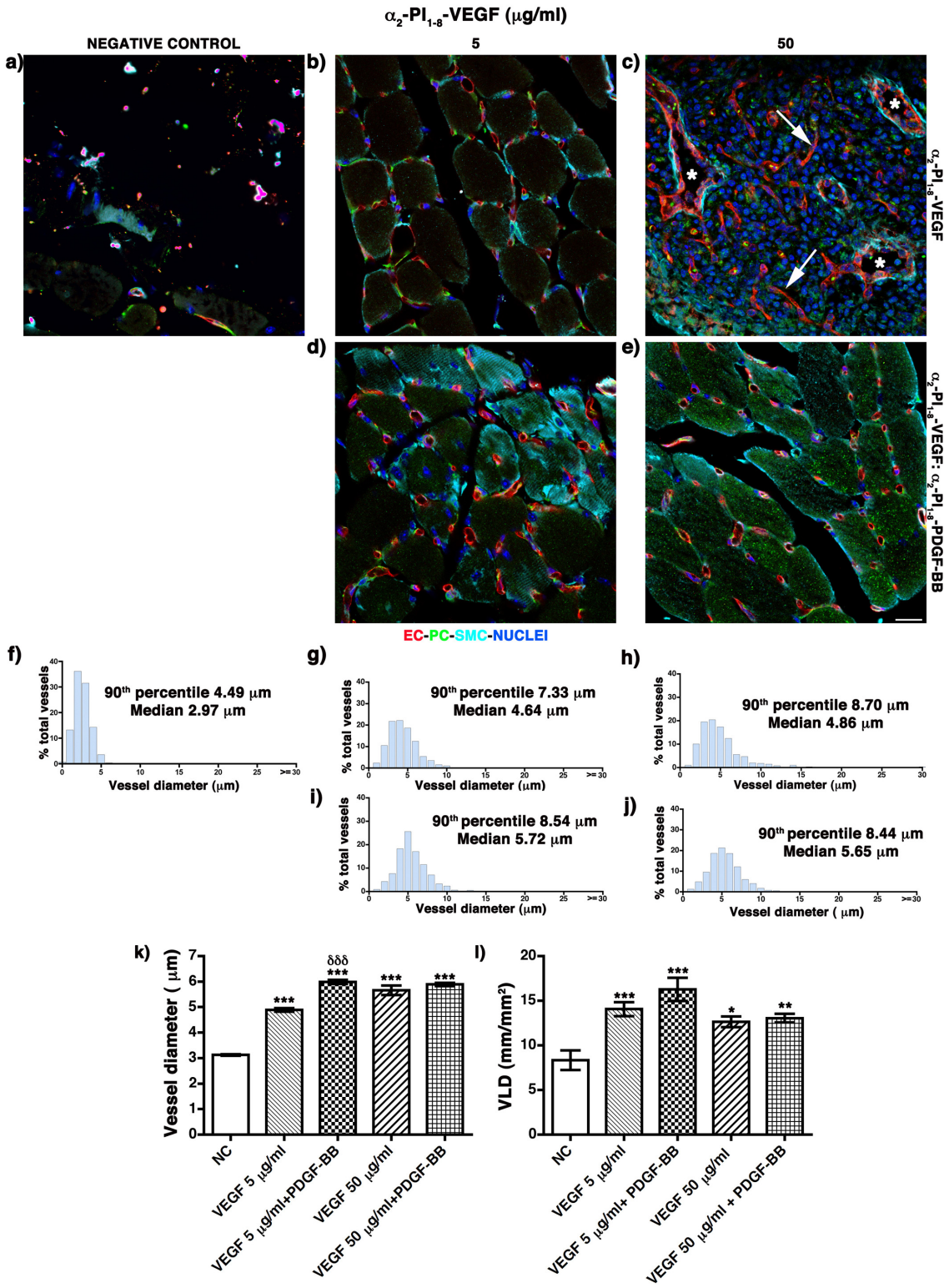

Figure 7 Short term co-delivery of α_2-PI$_{1-8}$-PDGF-BB and α_2-PI$_{1-8}$-VEGF$_{164}$ not only normalize aberrant angiogenesis induced by high α_2-PI$_{1-8}$-VEGF$_{164}$ levels, but also increased diameters of morphologically normal vessels induced by α_2-PI$_{1-8}$-VEGF$_{164}$ at a safe concentration.

(a-e) Fibrin gels of 50μl volume with inserted two α_2-PI$_{1-8}$-VEGF$_{164}$ concentration, 5μg/ml and 50μg/ml, alone (b and c) or co-delivered with α_2-P$_{l1-8}$-PDGF-BB at 1/20th of the α_2-PI$_{1-8}$-VEGF$_{164}$ concentration (d

and e), were injected into GC muscles of SCID and harvested 2 weeks later after perfusion with PFA 1%. Endothelial cells (CD31, in red), pericytes (NG2, in green), and smooth muscle cells (α-SMA, in cyan) were immuno-stained on frozen section. Scale bar= 20 μm

(f-k) Vessel diameters were quantified in each group and their distribution (f, negative control: g-h α_2-$PI_{1\text{-}8}$-$VEGF_{164}$ groups, i-j α_2-$P_{I1\text{-}8}$-PDGF-BB and α_2-$PI_{1\text{-}8}$-$VEGF_{164}$ groups) and average values (μm) (k) were calculated. (l) The amount of angiogenesis was quantified as vessel length density (VLD), calculated as the ratio between the total vessel length and the area of each measured field (mm/mm^2). Results in (k) and (l) are shown as mean ± SEM; n = 3 muscles/group; ***, $P< 0.001$, ** $P<0.01$ vs negative control, δδδ $P< 0.001$, δ $P< 0.05$ vs α_2-$PI_{1\text{-}8}$-PDGF-BB group. Balanced co-delivery of α_2-$P_{I1\text{-}8}$-PDGF-BB and α_2-$PI_{1\text{-}8}$-$VEGF_{164}$ significantly increased the size of vessels induced from the lowest α_2-$PI_{1\text{-}8}$-$VEGF_{164}$ concentration.

6.4 Discussion

Here we showed that balanced co-delivery of α_2-PI_{1-8}-PDGF-BB and α_2-PI_{1-8}-$VEGF_{164}$ by fibrin gel in concentration ratio 1:20 could normalize aberrant angiogenesis induced by high α_2-PI_{1-8}-$VEGF_{164}$ levels alone, promoting the growth of normal, stable and functional capillaries. Thus, this is a potential strategy to reliably induce normal and stable angiogenesis without the need to strictly control the α_2-PI_{1-8}-$VEGF_{164}$ concentration. Further, taking advantage of this highly flexible tool that allow an easy variation of the growth factors ratio, we could assess that α_2-PI_{1-8}-PDGF-BB at $1/20^{th}$ of the α_2-PI_{1-8}-$VEGF_{164}$ concentration is the minimum concentration necessary to normalize aberrant angiogenesis. This ratio was validated using a second higher α_2-PI_{1-8}-$VEGF_{164}$ concentration, confirming that absolute levels of the two growth factors were not important as the relative dosage present in the microenviroment of the growing vessels. It is relevant the definition that a 5-fold less amount of α_2-PI_{1-8}-PDGF-BB compared to what previously defined using cell-based and viral gene delivery (10) is sufficient to prevent the loss of pericytes and convert vascular remodeling into a network of mature homogenous capillaries. However, further investigations are necessary to identify if the reducing of α_2-PI_{1-8}-PDGF-BB from $1/3^{rd}$ to $1/20^{th}$, which did not affect the normalization effect, had an effect on the vessel size and amount of induced vasculature.

After 2 months, α_2-PI_{1-8}-$VEGF_{164}$ injected alone induced only normal and mature capillaries, as when co-delivered with α_2-PI_{1-8}-PDGF-BB and in contrast to the aberrant vessels induced after 2 weeks. However, the balanced co-delivery of

α_2-PI_{1-8}-PDGF-BB and α_2-PI_{1-8}-$VEGF_{164}$ produce vessels significantly larger than those induced from α_2-PI_{1-8}-$VEGF_{164}$ injected alone. These results can have an impact on the therapeutic potential of the system, as others and we have previously found that the size of newly induced vessels is key to determine the efficacy of therapeutic angiogenesis approaches (19, 20).

The normalization potential of α_2-PI_{1-8}-PDGF-BB was maintained even when we did not use aprotinin-α_2-PI_{1-8} and thus growth factor release was accelerated. Further, in this gel composition, α_2-PI_{1-8}-PDGF-BB increased vessels size induced by α_2-PI_{1-8}-$VEGF_{164}$ alone when α_2-PI_{1-8}-$VEGF_{164}$ was at a concentration of 5 μg/ml, which per se induced normal angiogenesis. This potentially could improve the therapeutic efficacy of this α_2-PI-$_{1-8}$-$VEGF_{164}$ concentration that per se induces normal angiogenesis, since, as discussed above, newly induced vessels size is determinant for therapeutic efficacy in ischemia (19, 20).

6.5 Conclusions and future perspectives

In conclusion, with this work we demonstrated that controlled co-delivery of α_2-$PI_{1\text{-}8}$-$VEGF_{164}$ and α_2-$PI_{1\text{-}8}$-PDGF-BB proteins is a convenient, safe and clinically applicable approach to expand the range of VEGF doses within which normal and stable angiogenesis can be reliably and efficiently induced. Additionally, co-delivery of α_2-$PI_{1\text{-}8}$-PDGF-BB and α_2-$PI_{1\text{-}8}$-$VEGF_{164}$ when is at a low concentration which *per se* induced safe angiogenesis is a strategy to potentiate the possible therapeutic effect by increasing induced vessels size. Further analyses are ongoing to determine the minimum duration of factor co-delivery necessary to achieve vessel stabilization and indefinite persistence, in order to define a complete set of parameters (dose, ratio and duration) for clinical application.

References

1. Carmeliet, P., and Jain, R.K. 2011. Molecular mechanisms and clinical applications of angiogenesis. *Nature* 473:298-307.
2. Gupta, R., Tongers, J., and Losordo, D.W. 2009. Human studies of angiogenic gene therapy. *Circ Res* 105:724-736.
3. Yla-Herttuala, S., Markkanen, J.E., and Rissanen, T.T. 2004. Gene therapy for ischemic cardiovascular diseases: some lessons learned from the first clinical trials. *Trends Cardiovasc Med* 14:295-300.
4. Karvinen, H., and Yla-Herttuala, S. 2010. New aspects in vascular gene therapy. *Curr Opin Pharmacol* 10:208-211.
5. Dor, Y., Djonov, V., Abramovitch, R., Itin, A., Fishman, G.I., Carmeliet, P., Goelman, G., and Keshet, E. 2002. Conditional switching of VEGF provides new insights into adult neovascularization and pro-angiogenic therapy. *EMBO J* 21:1939-1947.
6. Ozawa, C.R., Banfi, A., Glazer, N.L., Thurston, G., Springer, M.L., Kraft, P.E., McDonald, D.M., and Blau, H.M. 2004. Microenvironmental VEGF concentration, not total dose, determines a threshold between normal and aberrant angiogenesis. *J Clin Invest* 113:516-527.
7. Tafuro, S., Ayuso, E., Zacchigna, S., Zentilin, L., Moimas, S., Dore, F., and Giacca, M. 2009. Inducible adeno-associated virus vectors promote functional angiogenesis in adult organisms via regulated vascular endothelial growth factor expression. *Cardiovasc Res* 83:663-671.
8. Gaengel, K., Genove, G., Armulik, A., and Betsholtz, C. 2009. Endothelial-mural cell signaling in vascular development and angiogenesis. *Arterioscler Thromb Vasc Biol* 29:630-638.
9. Reginato, S., Gianni-Barrera, R., and Banfi, A. 2011. Taming of the wild vessel: promoting vessel stabilization for safe therapeutic angiogenesis. *Biochem Soc Trans* 39:1654-1658.
10. Banfi, A., von Degenfeld, G., Gianni-Barrera, R., Reginato, S., Merchant, M.J., McDonald, D.M., and Blau, H.M. 2012. Therapeutic angiogenesis due to balanced single-vector delivery of VEGF and PDGF-BB. *FASEB J* 26:2486-2497.
11. Groppa, E. Manuscritpt in preparation.
12. Tayalia, P., and Mooney, D.J. 2009. Controlled growth factor delivery for tissue engineering. *Advanced materials* 21:3269-3285.
13. Banfi, A., von Degenfeld, G., and Blau, H.M. 2005. Critical role of microenvironmental factors in angiogenesis. *Current atherosclerosis reports* 7:227-234.
14. Schense, J.C., and Hubbell, J.A. 1999. Cross-linking exogenous bifunctional peptides into fibrin gels with factor XIIIa. *Bioconjugate chemistry* 10:75-81.
15. Breen, A., O'Brien, T., and Pandit, A. 2009. Fibrin as a delivery system for therapeutic drugs and biomolecules. *Tissue Eng Part B Rev* 15:201-214.
16. Schense, J.C., Bloch, J., Aebischer, P., and Hubbell, J.A. 2000. Enzymatic incorporation of bioactive peptides into fibrin matrices enhances neurite extension. *Nat Biotechnol* 18:415-419.

17. Lorentz, K.M., Kontos, S., Frey, P., and Hubbell, J.A. 2011. Engineered aprotinin for improved stability of fibrin biomaterials. *Biomaterials* 32:430-438.
18. Muller, N., Girard, P., Hacker, D.L., Jordan, M., and Wurm, F.M. 2005. Orbital shaker technology for the cultivation of mammalian cells in suspension. *Biotechnol Bioeng* 89:400-406.
19. von Degenfeld, G., Banfi, A., Springer, M.L., Wagner, R.A., Jacobi, J., Ozawa, C.R., Merchant, M.J., Cooke, J.P., and Blau, H.M. 2006. Microenvironmental VEGF distribution is critical for stable and functional vessel growth in ischemia. *FASEB J* 20:2657-2659.
20. Korpisalo, P., Hytonen, J.P., Laitinen, J.T., Laidinen, S., Parviainen, H., Karvinen, H., Siponen, J., Marjomaki, V., Vajanto, I., Rissanen, T.T., et al. 2011. Capillary enlargement, not sprouting angiogenesis, determines beneficial therapeutic effects and side effects of angiogenic gene therapy. *Eur Heart J* 32:1664-1672.

7. Summary and future perspectives

Therapeutic angiogenesis, which aims to stimulate the growth of new capillaries from pre-existing ones to increase blood supply and support tissue function and recovery, is a promising strategy both for treating ischemic diseases and support engraftment and survival of transplanted engineered tissues(1, 2). VEGF-A is the master regulator of angiogenesis (3) and thus it has been tested in several clinical trials, but with disappointing results(4).

In this work, we aimed to establish an optimized platform to induce stable and functional angiogenesis in relevant target tissues using recombinant proteins engineered to covalently bind to fibrin gel. In the fifth chapter, we demonstrated that delivery of α_2-PI_{1-8}-$VEGF_{164}$ from fibrin gels is a suitable system to induce angiogenesis in skeletal mouse muscle tissues. The optimization of the different parameters influencing the effective delivered dose of α_2-PI_{1-8}-$VEGF_{164}$ and the duration of the α_2-PI_{1-8}-$VEGF_{164}$ release, such as the fibrin gel composition and the concentration of the plasmin inhibitor aprotinin-α_2-$PI_{1-8,}$ allowed us to reliably induce exclusively normal and mature micro-vascular networks, which were stable and functionally perfused, over a very wide range (at least 500-fold) of α_2-PI_{1-8}-VEGF-A_{164} concentrations. Remarkably, newly induced vessels did not regress for at least 3 months, whereas the injected gels were almost completely degraded by 4 weeks, demonstrating that they achieved independence from exogenous VEGF signaling for their survival and suggesting that they could likely persist indefinitely. This is particularly relevant for the therapeutic potential of this approach, since until now one of the main limits of recombinant protein delivery for therapeutic angiogenesis has been the insufficient duration of GF release to achieve stable and persistent effects(5).

The flexibility of the fibrin-bound delivery platform allowed us to define an extremely wide range of VEGF doses that efficiently induce angiogenesis, including those determining the transition between normal and aberrant vessels, which is a key feature for the design of preclinical dose-escalation studies.

The concentration of α_2-PI_{1-8}-$VEGF_{164}$ did not influence the amount of induced vasculature, which was maximal already with the minimum concentration and was maintained over a 500-fold range. Nevertheless, the concentration of α_2-PI_{1-8}-$VEGF_{164}$ influenced the size of induced vessels, which remained unaffected by concentrations up to 0.1 µg/ml, but was significantly increased by 5 µg/ml. These results are relevant for the therapeutic potential of α_2-PI_{1-8}-$VEGF_{164}$ delivery, as others and we have previously found that the size of newly induced vessels is key to determine the efficacy of therapeutic angiogenesis approaches(6, 7). Based on these considerations, we chose a concentration of 2 µg/ml to test the ability of fibrin-bound α_2-PI_{1-8}-$VEGF_{164}$ delivery to induce functional improvement in an ischemic wound-healing model. The treatment with α_2-PI_{1-8}-$VEGF_{164}$ stimulated a significant increase in normal angiogenesis, which significantly improved tissue perfusion and wound closure in ischemic conditions, restoring healing in ischemia to non-ischemic levels (36% still open wound size by 7 days), thereby demonstrating that α_2-PI_{1-8}-$VEGF_{164}$ from an optimized fibrin platform induced functional improvement in an ischemic model.

These promising results warrant a preclinical evaluation of the therapeutic potential of this approach. The first step will require the comparison of several α_2-PI_{1-8}-$VEGF_{164}$ concentrations, in the range that proved able to induce normal and stable angiogenesis in healthy muscle, for their functional effects in a pre-

clinical model of hind limb ischemia, in order to define the actual therapeutic window. In fact, it has been previously shown that differences in the size of induced vessels may produce significant disparities in therapeutic efficacy (6, 7)and a range of lower doses, which did not show any increase in vessel size, may prove inefficacious. The second step should then focus on the obvious differences between rodents and human patients suffering from ischemic diseases, including physiology, body size and distance over which collateral arteries need to grow, using more relevant large animal models (2).

In the sixth chapter, we determined that balanced co-delivery of α_2-PI_{1-8}-PDGF-BB and α_2-PI_{1-8}-$VEGF_{164}$ from fibrin hydrogels had the potential to normalize aberrant angiogenesis induced by high α_2-PI_{1-8}-$VEGF_{164}$ alone, while also achieving long-term stability. Therefore, this approach provides a tool to expand the range of α_2-PI_{1-8}-$VEGF_{164}$ doses within which normal and stable angiogenesis can be reliably induced. Further, taking advantage of the robust flexibility of this platform, we could determine, with two different α_2-PI_{1-8}-$VEGF_{164}$ concentrations, that complete normalization of induced angiogenesis was ensured by a ratio of α_2-PI_{1-8}-PDGF-BB: α_2-PI_{1-8}-$VEGF_{164}$ as low as 1:20, which is 5-fold lower than the ratio previously defined using cell-based and viral gene delivery (8). Interestingly, co-delivery of α_2-PI_{1-8}-PDGF-BB and α_2-PI_{1-8}-$VEGF_{164}$ produced significantly larger vessels than the same dose of α_2-PI_{1-8}-$VEGF_{164}$ alone, which could have significant therapeutic implications, since, as discussed above, vessel size is the main determinant of therapeutic efficacy in ischemia(6, 7).

α_2-$PI_{1\text{-}8}$-PDGF-BB co-delivery not only increased the size of vessels induced by α_2-$PI_{1\text{-}8}$-$VEGF_{164}$ alone, but also significantly accelerated vascular stabilization, thereby allowing persistent angiogenesis to be generated by fibrin gels with a duration as short as 2 weeks, thereby providing a strategy to potentiate both the therapeutic efficacy and the safety of α_2-$PI_{1\text{-}8}$-$VEGF_{164}$ alone.

Further investigations will be needed in order to rigorously determine the minimum duration of growth factor co-delivery necessary to achieve vessel stabilization and indefinite persistence, to define a complete set of parameters (dose, ratio and duration) for therapeutic applications.

The optimized platform that was developed in the work here described proved also to be a flexible tool for investigating the cellular and molecular mechanisms of VEGF dose- and time-dependent angiogenesis, thanks to its high tunability that allowed us to finely and precisely control VEGF dose over an extremely wide range of concentrations. For instance, our group has previously found, using myoblast-mediated gene delivery, that VEGF over-expression in skeletal muscle at the doses required for therapeutic benefit induces angiogenesis by intussusception rather than by sprouting (9). However, using the cell-based platform it was not possible to investigate whether the induction of intussusceptive angiogenesis rather than sprouting was a function of VEGF dose or a tissue-specific feature of muscle vascular networks. Initial observations we recently obtained with the fibrin-bound platform confirmed that higher concentrations of α_2-$PI_{1\text{-}8}$-$VEGF_{164}$ induce vascular enlargement and splitting (intussusception) around the implanted gel. However, reducing sufficiently the α_2-$PI_{1\text{-}8}$-$VEGF_{164}$ concentration caused a switch in the mode of

angiogenic growth to sprouting inside the gel, suggesting that VEGF dose and gradient shape in the microenvironment dictate the endothelial cell fate decision whether to sprout or to split. Based on these results, the flexibility of this platform is expected to provide valuable insights in the molecular mechanisms underlying the dose-dependent angiogenic response to therapeutic VEGF over-expression in skeletal muscle.

References

1. Bae, H., Puranik, A.S., Gauvin, R., Edalat, F., Carrillo-Conde, B., Peppas, N.A., and Khademhosseini, A. 2012. Building vascular networks. *Sci Transl Med* 4:160ps123.
2. Dragneva, G., Korpisalo, P., and Yla-Herttuala, S. 2013. Promoting blood vessel growth in ischemic diseases: challenges in translating preclinical potential into clinical success. *Dis Model Mech* 6:312-322.
3. Carmeliet, P., and Jain, R.K. 2011. Molecular mechanisms and clinical applications of angiogenesis. *Nature* 473:298-307.
4. Gupta, R., Tongers, J., and Losordo, D.W. 2009. Human studies of angiogenic gene therapy. *Circ Res* 105:724-736.
5. Ehrbar, M., Zeisberger, S.M., Raeber, G.P., Hubbell, J.A., Schnell, C., and Zisch, A.H. 2008. The role of actively released fibrin-conjugated VEGF for VEGF receptor 2 gene activation and the enhancement of angiogenesis. *Biomaterials* 29:1720-1729.
6. von Degenfeld, G., Banfi, A., Springer, M.L., Wagner, R.A., Jacobi, J., Ozawa, C.R., Merchant, M.J., Cooke, J.P., and Blau, H.M. 2006. Microenvironmental VEGF distribution is critical for stable and functional vessel growth in ischemia. *FASEB J* 20:2657-2659.
7. Korpisalo, P., Hytonen, J.P., Laitinen, J.T., Laidinen, S., Parviainen, H., Karvinen, H., Siponen, J., Marjomaki, V., Vajanto, I., Rissanen, T.T., et al. 2011. Capillary enlargement, not sprouting angiogenesis, determines beneficial therapeutic effects and side effects of angiogenic gene therapy. *European heart journal* 32:1664-1672.
8. Banfi, A., von Degenfeld, G., Gianni-Barrera, R., Reginato, S., Merchant, M.J., McDonald, D.M., and Blau, H.M. 2012. Therapeutic angiogenesis due to balanced single-vector delivery of VEGF and PDGF-BB. *FASEB J* 26:2486-2497.
9. Gianni-Barrera, R., Trani, M., Fontanellaz, C., Heberer, M., Djonov, V., Hlushchuk, R., and Banfi, A. 2013. VEGF over-expression in skeletal muscle induces angiogenesis by intussusception rather than sprouting. *Angiogenesis* 16:123-136.

CURRICULUM VITAE

PERSONAL INFORMATION

Full name	Veronica, SACCHI
Place and Date of Birth	Siena (Italy), February 2nd 1984
Home Address	Baerenfelserstrasse 3, CH-4057, Basel, Switzerland
Cell Phone	0041/(0)765931247
E-mail address - personal	veronica.sacchi.84@gmail.com
- work	veronica.sacchi@usb.ch

EDUCATION & TRAINING

June 2013 PhD Degree

Institute for Surgical Research and Hospital Management, Cell and Gene Therapy Laboratory
20,Hebelstrasse CH-4031 Basel Switzerland

Thesis title: Highly tunable delivery of matrix-bound growth factors for therapeutic angiogenesis

February 2009 Master's Degree in Medical Biotechnologies (110/110 *cum laude*)

University of Siena, Interfaculty of Faculty of Pharmacy, Medicine, Mathematics Physics and Natural Sciences
4, Strada Delle Scotte , 53100, Siena, Italy

Thesis title: Metabolomic and proteomic analysis for prostate cancer biomarkers using cell culture model

July 2006 Bachelor's Degree in Biotechnology (110/110 *cum laude*)

University of Siena, Interfaculty of faculty of Pharmacy, Medicine, Matematics Physics and Natural Sciences
2, Via Aldo Moro, 53100 Siena, Italy

Thesis title: Synthesis and stability of multimeric peptides for tumor targeting

June 2003 Scientific school leaving-examination (82/100)

Liceo Scientifico A. da Sangallo
12, Via San Martino, 53045 Montepulciano (SI) Italy

WORK EXPERIENCE

June 2013- Research Fellow

Institute for Surgical Research and Hospital Management, Cell and Gene Therapy Laboratory, Supervisor Dr Andrea Banfi
20,Hebelstrasse CH-4031 Basel, Switzerland

Research project: determine whether precise co-localization of PDGF-BB and VEGF gradients is required to normalize VEGF-induced aberrant angiogenesis in skeletal muscle with injectable Poly(L-lactide) and Poly(glycolide) (PLGA) microparticles loaded with recombinant proteins.

November 2009-June 2013	PhD student Institute for Surgical Research and Hospital Management, Cell and Gene Therapy Laboratory, Supervisor Dr Andrea Banfi 20,Hebelstrasse CH-4031 Basel, Switzerland Research project: my PhD project aimed to I) Optimize a fibrin platform for controlled and sustained delivery of recombinant $VEGF_{164}$ to induce normal, stable and functional angiogenesis II) Explore the potential of recombinant PDGF-BB and $VEGF_{164}$ protein co-delivery from fibrin gels to normalize aberrant angiogenesis induced from high $VEGF_{164}$ levels and accelerates vascular stabilization.
May 2009- September 2009	Graduate student fellowship Novartis Vaccine & Diagnostics Research Center, Supervisor Dr Enrico Balducci 1, Via Fiorentina, 53100 Siena, Italy Research Project: purification and biochemical characterization of a human antimicrobial peptide, LL-37, modified by ADP-ribosyltransferases toxins to reduce its cytotoxic activity, in order to understand its mechanisms of inactivation by bacterial toxins.
February 2008- September 2008	Foreign training as undergraduate student Swansea University of Wales, School of Biological Sciences, Laboratory of Biochemistry, Supervisor Prof Lorenza Trabalzini & Dr Edward Dudley Singleton Park, SA2 8PP Swansea, UK Research project: Proteomics and metabolomics analyses in order to identify new prostate cancer biomarkers using cell culture 2D- models (PC-3 and PNT2 cells line).
February 2006-July 2006	Internal training as undergraduate student University of Siena, Department of Molecular Biology, Laboratory of Molecular Biotechnology, Supervisor Prof Luisa Bracci & Dr Chiara Falciani 1, Via Fiorentina, 53100 Siena, Italy Research project: synthesis and characterization of tetrabranched peptides for tumor targeting, in order to develop proteases- resistant peptides highly specific for several tumors applicable as carriers for chemotherapeutics agents and tumor-imaging compounds.

PERSONAL SKILLS AND COMPETENCES

Mother tongue	Italian
Other language	English (Speaking: Good; Writing: Good; Reading: Good)
Technical skills and competence	Fibrin gel preparation for in vitro assay and in vivo injection as liquid in hind limb skeletal mouse. Immunohistochemistry, immunofluorescence techniques and imaging by confocal microscopy (Carl Zeiss LSM 710 controlled via the ZEN software utility) Cell culture handling in conventional monolayer Cell transfection and transduction (with retrovirus) RNA, DNA & Protein extraction, quantitative real time PCR

	Bacteria culture and cloning
	ELISA & Western Blot
	In vivo experiments (with mice)
	Cytofluoremetric analyses with BD FACS Calibur
	Purification of Nucleotides and Peptides by HPLC chromatography
Computer skills and competence	OS: Windows and Macintosh
	Good command of internet and Microsoft Office tool, in particular Word, Power Point, Excel, and Access.
	GraphPad Prism 5.0, Adobe Photoshop CS5, ImageJ and FlowJo.
Social skills and competence	Able and ready to work both independently as well as in team
	Hard-worker with very strong determination and passion
	High organizational capacity in- and outside work
	High ability and adaptability to new working and social environments
Driving licence	Italian driving licence, category B
Work Permit	B permit for Switzerland

PUBLICATIONS LIST

Sacchi, V., Mittermayr, R., Hartinger, J., Martino MM, Lorentz KM, Morton T., Hofmann A., Wolbank S., Largo R., Marshall J., Groppa E., Gianni-Barrera R., Ehrbar M., Hubbell JAH, Redl H., Banfi A. **Sustained and highly tunable delivery of recombinant $VEGF_{164}$ from optimized fibrin matrices ensures normal, stable and functional angiogenesis** (Proceedings of the National Academy of Sciences, 2014 May 13;111(19): 6952-7).

Sacchi V., Martino MM, Gianni-Barrera R., Hubbell JAH, Banfi A. **Recombinant PDGF-BB and $VEGF_{164}$ balanced co-delivery from fibrin gels normalizes aberrant angiogenesis induced by high $VEGF_{164}$ concentration** (manuscript in preparation).

Groppa E., Brkic S., Sacchi V., Trani M., Muraro M.G,, Heberer M., Banfi A. **EphrinB2/EphB4 signaling controls the switch from normal to aberrant angiogenesis caused by VEGF dose** (manuscript in preparation).

Bichet S., Fogli B., Sacchi V., Heberer M., Banfi A., Gianni-Barrera R. **Sustained activation of Notch4 by Jagged-1 correlates with aberrant angiogenesis induced by VEGF in skeletal muscle** (manuscript in preparation).

PARTECIPATION AT CONFERENCES AND SYMPOSIA

Oral Presentation	*Recombinant PDGF-BB and $VEGF_{164}$ balanced co-delivery by fibrin gels normalizes aberrant angiogenesis induced by high $VEGF_{164}$ concentrations. Tissue Engineering and Regenerative Society, Annual EU Meeting, Genoa 2014* *Sustained and highly tunable delivery of recombinant $VEGF_{164}$ from optimized fibrin matrices ensures normal, stable and functional angiogenesis*. Tissue Engineering and Regenerative Society, Annual EU Meeting, Istanbul, Turkey (2013)*.* *Dose and time-dependent angiogenesis by controlled delivery of matrix-bound VEGF*. Tissue Engineering and Regenerative Society, Annual EU Meeting, Granada, Spain (2011).

Poster Presentation	*Recombinant PDGF-BB and VEGF164 balanced co-delivery by fibrin gels normalizes aberrant angiogenesis induced by high VEGF164 concentrations.* American Society of Cell and Gene Therapy, Washington 2014. *Long-lasting fibrin matrices ensure stable and functional angiogenesis by highly tunable, sustained delivery of recombinant VEGF$_{164}$.* 3rd Cardiovascular and metabolic research conference, Fribourg, Switzerland (2013) *Recombinant PDGF-BB and VEGF$_{164}$ balanced co-delivery by fibrin gels normalizes aberrant angiogenesis induced by high VEGF$_{164}$ concentrations*. Tissue Engineering and Regenerative Society, Annual EU Meeting, Istanbul, Turkey (2013). *Sustained and highly tunable delivery of engineered VEGF$_{164}$ from optimized fibrin matrices ensures normal, stable and functional angiogenesis***.** 9th Swiss Stem Cells Network, Bern, Switzerland, (2013) *Dose and time-dependent angiogenesis by controlled delivery of matrix-bound VEGF*. Tissue Engineering and Regenerative Medicine Society, 3rd World Congress, Vienna, Austria *Dose and time-dependent angiogenesis by controlled delivery of matrix-bound VEGF* Frontiers in Cardiac and Vascular Regeneration, Trieste, Italy (2012). *Dose and time-dependent angiogenesis by controlled delivery of matrix-bound VEGF*. 8th International Symposium on the Biology of Endothelial Cells, Zurich, Switzerland(2011)***.**

ADDITIONAL INFORMATIONS

Personal interests	Travelling, Reading, Enjoy with friends
Sports	Swimming, Biking, Skiing, Volleyball, Hiking

REFERENCES:

- PD, Dr Andrea Banfi: andrea.banfi@usb.ch
- Prof Heinz Redl: Office@TRAUMA.LBG.AC.AT
- Dr Enrico Balducci: enrico.balducci@novartis.com
- Prof Lorenza Trabalzini: trabalzinil@unisi.it
- Dr Edward Dudley: e.dudley@swansea.ac.uk